INVESTIGATION OF GEOSYNTHETIC-SOIL CONFINEMENT USING ASPHALT PAVEMENT ANALYZER

By

Yuze Zhang

A thesis submitted to the Department of Civil Engineering and the Graduate Faculty of the University of Kansas in partial fulfillment of the requirements for the degree of Master's of Science

Dr. Jie Han, Chairperson

Committee members

Dr. Robert L. Parsons

Dr. Oswald Chong

Date defended:

The Thesis Committee for Yuze Zhang certifies

That this is the approved version of the following thesis:

INVESTIGATION OF GEOSYNTHETIC-SOIL CONFINEMENT USING ASPHALT PAVEMENT ANALYZER

Committee:

Dr. Jie Han, Chairperson

Dr. Robert L. Parsons

Dr. Oswald Chong

Date approved: _____

ACKNOWLEDGEMENT

I would like to express my appreciation to my advisor Dr. Jie Han for giving his advice and the opportunity of working on such an interesting project. Every progress would not be possible without his guidance and support. I would also like to thank Dr. Robert Parsons and Dr. Jungjo Yuu, for their suggestion and interest in my work.

Special thanks to Jim Weaver for the technical support and Pei-Ling for the helps on program and image processing.

Thanks also to the Transportation Research Institute at the University of Kansas and Tensar Earth Technologies, Inc., for funding the research.

Last, but not the least, I want to thank my parents for their understanding, support, and encouragement.

TABLE OF CONTENTS

Title Page **i**

Acceptance Page **ii**

ACKNOWLEDGEMENT **iii**

ABSTRACT **xii**

LIST OF FIGURES **vii**

LIST OF TABLES **xi**

Chapter 1 INTRODUCTION **1**

1.1 Background **1**

1.2 Problem statement **1**

1.3 Objective **3**

1.4 Organization **3**

Chapter 2 LITERATURE REVIEW **5**

2.1 Mechanism of geosynthetic reinforcement **5**

2.1.1 Separation 5

2.1.2 Lateral confinement 6

2.1.3 Tension membrane effect 7

2.2 Previous works **8**

2.2.1 Generalization of previous work 8

2.2.2 Review of previous work 9

Chapter 3 EXPERIMENTAL STUDIES **18**

3.1 Introduction **18**

3.2 Soil properties **18**

3.2.1 Kansas River sand 18

3.2.2 AB-3 22

3.3 Geosynthetic types and properties **26**

3.4 Test equipment **31**

3.4.1 Specification 32

3.4.2 Parts of the APA 33

3.4.3 Calibration 39

3.4.4 Data acquisition 41

3.5 Modification **42**

3.6 Test procedures **54**

3.6.1 Sample preparation 54

3.6.2 Surcharge 56

3.6.3 Wheel load and hose pressure 57

3.6.4 Data acquisition 57

Chapter 4 TEST RESULTS AND ANALYSIS **59**

4.1 Introduction **59**

4.2 Repeatability of test results **59**

4.3 Effect of base material **61**

4.4 Effect of surcharge **66**

4.5 Effect of geosynthetic **75**

4.6 Traffic benefit ratio **82**

4.7 Rut reduction ratio **85**

Chapter 5 CONCLUSIONS AND RECOMMENDATIONS **88**

5.1 Summary **88**

5.2 Conclusions **89**

5.3 Recommendations **89**

REFERENCES **90**

LIST OF FIGURES

Figure 2.1 Schematic of mixing and separation.....6

Figure 2.2 Snooker ball rack analogy.....7

Figure 2.3 The mechanism of interlock.....7

Figure 2.4 Tension membrane effect.....8

Figure 2.5 The University of Oxford experiment without and with reinforcement.....10

Figure 2.6 Trials of different geosynthetics by TRL.....11

Figure 2.7 Cyclic plate tests.....12

Figure 2.8 Pavement trials by USACE.....14

Figure 2.9 The Newcastle University trafficking trails.....15

Figure 2.10 Full scale plate load tests on reinforced foundations.....16

Figure 3.1 Grain size distribution of Kansas River sand.....20

Figure 3.2 CD triaxial test of Kansas River sand.....20

Figure 3.3 Mohr circle from CD test.....21

Figure 3.4 Large direct shear test of Kansas River sand.....21

Figure 3.5 Grain size distribution of AB-3 base course.....23

Figure 3.6 Compaction curve of AB3 base course.....24

Figure 3.7 Large direct shear test for AB-3 aggregate.....24

Figure 3.8 Grain size distribution of modified AB-3.....25

Figure 3.9 Geosynthetics used in this study.....26

Figure 3.10 Asphalt Pavement Analyzer (APA).....32

Figure 3.11 Three metal wheels on three rubber hoses.....33

Figure 3.12 Hose rack.....34

Figure 3.13 Sample tray.....35

Figure 3.14 Three sample molds.....36

Figure 3.15 Three original test molds on the tray.....37

Figure 3.16 Control panel of APA.....38

Figure 3.17 Load cell for calibration.....39
Figure 3.18 Manual measurement.....42
Figure 3.19 Modified test box.....43
Figure 3.20 Geosynthetics in soil.....43
Figure 3.21 Dimension of the modified box.....44
Figure 3.22 Cross section of the box under three wheel loads.....45
Figure 3.23 Uniform vertical loads near a retaining wall.....46
Figure 3.24 Stress below a strip load.....48
Figure 3.25 Uniform vertical loading.....50
Figure 3.26 Stresses on 480 mm side.....51
Figure 3.27 Three teeth supporting the 480 mm side.....53
Figure 3.28 Dimensions of the modified test box.....54
Figure 3.29 Surcharge.....57

Figure 4.1 Repeatability test of Kansas River sand.....60
Figure 4.2 Repeatability test of AB-3 aggregate.....60
Figure 4.3 Without reinforcement.....61
Figure 4.4 BX1100 at 25 mm below the surface.....62
Figure 4.5 BX1200 at 25 mm below the surface.....62
Figure 4.6 BX1500 at 25 mm below the surface.....63
Figure 4.7 Geotextile at 25 mm below the surface.....63
Figure 4.8 BX1100 at 13 mm below the surface.....64
Figure 4.9 BX1200 at 13 mm below the surface.....64
Figure 4.10 BX1500 at 13 mm below the surface.....65
Figure 4.11 Geotextile at 13 mm below the surface.....65
Figure 4.12 Test results of unreinforced cases under 44 N wheel loads without and with surcharge.....66
Figure 4.13 Test results of unreinforced cases under 88 N wheel loads without and with surcharge.....67

Figure 4.14 Test results of reinforced cases with BX1100 at 25mm deep under 44 N wheel loads without and with surcharge.....68
Figure 4.15 Test results of reinforced cases with BX1100 at 25mm deep under 88 N wheel loads without and with surcharge.....68
Figure 4.16 Test results of reinforced cases with BX1200 at 25mm deep under 88 N wheel loads without and with surcharge.....69
Figure 4.17 Test results of reinforced cases with BX1500 at 25mm deep under 44 N wheel loads without and with surcharge.....69
Figure 4.18 Test results of reinforced cases with BX1500 at 25mm deep under 88 N wheel loads without and with surcharge.....70
Figure 4.19 Test results of reinforced cases with geotextile at 25mm deep under 44 N wheel loads without and with surcharge.....70
Figure 4.20 Test results of reinforced cases with geotextile at 25mm deep under 88 N wheel loads without and with surcharge.....71
Figure 4.21 Test results of reinforced cases with BX1100 at 13mm deep under 44 N wheel loads without and with surcharge.....71
Figure 4.22 Test results of reinforced cases with BX1100 at 13mm deep under 88 N wheel loads without and with surcharge.....72
Figure 4.23 Test results of reinforced cases with BX1200 at 13mm deep under 88 N wheel loads without and with surcharge.....72
Figure 4.24 Test results of reinforced cases with BX1500 at 13mm deep under 44 N wheel loads without and with surcharge.....73
Figure 4.25 Test results of reinforced cases with BX1500 at 13mm deep under 88 N wheel loads without and with surcharge.....73
Figure 4.26 Test results of reinforced cases with geotextile at 13mm deep under 44 N wheel loads without and with surcharge.....74
Figure 4.27 Test results of reinforced cases with geotextile at 13mm deep under 88 N wheel loads without and with surcharge.....74
Figure 4.28 Test results of unreinforced and reinforced Kansas River sands with geosynthetics at 25mm deep under 44 N loads.....75

Figure 4.29 Test results of unreinforced and reinforced Kansas River sands with geosynthetics at 25mm deep under 88 N loads.....76
Figure 4.30 Test results of unreinforced and reinforced Kansas River sands with geosynthetics at 13mm deep under 44 N loads.....76
Figure 4.31 Test results of unreinforced and reinforced Kansas River sands with geosynthetics at 13mm deep under 88 N loads.....77
Figure 4.32 Test results of unreinforced and reinforced Kansas River sands with geosynthetics at 25mm deep under 44 N loads and with surcharge.....78
Figure 4.33 Test results of unreinforced and reinforced Kansas River sands with geosynthetics at 25mm deep under 88 N loads and with surcharge.....78
Figure 4.34 Test results of unreinforced and reinforced Kansas River sands with geosynthetics at 13mm deep under 44 N loads and with surcharge.....79
Figure 4.35 Test results of unreinforced and reinforced Kansas River sands with geosynthetics at 13mm deep under 88 N loads and with surcharge.....79
Figure 4.36 Test results of unreinforced and reinforced AB-3 aggregates with geosynthetics at 25mm deep under 353 N loads.....80
Figure 4.37 Test results of unreinforced and reinforced AB-3 aggregates with geosynthetics at 13mm deep under 353 N loads.....81
Figure 4.38 Sample calculation of TBR.....83
Figure 4.39 Sample calculation of RRR.....86

LIST OF TABLES

Table 3.1 Specifications of BX1100 geogrid.....27

Table 3.2 Specifications of BX1200 geogrid.....28

Table 3.3 Specifications of BX1500 geogrid.....29

Table 3.4 Specifications of HP370 woven geotextile.....30

Table 4.1 TBR of four geosynthetics at all conditions.....90

Table 4.2 RRR of four geosynthetics at all conditions.....93

ABSTRACT

Interaction between geosynthetics (geogrid or geotextile) and aggregates under traffic wheel loading has been considered one of high-priority problems by the Transportation Research Board. The practical use of geosynthetics above the subgrade or in base course has demonstrated their effects on the reduction of rut depths and the prolonging of pavement life. However, no standard test method is available to appropriately evaluate the geosynthetic-soil confinement effect and distinguish the benefits among different types of geosynthetics and soils. This proposed test method is to modify the asphalt pavement analyzer to evaluate geosynthetic-soil confinement. In this test, a geosynthetic sheet is placed within a base course to form a reinforced base course, which is subjected to wheel loading. The measured rut depth with the number of cycles of wheel loading can be used to evaluate the geosynthetic-soil confinement. In this study, two different base course materials and four different geosynthetics were used. The experimental results clearly show that this proposed new test method can distinguish the benefits of rut reduction among different types of geosynthetics and base course materials.

Chapter 1 INTRODUCTION

1.1 Background

Geosynthetic materials have gained considerable popularity because of their wide applications in earthwork construction such as roadways and embankments. It has been demonstrated that geosynthetics are successfully used to enhance the performance not only in the newly constructed but also the rehabilitated pavement systems. Geosynthetics provide tensile reinforcement through frictional interaction with base course materials, thus confine the soil particles from moving apart and reduce the rut depth. By improving the performance of the base course, the geosynthetic inclusion can help increase the service life of the road system. Geosynthetics are particularly attractive in areas where quality aggregate sources are scarce, in urban areas where these resources have been depleted, or in environmentally sensitive areas where the aggregate quarries is not permitted.

1.2 Problem statement

Although many studies have been conducted on the use of geosynthetics for roadway applications, the development of methods of analysis still somewhat falls behind the rapid development of geosynthetic reinforcement technology and there is still a lack of understanding about the behavior of geosynthetic-soil confinement, which is an important mechanism in roadway applications.

A few studies were conducted in the past to develop test methods that aid in describing the behavior of geosynthetic-soil confinement, but they all have deficiencies. The aperture stability modulus test was developed by Kinney (2000) to measure the rigidity of geogrid subjected to a torque action, however, it provides no interaction between geogrid and base course material and the test is not under a repeated wheel load. The TRI bending confinement test (Prague *et al*., 2005) is to apply uniform pressure on soil-geosynthetic-soil "sandwich" and measure the deflection under such a pressure, however, it is not under a repeated wheel load either and has significant influence of shear resistance between soil and chamber. Cyclic plate loading test, which were used for a few studies (for example, Gabr, 2000; Perkins, 1997), can not simulate rolling wheel action, and they are tedious, slow, and costly. Cyclic triaxial tests were used to evaluate the reinforcement effect of geosynthetics in soil (for example, Perkins *et al*., 2004), however, they do not have any localized deformation and can not simulate wheel loading. Accelerated pavement testing facility is ideal for evaluating the benefit of geosynthetics in roadways (White *et al.*, 1999); however, it is slow and very costly. Therefore, it is not feasible as a routine test method. Field track testing is another ideal method for evaluating the performance; however, it is difficult, slow, and very costly. Thus, it is not suitable for routine testing. Therefore, a new method is needed, which can efficiently and effectively evaluate the geosynthetic-soil confinement and avoid all the deficiencies mentioned above.

1.3 Objective

The purpose of this study is to propose a new test method using the Asphalt Pavement Analyzer (APA) to evaluate the confinement effect of geosythetics in the soil. In this study, different geosythetics including biaxial geogrid and woven geotextile were tested at different locations in the base course with two different soil types.

The research scope is focused on experimental studies which evaluated how the geosynthetic reinforcement affected the rut depth of the base course material under rolling wheel loading. This proposed test method was proved in this study that it can distinguish the difference in the geosynthetic-soil confinement by different geosynthetic products and base course materials. This new test method is quick, easy, and not costly to perform, therefore, it can be used as a routine test method to evaluate the geosynthetic-soil confinement for base reinforcement.

1.4 Organization

In addition to Chapter 1 - Introduction, Chapter 2 reviews the basic concepts of geosynthetics and base course reinforcement, which include lateral confinement, improvement of bearing capacity, and tension membrane effect. Current test methods and results related to geosynthetic-soil confinement are also discussed in this chapter.

Chapter 3 provides the experimental parameters and results, which include soil and geosynthetics properties, the Asphalt Pavement Analyzer (APA), test box design, test

procedures, measured rut depths under different load conditions. In this study, four different geosynthetics and two types of base course materials were used. One geosynthetic sheet was placed at a depth of either 25 mm (1 in) or 13 mm (0.5 in) below the surface.

Chapter 4 presents the interpretation and analysis of the test data. The analysis is focused on the effect of base course material, the effect of surcharge, the effect of geosynthetic, and the traffic benefit ratio (defined as the ratio of the number of cycles to reach a certain rut depth when reinforced to the number of cycles to reach the same rutting depth when unreinforced).

The conclusions and recommendations from this study are provided in Chapter 5.

Chapter 2 LITERATURE REVIEW

2.1 Mechanism of geosynthetic reinforcement

Geogrid and geotextile have been commonly used as reinforcement in the earthwork. Nonwoven geotextiles are usually used for separation, filtration, and drainage while woven geotextiles are usually used for reinforcement. Geogrids are typically used for soil reinforcement. Previous studies have identified three key mechanisms for geosynthetics used for roadway applications: separation, lateral confinement, and tension membrane effect.

2.1.1 Separation

The failure of a road section may occur when the fines from the subgrade migrate into the overlying granular base. A wheel load applied on the road surface would be transferred from base to subgrade and cause the mixing of base and subgrade. This mixing would then result in decrease of modulus and thickness of the base course, thereby weaken the base layer and cause the section failure. A layer of geosynthetic can be placed between base and subgrade as separator to avoid the mixing. Figure 2.1 shows the schematic of mixing and separation. A separation condition is crucial since the stronger base layer can be weakened and thinned when the fines from the subgrade are mixed into the base layer.

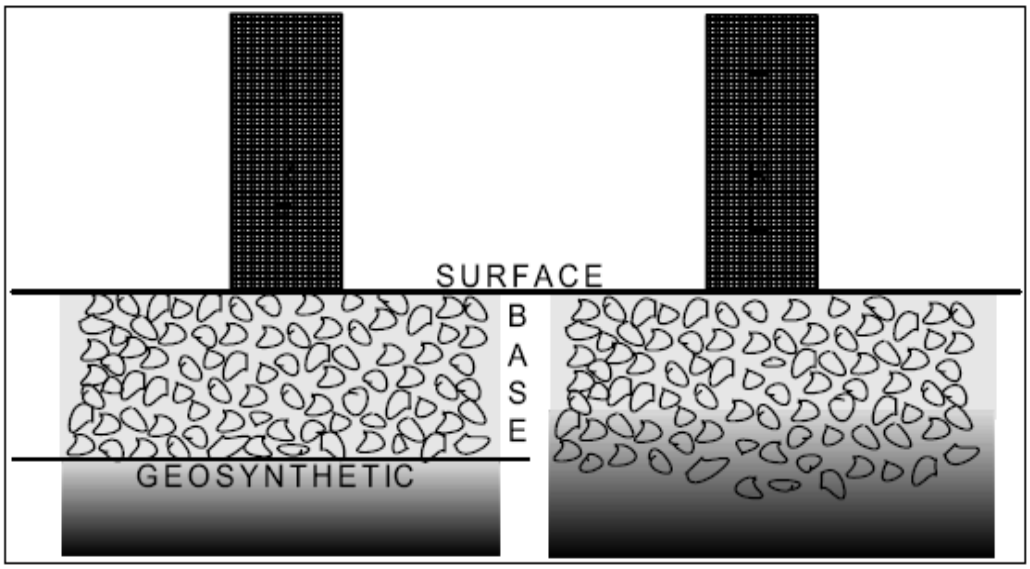

Figure 2.1 Schematic of mixing and separation (Maxwell *et al.*, 2005)

2.1.2 Lateral confinement

The wheel loads induce the shear stresses and create the spreading effect of base layer above the subgrade. This spreading effect leads to vertical strain and cause rutting at the surface. The geosynthetics can limit this lateral movement by providing the frictional force between the base course and the geosynthetics. When the base material is compacted over the geosynthetics, it partially penetrates and projects through the apertures, especially for geogrid, to create a strong interlocking effect. This mechanism can be best pictured as the effect of a snooker ball rack (Figure 2.2). By interlocking the aggregates, the geosynthetics reduce the lateral movement, provide the confinement effect and therefore increase the modulus of the base layer. Figure 2.3 shows the mechanism of the interlock.

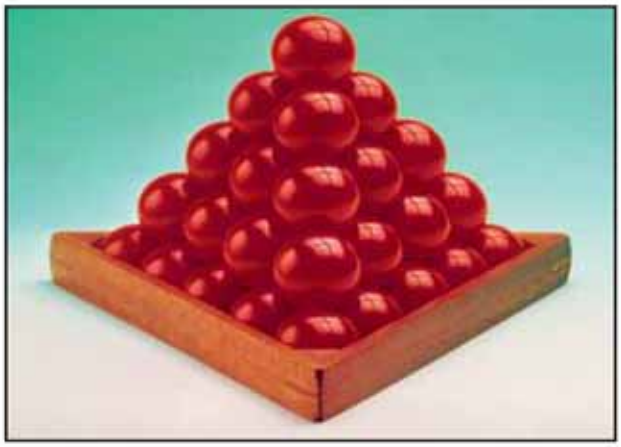

Figure 2.2 Snooker ball rack analogy (Tensar Earth Technologies, Inc.)

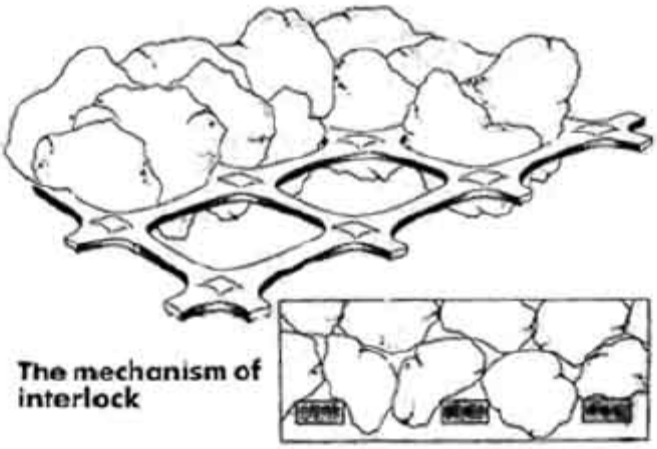

Figure 2.3 The mechanism of interlock (Wrigley, 1989)

2.1.3 Tension membrane effect

A tension membrane effect develops when the vertical deformation at the bottom of the base layer create a concave shape in the geosynthetic layer. The vertical component generated from the tensile force of geosynthetics reduces the vertical stress acting on the subgrade. This effect, of course, requires a relatively large deformation of the geosynthetics to mobilize the tensile resistance and show the

benefit. Figure 2.4 shows the tension membrane effect.

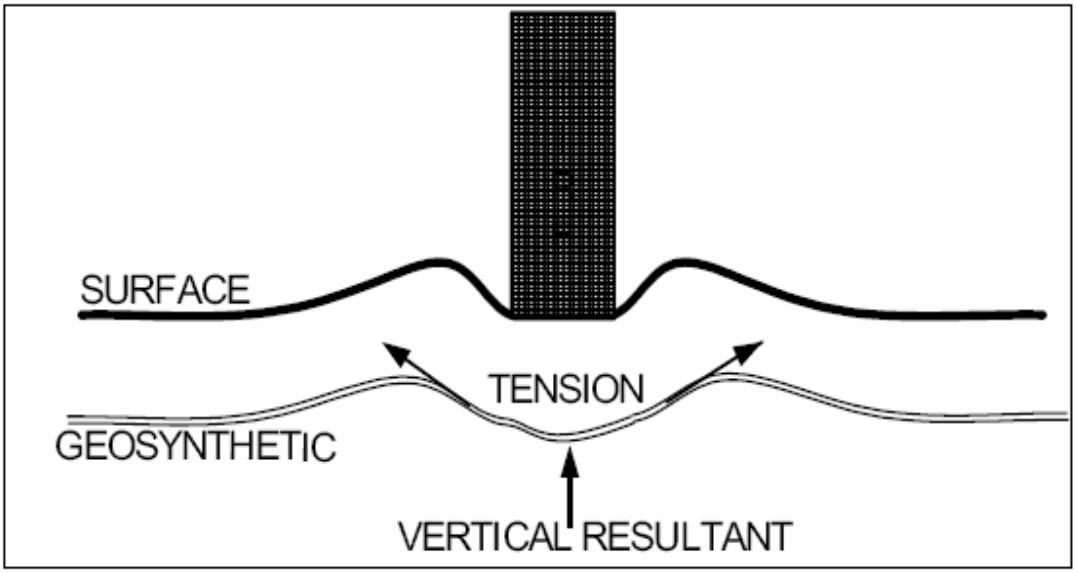

Figure 2.4 Tension membrane effect (Maxwell *et al.*, 2005)

2.2 Previous work

The fundamental objective of the pavement design is to prolong the service life of the pavement systems and thus reduce the life-cycle cost. Geosynthetics are successfully used to enhance the performance not only in the newly constructed but also the rehabilitated pavement systems. The increased use of geosynthetics motivated a number of researchers to conduct the studies on geosynthetic-reinforced pavement systems in the past three decades, like Hass *et al.* (1988) using a stationary cyclic load test, Barksdale *et al.* (1989) using a moving single wheel test, and many others.

2.2.1 Generalization of previous work

In general, four categories of studies were conducted in the past: (1) A stationary

cyclic load is applied onto test sections constructed in large, stiff cubical containers, for example, Hass *et al.* (1988), Kinney *et al.* (1998), and Perkins (1999); (2) Controlled loading using standard trucks or moving wheel loads (MWL), for example, Barksdale *et al.* (1989) and Cancelli *et al.* (1996); (3) Field tests by random public vehicular traffic, for example, Bhutta *et al.* (1998), Hayden *et al.* (1999), and Huntington and Ksaibati (1999); and (4) Numerical analyses, for example, Barksdale *et al.* (1989), Dondi (1994), Miura *et at.* (1990), Perkins and Edens (2003), and Wathugala *et al.* (1996).

2.2.2 Review of previous work

The potential benefits of geosynthetic reinforcement were examined by researchers through laboratory, field, and numerical modeling investigations. A series of studies are reviewed in this section.

In early 1980s, static load tests were conducted by the University of Oxford to investigate the benefit of reinforcing a granular layer over soft clay. The experiment consistently demonstrated that an enhancement in bearing capacity of about 40% was achieved in reinforced cases. Figure 2.5 demonstrated that the geosynthetics prevented the particles from moving laterally under a loaded area and the tests without and with geosynthetics under a similar load showed different behavior.

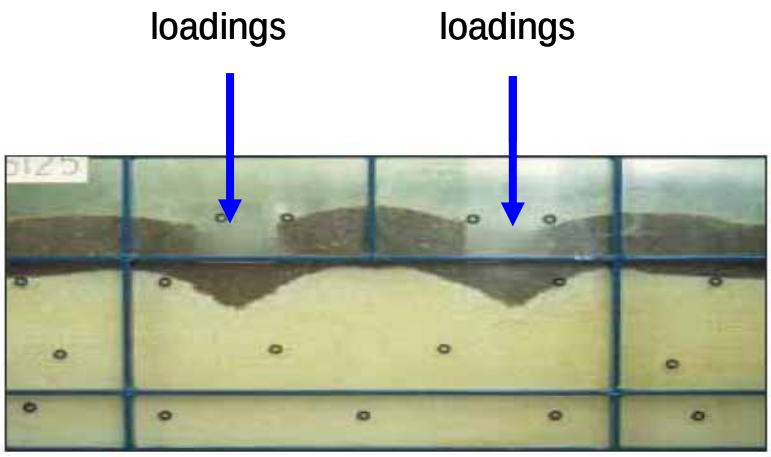

Unreinforced case

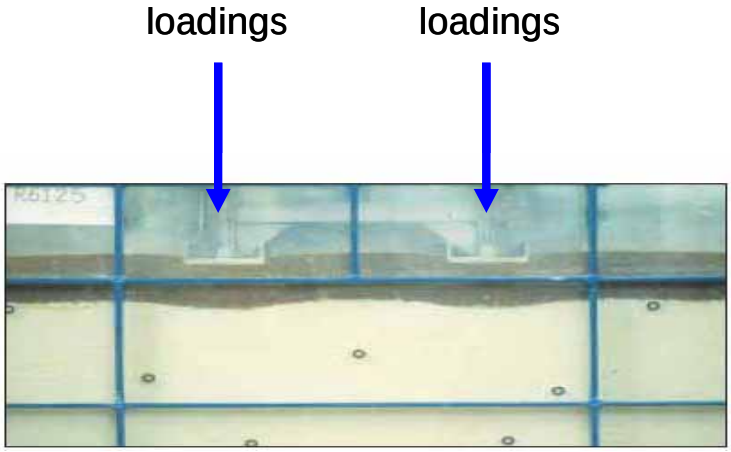

Reinforced case

Figure 2.5 The University of Oxford experiment without and with reinforcement (The University of Oxford, 1980)

UK's Transport and Road Research Laboratory (TRRL- now known as TRL) conducted the trials both in the test facility and in the field in mid 1980s (Chaddock, 1988). They found that a given subbase could carry approximately 3.5 times more traffic if a geosynthetic reinforcement was used.

Further trials were carried out by TRL later in 2000 incorporating a variety of geosynthetic materials (Blackman *et al*.). A 40 kN dual wheel was used to traffick on a fixed path consisting of 320 mm sub-base over a clay subgrade with CBR of 1.5%. The results in Figure 2.6 show that the geogrid section had much better performance than the geotextile and welded geogrid sections.

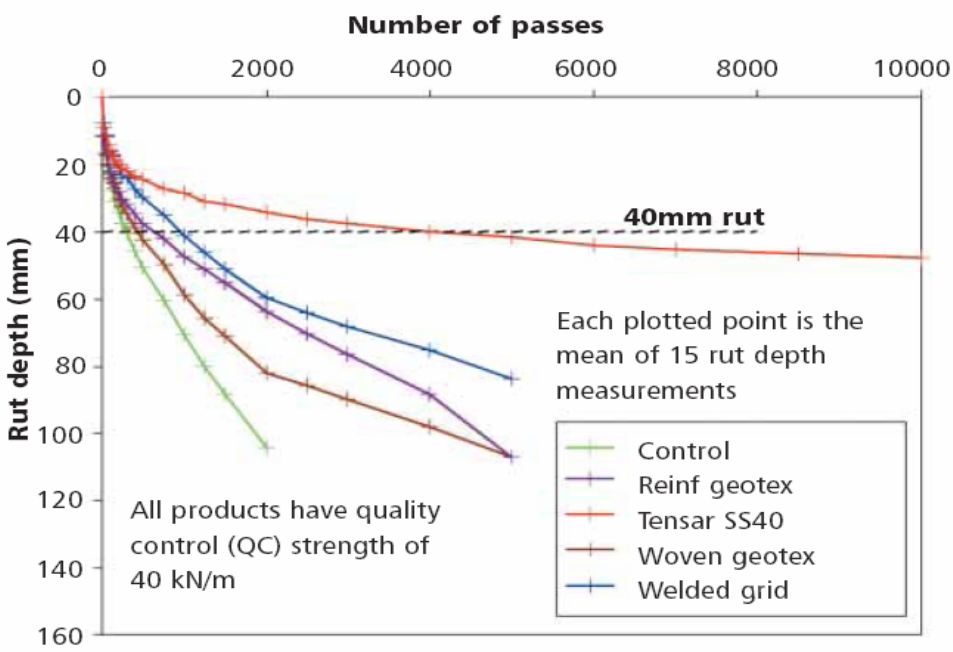

Figure 2.6 Trials of different geosynthetics by TRL (Blackman et al., 2000)

Through the cyclic plate loading tests, Haas *et al.* (1988) found that the thickness of the base layer could be reduced by about 25%-50% as a result of using the geogrid, and observed that, after the first 10,000 load cycles, the rut depth decreased from 20.3 mm for the unreinforced pavement section to 11.6 mm for the reinforced one. Such reduction was even higher when a weaker subgrade was used. Moreover, the geogrid placed at the middle of a 304.8 mm thick base layer did not produce any benefit until

large deformations occurred. Figure 2.7 is the complete result of the cyclic plate loading tests by Haas *et al.* (1988).

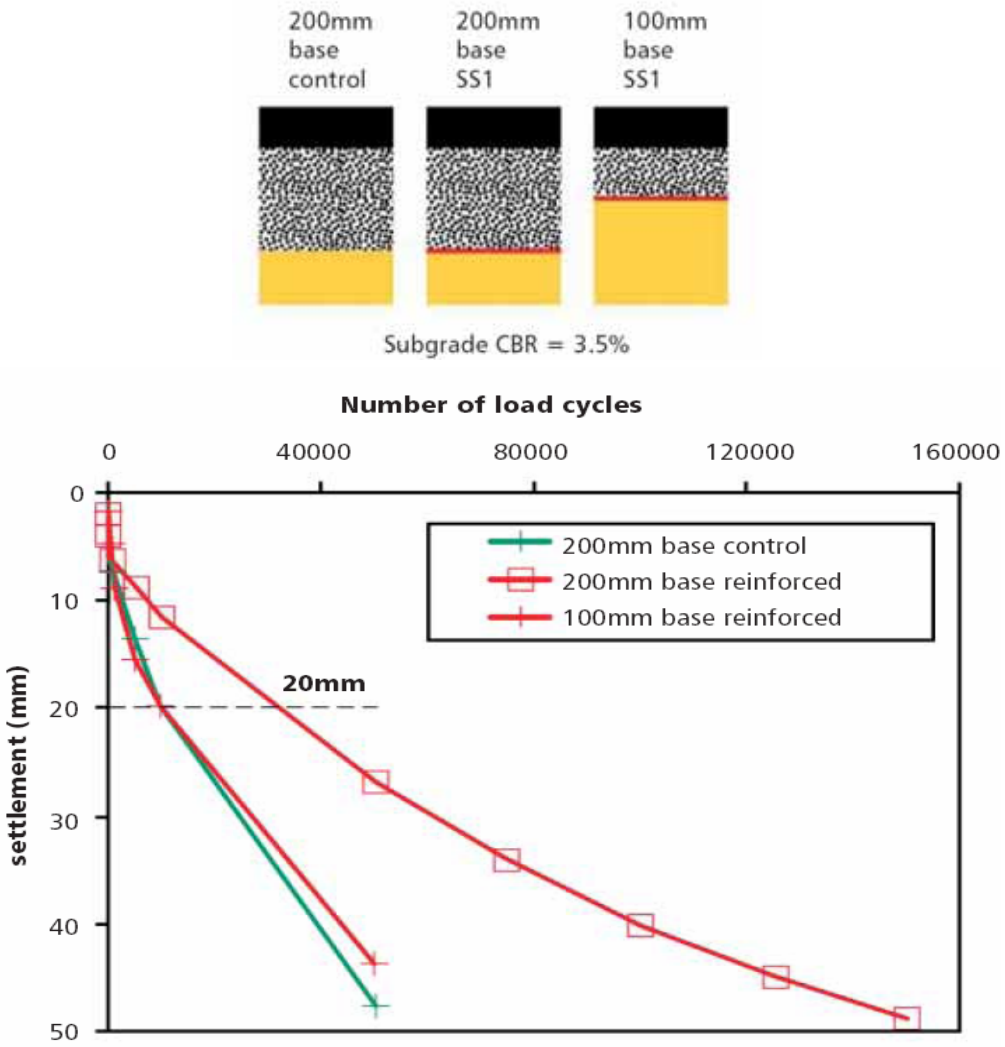

Figure 2.7 Cyclic plate tests (Haas *et al.*, 1988)

Miura *et al.* (1988) carried out a comprehensive laboratory study to investigate the role of geosynthetic membrane. They concluded: (1) the peak tensile strain in the geogrid happened at the center of the loading plate when the grid was placed at the

base-subgrade interface; (2) the induced tensile stress in the higher modulus grid was greater than that in the lower modulus grid, thus reduced rut depth more effectively; and (3) if strong bonding was maintained between the asphalt concrete (AC) layer and the geogrid, the performance was enhanced when the grid was placed at the bottom of the AC layer.

Barksdale *et al.* (1989) indicated that even though the geogrid had lower stiffness, it showed a better performance against permanent deformation than the geotextile when placed in the middle and bottom of the base course. Also, their finite element simulations suggested that the geosynthetic benefit was obscured for pavements with a strong subgrade, which matched well with the results of Haas *et al.* (1988) as mentioned above.

A major trafficking trial test was carried out by the US Army Corps of Engineers (USACE) in the early 1990s (Webster, 1992). A 130 kN wheel was used as the load acting on a 50 mm thick asphalt underlain by the base with different thickness and the clay subgrade with CBR of 3% and 8%. It was observed that the relatively rigid geogrid performed the best of all the products. However, one woven geotextile with good strength did not provide any benefit and the rest of the woven geotextile products provided only marginal improvement. In summary, the performance of different geosynthetic products as shown in Figure 2.8 ranged from no improvement up to about 40% reduction of the total pavement thickness requirement.

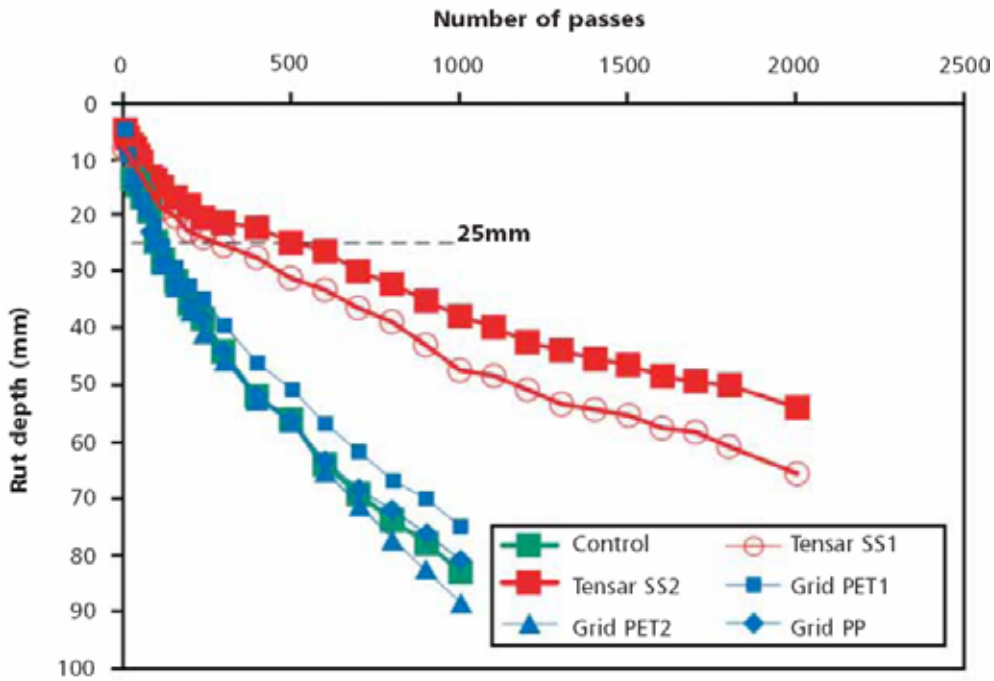

Figure 2.8 Pavement trials by USACE (Webster, 1992)

Dondi (1994) applied the commercial finite element program ABAQUS to model a geosynthetic reinforced flexible pavement. A dual-wheel was simulated by two rectangular areas with the contact pressure of 1500 kPa. Their studies showed: (1) a reduction in the shear strain and the stress transmitted to the top of subgrade; (2) the rut depth of the loaded area reduced by 15-20% for the reinforced section as compared with the unreinforced one; and (3) the fatigue life for the reinforced section 2 to 2.5 times longer than the unreinforced section.

Trial tests (Vanggaard, 1996) conducted by the Newcastle University in 1996 showed that the rut depths of sections with the coated woven polyester geogrid and the extruded PP geogrid were similar to the rut depth of the unreinforced section (Figure 2.9), and the rut depths of two Tensar geogrid-reinforced sections were only about

half the rut depth of the controlled unreinforced section.

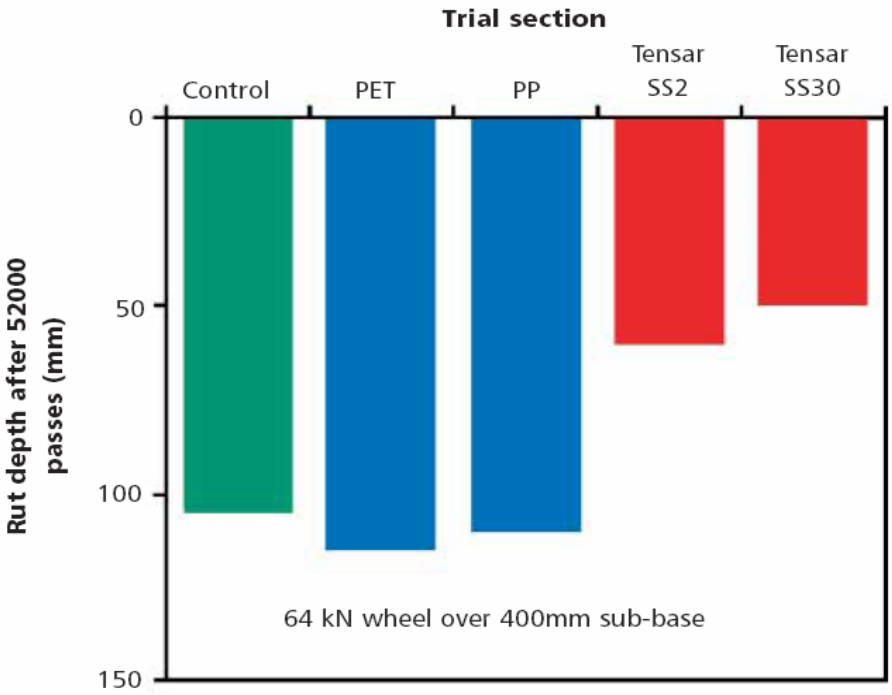

Figure 2.9 The Newcastle University trafficking trails (Vanggaard, 1996)

Adams and Collin (1997) conducted full scale plate load tests on reinforced foundations and they found that a single layer of geosynthetic could increase the bearing capacity of approximately 50%, but that the narrow geogrid layer (TL 146) and the wide geogrid layer (TL 186) had the same performance as shown in Figure 2.10. The observation showed that the reinforcement provided by the interlock mechanism was localized.

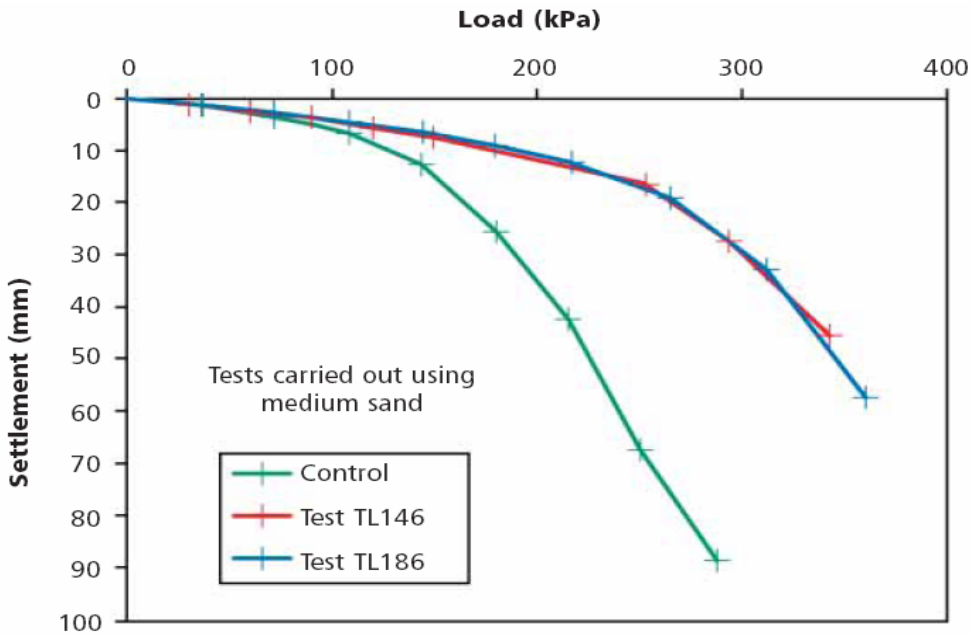

Figure 2.10 Full scale plate load tests on reinforced foundations

(Adams and Collin, 1997)

Wathugala *et al.* (1998) also used the ABAQUS finite element program to explore the reduction in the rut depth resulting from placement of the geogrid sheet at the base-subgrade interface. The asphalt concrete and the crushed stone base were simulated by Drucker-Prager materials. The use of geogrid reduced the permanent rut depth by about 20% for a single cycle of load.

In their overview, Berg *et al.* (2000) summarized that a geosynthetic sheet placed in the pavement section can provide pronounced benefits in load-carrying capacity under certain conditions controlled by subgrade strength, aggregate base characteristics, design requirements, and geosynthetic characteristics.

Perkins (2001) examined factors of geogrid location, geogrid stiffness, base thickness, and subgrade strength and he found that the geogrid having higher stiffness gave a better traffic benefit ratio (TBR). Besides, the increase of TBR was higher when the grid was placed in the middle than the same geogrid placed at the base-subgrade interface. However, Perkins (2001) found from his finite element study that many models did not result in the anticipated results, for example, when the geogrid was placed in the base. He indicated that in order to account for the effect of reinforcement, the base aggregate model had to be improved.

In their experimental studies, Ling and Liu (2001) placed the geogrid between the AC layer and Ottawa sand, and reported that the pavement section performance was enhanced if the bonding was maintained effectively between the AC layer and the geogrid. This finding is consistent with that by Miura *et al.* (1988). In addition, more recently, Ling and Liu (2003) used the two-dimensional commercial finite element program PLAXIS to obtain a favorable comparison with the test results. Moreover, their results indicated that the geosynthetic benefit was more apparent when the subgrade is weak. This finding is in good agreement with the results from Haas *et al.* (1988) and Barksdale *et al.* (1989).

Chapter 3 EXPERIMENTAL STUDIES

3.1 Introduction

As mentioned in Chapter 1, the APA was used in the experimental studies since it has the ability of simulating the rolling wheel load and is readily available at most Departments of Transportation (DOT) in the U.S. Two types of soil, Kansas River sand and AB-3, were used as the base course material, interacting with four types of geosynthetics: Tensar BX1100, BX1200, BX1500 geogrids, and Mirafi HP370 woven geotextile. These geosynthetics were placed 25 mm (1 in) or 13 mm (0.5 in) below the surface. Each test was designed to run for 8000 cycles and the rut depths were measured in different intervals manually or automatically. For a few tests, however, the data acquisition system of the APA machine stopped taking data before reaching 8000 cycles due to the malfunction of the software. The geosynthetic-soil confinement effect was then evaluated in the term of rut depth with number of cycles.

3.2 Soil properties

3.2.1 Kansas River sand

Kansas River sand is a local soil and its particles are subrounded due to the erosion effect of water. ASTM Standard D854-92 was used to determine the specific gravity of soil and ASTM Standards D4254-91 and D4253-93 were used to determine its minimum and maximum void ratios. ASTM Standard D422-63 was used for the sieve analysis of Kansas River sand. The grain size distribution is presented in Figure 3.1.

The average friction angle was obtained from the consolidated drained (CD) triaxial test (Figure 3.2 and 3.3) and the large direct shear test (Figure 3.4). The basic properties of Kansas River sand are listed below:

G_s= 2.651

γ_{min}= 16.7 kN/m^3

γ_{max}= 18.77 kN/m^3

e_{min}= 0.384

e_{max}= 0.56

C_u = 2.73

C_c = 0.98

ϕ'= 43.4 °

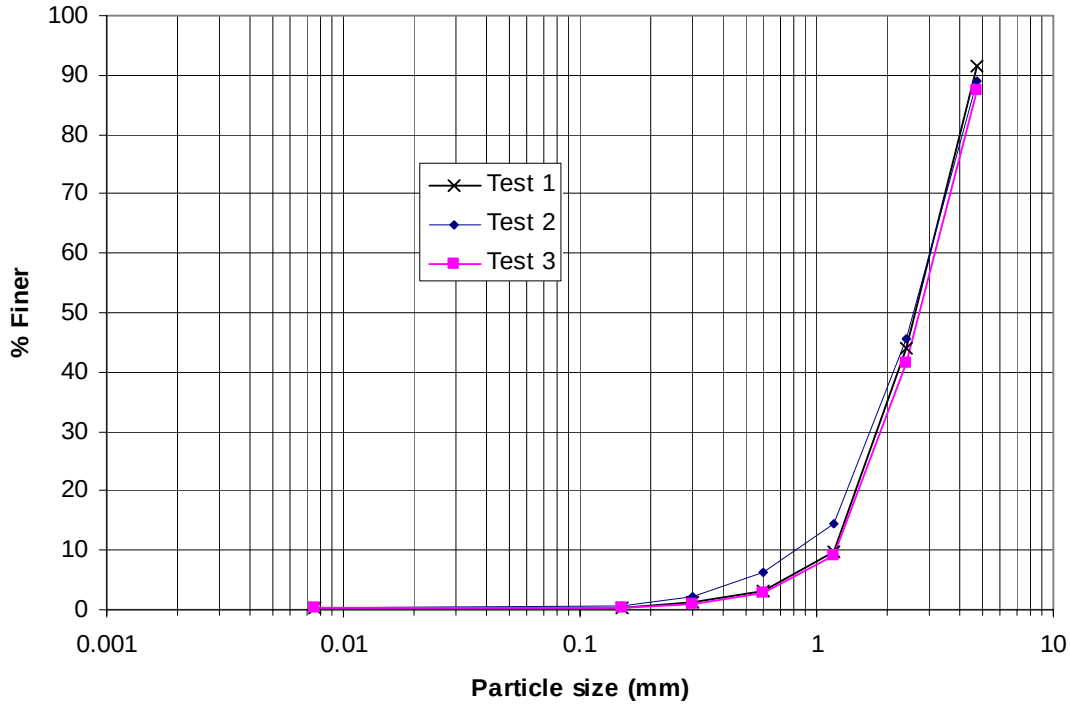

Figure 3.1 Grain size distribution of Kansas River sand

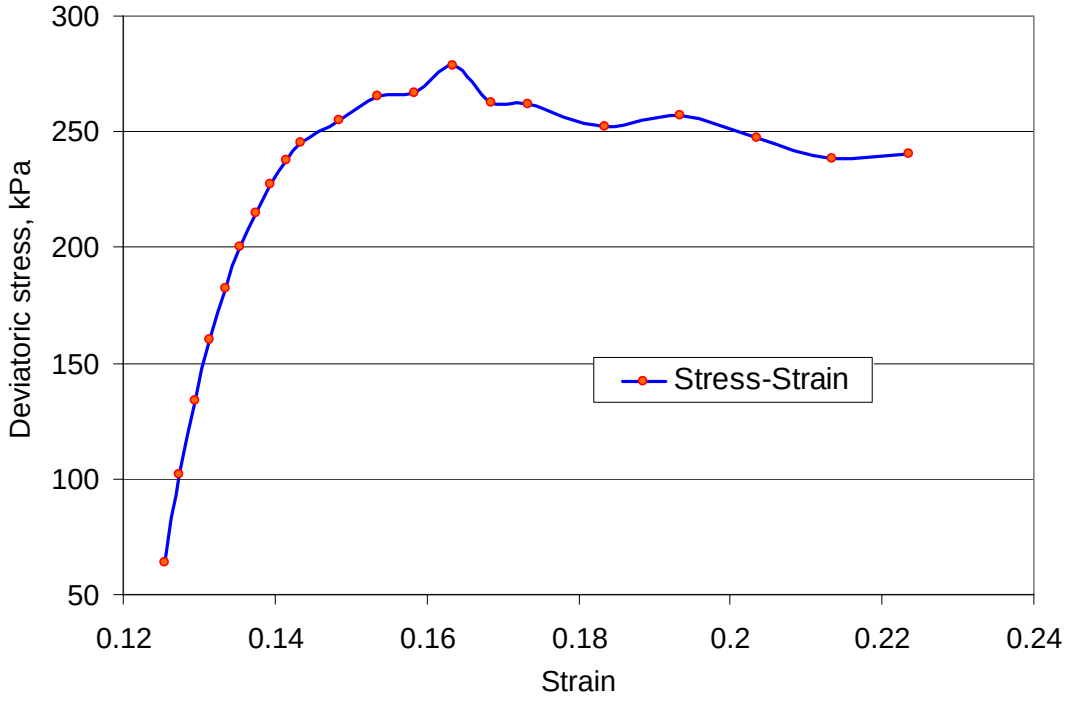

Figure 3.2 CD triaxial test of Kansas River sand

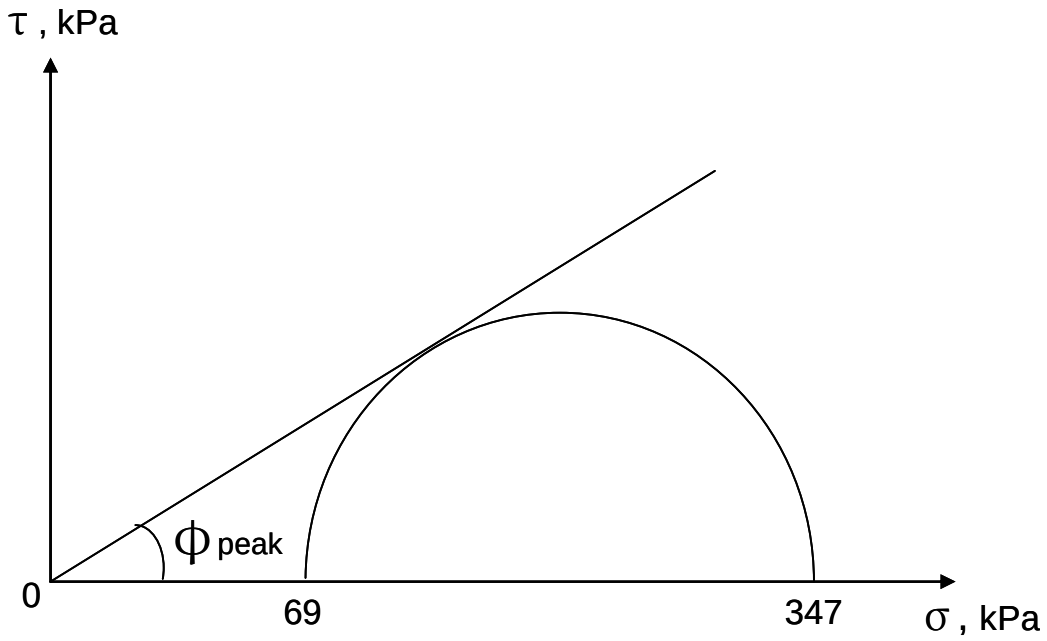

Figure 3.3 Mohr circle from CD test

$$\varphi_{peak} = \sin^{-1}\left(\frac{139}{208}\right) = 42^{\circ}$$

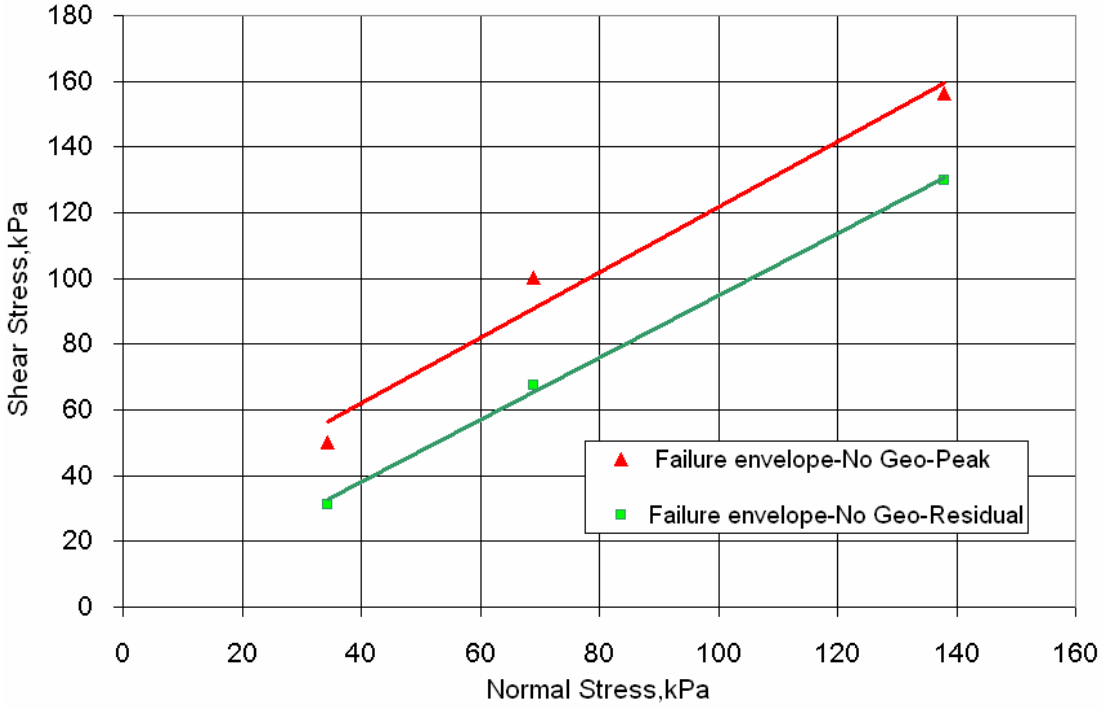

Figure 3.4 Large direct shear test of Kansas River sand

$$\varphi' = \tan^{-1}\left(\frac{160 - 56}{138 - 34}\right) = 45^{\circ}$$

Therefore, Kansas River sand is a poorly graded soil.

3.2.2 AB-3 aggregate

AB-3 is a commonly used base course material in Kansas, which is composed of particles of limestone from a local quarry. It is an angular material. ASTM Standard C127-88 and D5550-94 were used to determine the specific gravity of the soil. ASTM Standards D4254-91 and D4253-93 were used to determine its minimum and maximum unit weight. ASTM Standard D422-63 was used for sieve analysis of the raw material, and the grain size distribution is shown in Figure 3.5. ASTM D5080-93 was used to determine the maximum dry unit weight, and the compact curve is shown in Figure 3.6. ASTM Standard D4318-93 was used to determine the liquid limit and plastic limit (for soil particle passing No.40 sieve). Large direct shear tests (Figure 3.7) were used to determine the friction angle of AB-3. The basic properties of AB-3 course are listed below:

G_s= 2.64

γ_{min}= 17.01 kN/m^3

γ_{max}= 21.64 kN/m^3

C_u= 31.25

C_c= 1.8

LL= 18.6

PL= 14

ϕ '= 52 °

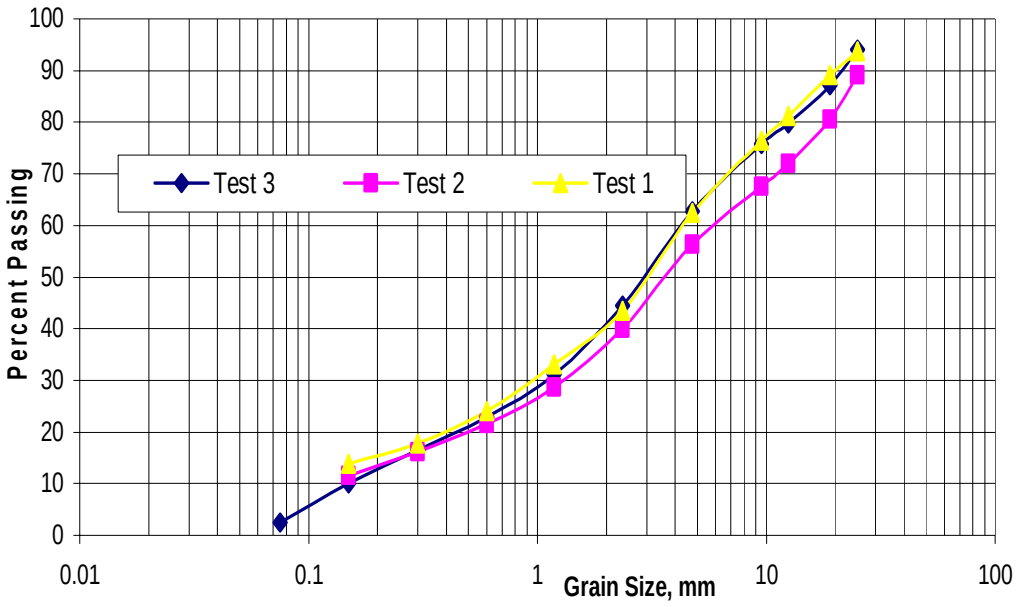

Figure 3.5 Grain size distribution of AB-3 base course

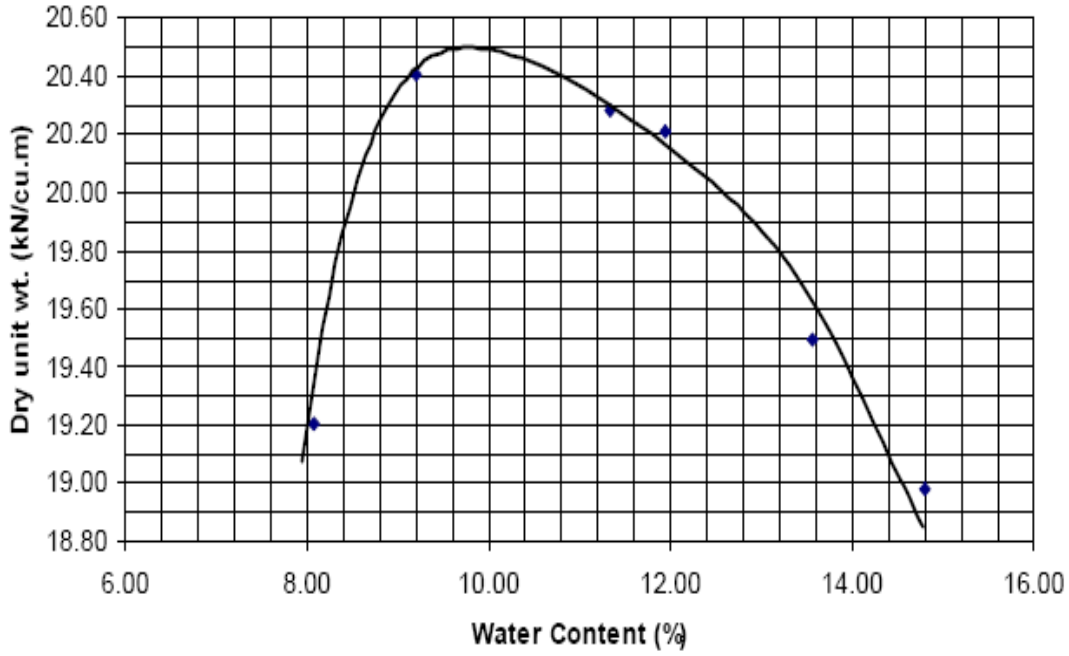

Figure 3.6 Compaction curve of AB3 base course

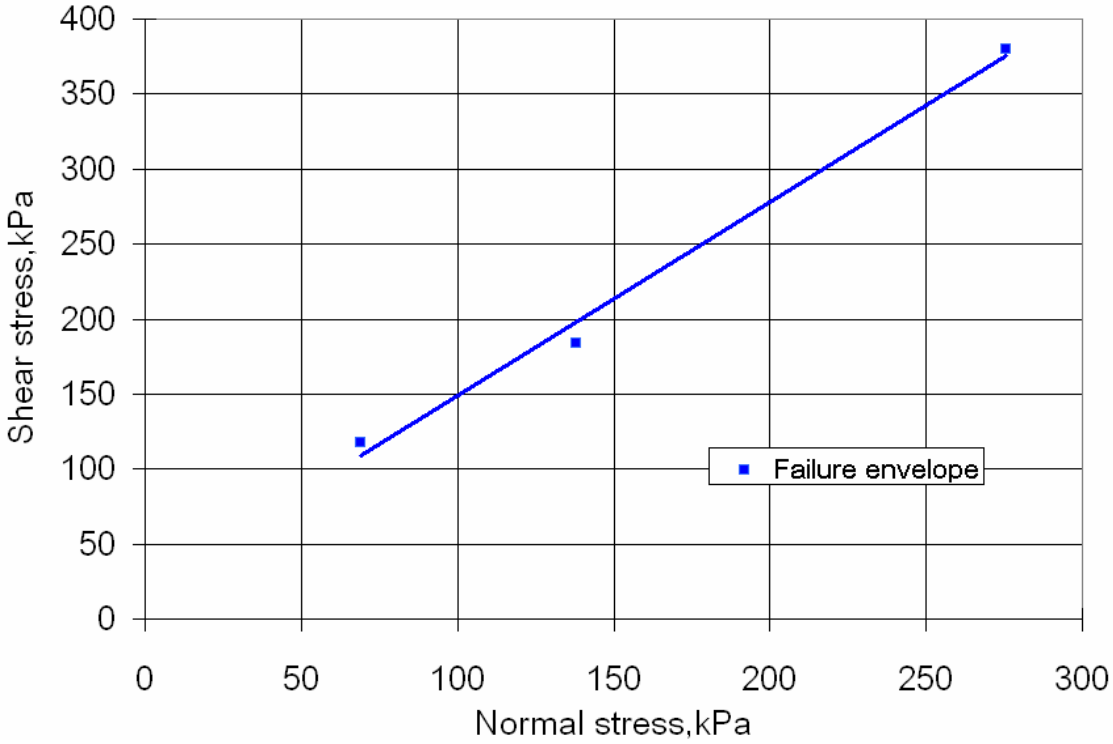

Figure 3.7 Large direct shear test for AB-3 aggregate

$$\varphi' = \tan^{-1}\left(\frac{380 - 118}{276 - 69}\right) = 52^{\circ}$$

Therefore, AB-3 is a well-graded base course material.

As mentioned earlier, one of the cases is that the geosynthetic sheet was placed at 13 mm (0.5 in) below the surface. The grain size distribution curve shows that at least 5% of the particles had the size larger than 13 mm, and the size of some particles was even over 20 mm. These oversized particles made the compaction of the soil above the geosynthetic difficult, therefore, they were removed in this study. The modified grain size distribution of AB-3 aggregates is shown in Figure 3.8.

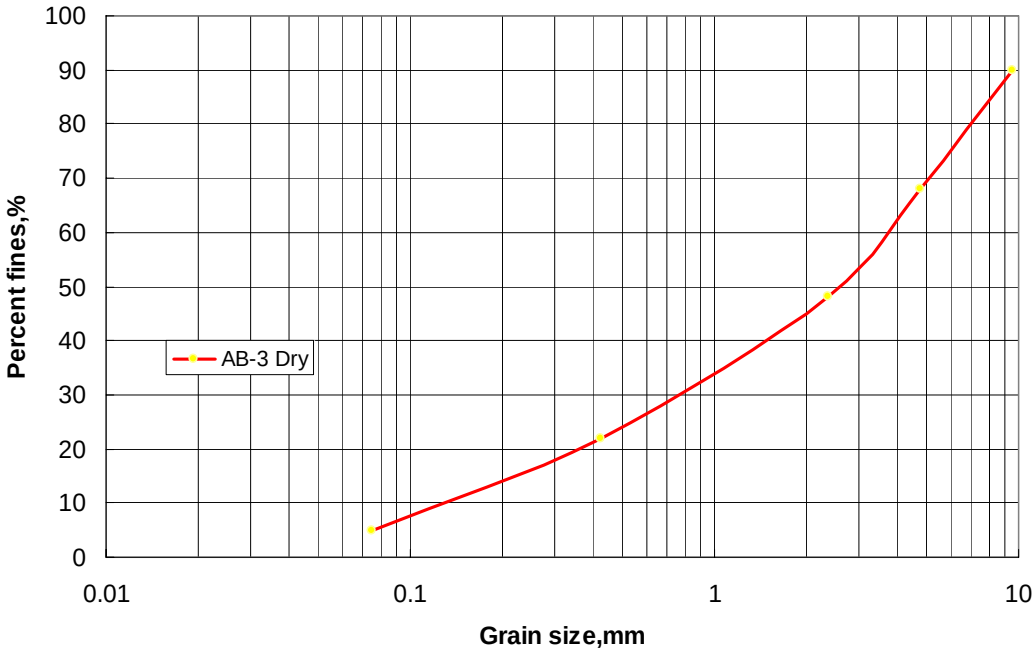

Figure 3.8 Grain size distribution of modified AB-3

3.3 Geosynthetic Types and Properties

Four types of geosynthetics were used in this study: Tensar BX1100, BX1200, BX1500 geogrids and Mirafi HP370 woven geotextile (Figure 3.9). The specifications of BX1100, BX1200 and BX1500 geogrids are provided in Tables 3.1 to 3.3. The specifications of the HP370 geotextile are provided in Table 3.4.

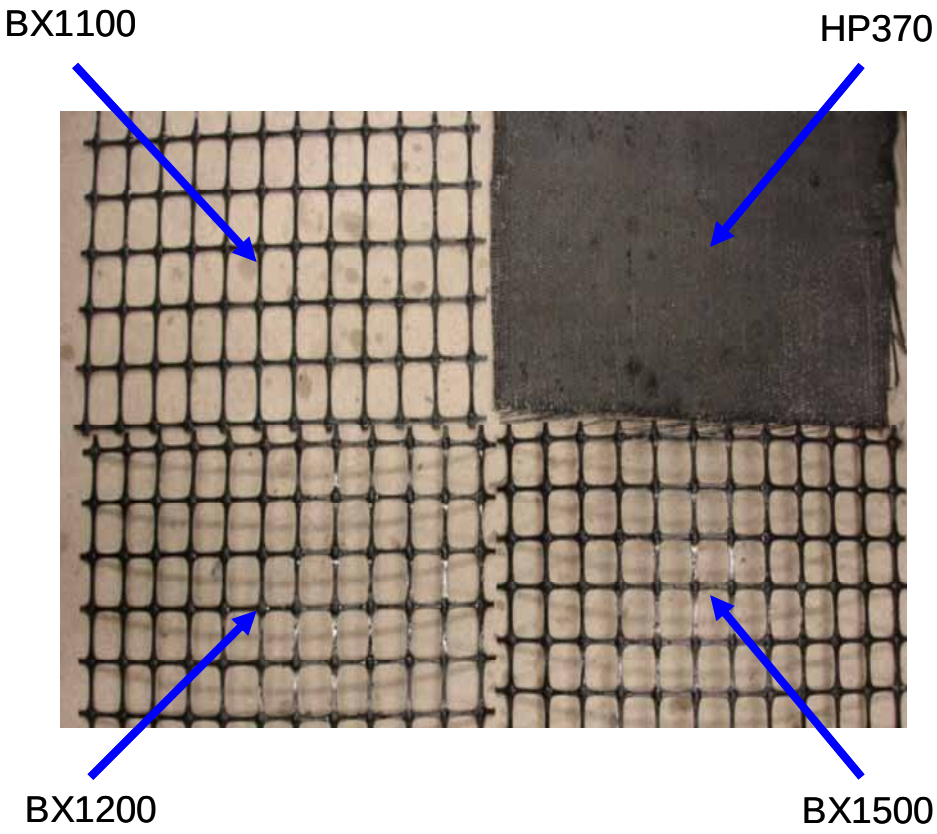

Figure 3.9 Geosynthetics used in this study

Product Type: Punched-drawn Biaxial Geogrid
Polymer: Polypropylene
Load Transfer Mechanism: Positive Mechanical Interlock
Primary Applications: Base Reinforcement and Subgrade Improvement

Product Properties			
Index Properties	**Units**	**MD Values**	**XMD Values**
Aperture Dimensions	mm (in)	25 (1.0)	33 (1.3)
Minimum Rib Thickness	mm (in)	0.76 (0.03)	0.76 (0.03)
Tensile Strength @ 2% Strain	kN/m (lb/ft)	4.1 (280)	6.6 (450)
Tensile Strength @ 5% Strain	kN/m (lb/ft)	8.5 (580)	13.4 (920)
Ultimate Tensile Strength	kN/m (lb/ft)	12.4 (850)	19.0 (1,300)
Structural Integrity			
Junction Efficiency	%	93	
Flexural Stiffness	mg - cm	250,000	
Aperture Stability	m - N/deg	0.32	
Durability			
Resistance to Installation Damage	%SC/%SW/%GP	95/93/90	
Resistance to Long Term Degradation	%	100	
Resistance to UV Degradation	%	100	

Table 3.1 Specifications of BX1100 geogrid (Tensar Earth Technologies, Inc.)

Product Type: Punched-drawn Biaxial Geogrid
Polymer: Polypropylene
Load Transfer Mechanism: Positive Mechanical Interlock
Primary Applications: Base Reinforcement and Subgrade Improvement

Product Properties			
Index Properties	**Units**	**MD Values**	**XMD Values**
Aperture Dimensions	mm (in)	25 (1.0)	33 (1.3)
Minimum Rib Thickness	mm (in)	1.27 (0.05)	1.27 (0.05)
Tensile Strength @ 2% Strain	kN/m (lb/ft)	6.0 (410)	9.0 (620)
Tensile Strength @ 5% Strain	kN/m (lb/ft)	11.8 (810)	19.6 (1,340)
Ultimate Tensile Strength	kN/m (lb/ft)	19.2 (1,310)	28.8 (1,970)
Structural Integrity			
Junction Efficiency	%	93	
Flexural Stiffness	mg - cm	750,000	
Aperture Stability	m - N/deg	0.65	
Durability			
Resistance to Installation Damage	%SC/%SW/%GP	95/93/90	
Resistance to Long Term Degradation	%	100	
Resistance to UV Degradation	%	100	

Table 3.2 Specifications of BX1200 geogrid (Tensar Earth Technologies, Inc.)

Product Type: Punched-drawn Biaxial Geogrid
Polymer: Polypropylene
Load Transfer Mechanism: Positive Mechanical Interlock
Primary Applications: Base Reinforcement and Subgrade Improvement

Product Properties			
Index Properties	**Units**	**MD Values**	**XMD Values**
Aperture Dimensions	mm (in)	25 (1.0)	30.5 (1.2)
Minimum Rib Thickness	mm (in)	1.78 (0.07)	1.78 (0.07)
Tensile Strength @ 2% Strain	kN/m (lb/ft)	8.5 (580)	10.0 (690)
Tensile Strength @ 5% Strain	kN/m (lb/ft)	17.5 (1,200)	20.0 (1,370)
Ultimate Tensile Strength	kN/m (lb/ft)	27.0 (1,850)	30.0 (2,050)
Structural Integrity			
Junction Efficiency	%	93	
Flexural Stiffness	mg - cm	2,000,000	
Aperture Stability	m - N/deg	0.75	
Durability			
Resistance to Installation Damage	%SC/%SW/%GP	95/93/90	
Resistance to Long Term Degradation	%	100	
Resistance to UV Degradation	%	100	

Table 3.3 Specifications of BX1500 geogrid (Tensar Earth Technologies, Inc.)

Mechanical Properties	Test Method	Unit	Minimum Average Roll Value	
			MD	CD
Tensile Strength (at ultimate)	ASTM D 4595	kN/m (lbs/ft)	47.3 (3240)	39.4 (2700)
Tensile Strength (at 2% strain)	ASTM D 4595	kN/m (lbs/ft)	7.9 (540)	7.9 (540)
Tensile Strength (at 5% strain)	ASTM D 4595	kN/m (lbs/ft)	19.8 (1356)	22.8 (1560)
Tensile Strength (at 10% strain)	ASTM D 4595	kN/m (lbs/ft)	35.0 (2400)	35.0 (2400)
Factory Seam Strength	ASTM D 4884	kN/m (lbs/ft)	24.6 (1688)	
Flow Rate	ASTM D 4491	l/min/m2 (gal/min/ft2)	1629 (40)	
Permeability	ASTM D 4491	cm/sec	0.050	
Permittivity	ASTM D 4491	sec-1	0.52	
Apparent Opening Size (AOS)	ASTM D 4751	mm (U.S. Sieve)	0.600 (30)	
UV Resistance (at 500 hours)	ASTM D 4355	% strength retained	70	

Table 3.4 Specifications of HP370 woven geotextile (Tencate Mirafi)

Physical Properties	Test Method	Unit	Typical Value
Mass/Unit Area	ASTM D 5261	g/m2 (oz/yd2)	284 (8.5)
Roll Dimensions (width╳ length)	ASTM D 5261	m (ft)	4.5 (15) ╳ 91 (300)
Roll Area	ASTM D 5261	m2 (yd2)	418 (500)
Estimated Roll Weight	ASTM D 5261	kg (lbs)	121 (266)

Table 3.4 Specifications of HP370 woven geotextile (continued, Tencate Mirafi)

3.4 Test equipment

The major facility in this study is the Asphalt Pavement Analyzer (APA) (Figure 3.10), which is a multifunctional Loaded Wheel Tester used for evaluating permanent deformation (rutting), fatigue cracking, and moisture susceptibility of both hot and cold asphalt mixes. This machine is available at most DOTs in the U.S.

Figure 3.10 Asphalt Pavement Analyzer (APA)

3.4.1 Specifications

This APA machine was manufactured by Pavement Technology Inc., (PTI) Covington, GA. It is 2.03 m (6.5 ft) long, 0.9 m (2.9 ft) wide, and 1.78 m (5.7 ft) high. The total weight is 1358.4 kg (3000 lb). It features retractable legs with wheels to make it portable and anchored while in use. Importantly, although the air consumption is low, the minimum pressure of 827.4 kPa (120 psi) is critical to maintain the adequate hose inflation. Since the machine is normally operated from the front, a space of one meter in the front of the APA should be adequate for the operation, and a space of one meter is also needed on both sides of the machine to access the service door. Manual and automatic modes can be used. The measurement can be recorded in a personal

computer when an automatic mode is used.

3.4.2 Parts of the APA

This section briefly discusses the major parts of the APA machine.

Wheel tracking/loading system

The APA is designed to simulate a rolling wheel condition by rolling three concave metal wheels on three rubber hoses which can provide the pressure ranging from 0 kPa to 827kPa (120 psi) to simulate the effect of tire pressures as shown in Figure 3.11). The rubber hoses are part of a hose rack (Figure 3.12), which can be taken out from the main chamber.

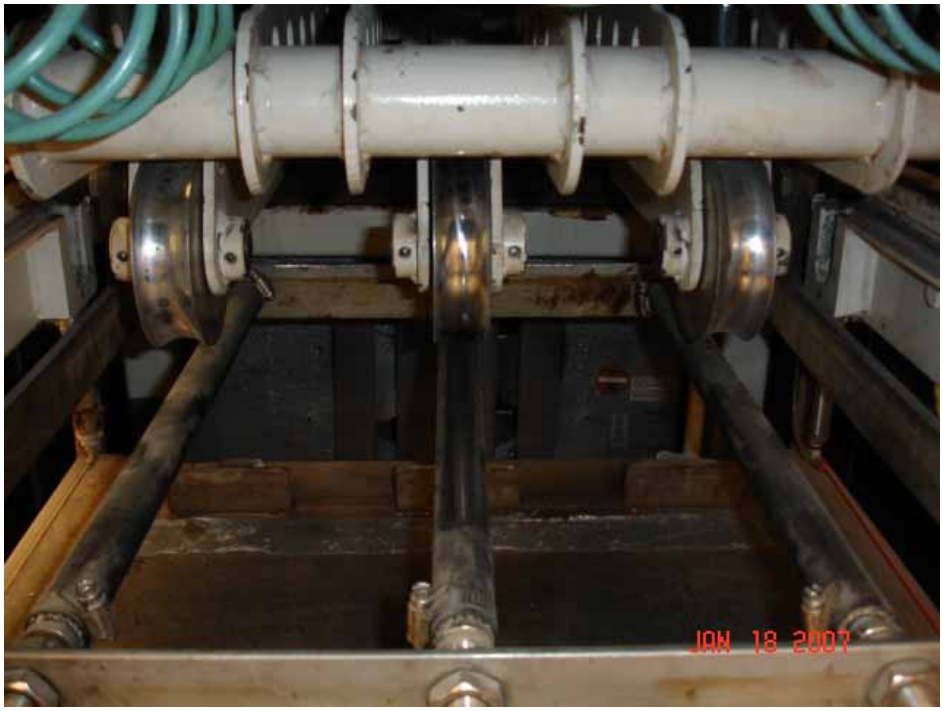

Figure 3.11 Three metal wheels on three rubber hoses

Figure 3.12 Hose rack

Sample holding assembly

The assembly holds the samples directly underneath the rubber hoses to allow the sample to be subjected to the wheel tracking action during the test. The tractable tray (Figure 3.13) allows the sample to be pulled out of the machine for manual measurements and sample installation. The tray can be locked by two toggle clamps when it is fully pushed. Three different sample molds are typically provided by the manufacturer: cylindrical rut test mold, beam rut test mold, and beam fatigue test mold (Figures 3.14 A to C). Figure 3.15 shows all three original sample molds on the tray, which are used for asphalt mix testing.

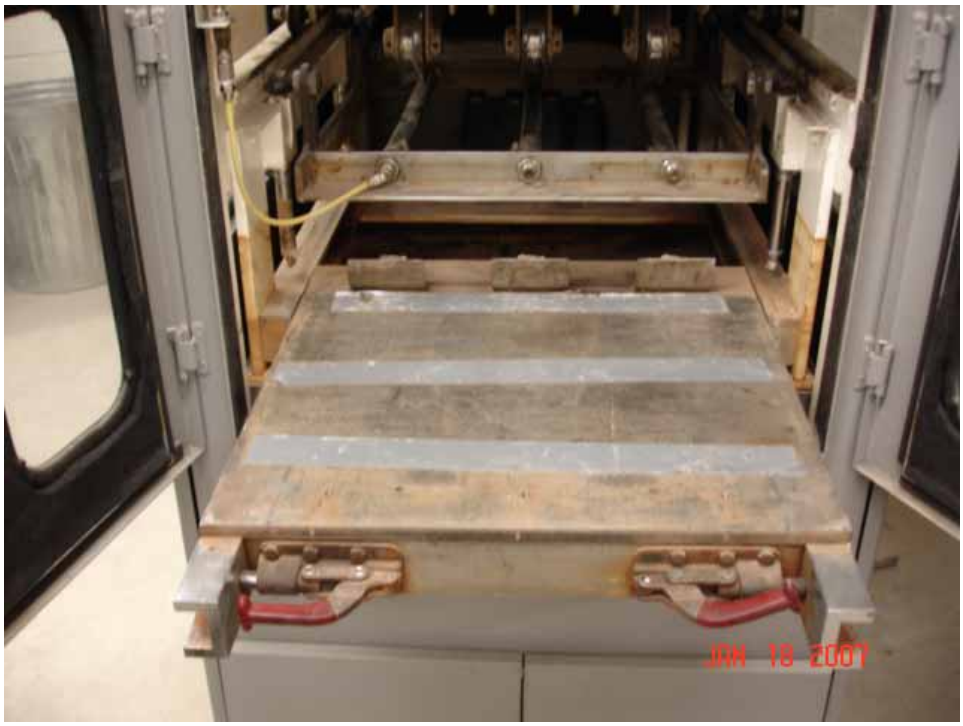

Figure 3.13 Sample tray

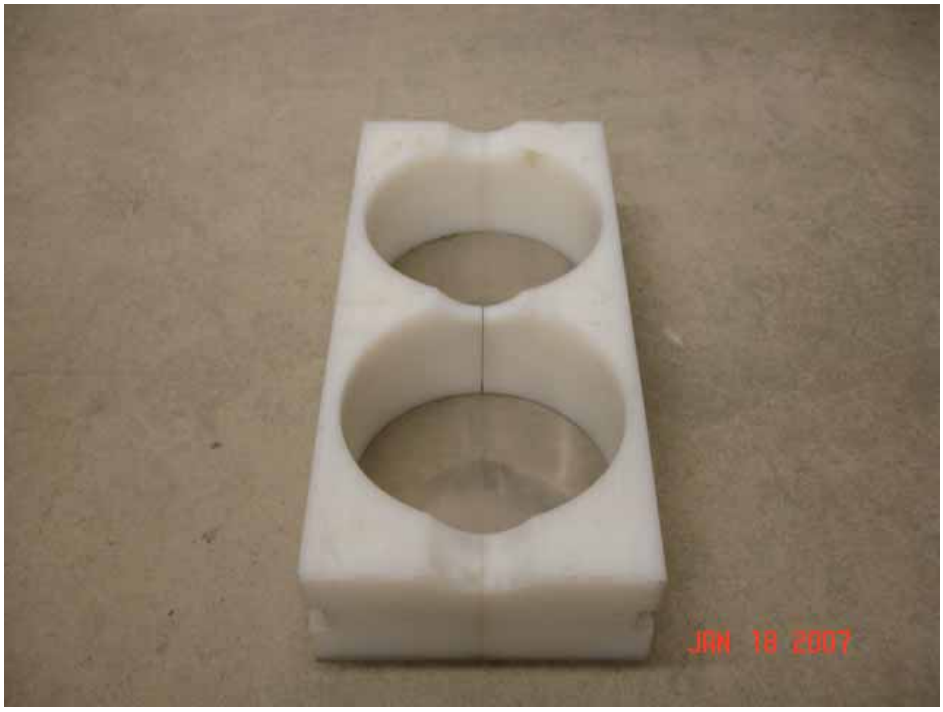

A Cylindrical test mold

B Beam rut test mold

C Beam fatigue test mold

Figure 3.14 Three sample molds

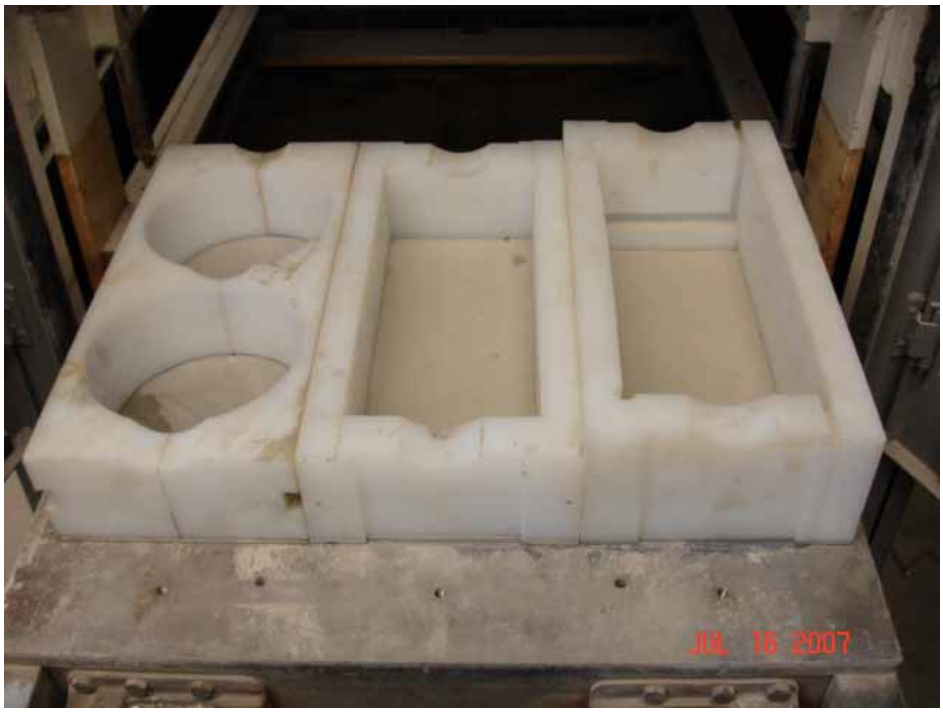

Figure 3.15 Three original test molds on the tray

Temperature control

Heating and cooling of the main chamber are provided by four heat strips, two fans, and a cooling unit, which are regulated by a solid state based temperature controller. In this study, the temperature control was not be used. All the tests were conducted at the room temperature.

Water submerge system

The water submerge system allows the water to cover the test samples in the submerge-in-water tests and automatically drains the water after completing the test before the tray is pulled out. All the tests in this study were not involved in the submerge-in-water situation.

Sample temperature conditioning shelf

The shelf is located inside the lower front doors. It allows the heat conditioning of extra beams or cylinders.

Air regulator

This system consists of an air inlet regulator controlling the maximum air pressure to the APA containing a water separator, the electronic regulator controlling the hose pressure, the left, middle, and right wheel cylinder regulators, and the pressure booster regulator doubling the incoming air pressure.

Operating controls

The APA is controlled by a PLC (Programmable Logic Computer). The control panel is shown in Figure 3.16.

Figure 3.16 Control panel of APA

3.4.3 Calibration

The following items should be calibrated no less than once per year: (1) the wheel load, (2) DAS Calibration of the Automated Vertical Measuring System, (3) the chamber temperature, and (4) the hose pressure. Instructions for each of these calibration procedures are included in this section. Load cell (Figure 3.17) was used to calibrate the wheel load, which was very important in this study because the tests were conducted under different wheel loads. The calibration of the load cell followed the following steps:

Figure 3.17 Load cell for calibration

1. Remove the hose rack.

2. Connect the load cell to the load cell meter located on the APA front panel. Turn on the meter using the toggle switch and zero the load cell by pressing the zero buttons located at the right of the meter.

3. Lower and raise each wheel 20 times by switching to CAL to loosen up the cylinders.

4. DO NOT LOCK the sample tray in place (release the “Red Toggle Clamps). It must be able to move freely during the calibration so that the load cell always rests evenly on the sample tray.

5. Place the load cell on the table under the first wheel.

6. If all three wheels are used during the test, then place two empty specimen molds (turned upside down) under the other two wheels. This setup simulates the loading condition the carriage is under during the test.

7. Lower the wheels by switching each one to CAL.

8. If adjustment needs to be made, raise the wheel that is being calibrated and turn the regulator up or down. (The other two wheels should be left in the down position.)

9. The final adjustment made to a regulator, should always be in a clockwise direction. The final adjustment should never be made in a counter clockwise direction to avoid a malfunction in the regulator.

10. Lower the wheel and allow the meter to stabilize.

11. All three wheels should be calibrated to within 5 pounds of each other.

12. Repeat steps 5-10 for each wheel.

3.4.4 Data acquisition

Automatic measurement

The APA machine is connected to a computer. Software installed in this computer can automatically perform data acquisition to take the measurements of the rut depth with the number of cycles. The measurements were taken at five different locations along the pressured hose, three of which close to the center were used to calculate permanent deformation of the rut.

Manual measurement

The measurement can also be achieved by using a steel plate and a dial gauge. The steel plate is fitted in the channel of the box, and a dial gauge is placed on the top of the plate to take a measurement (Figure 3.18). It should be noted that there is a unique position for the plate to fit in the channel on the box so that the plate is at the same level for every measurement.

Figure 3.18 Manual measurement

3.5 Modification of test box

A major modification had to be made for the APA test molds especially for this study. The original molds of APA have three separated boxes to hold the asphalt mixes as shown in Figure 3.15, which are not suitable for the confinement tests because the space for samples is very confined. Therefore, a modified test box three times as large as the original one was made to hold the base course materials as shown in Figure 3.19. Given the large space the modified test box can provide, the geosynthetic sheet can be placed within the soil as shown in Figure 3.20.

Figure 3.19 Modified test box

Figure 3.20 Geosynthetics in soil

Design of test box

According to the sizes of original sample molds and the tray, the modified box was determined to have the dimension shown in Figure 20. The worst case for the box is that three hoses are under three wheel loads at the same time as shown in Figure 21. This load condition was used in the design of the box.

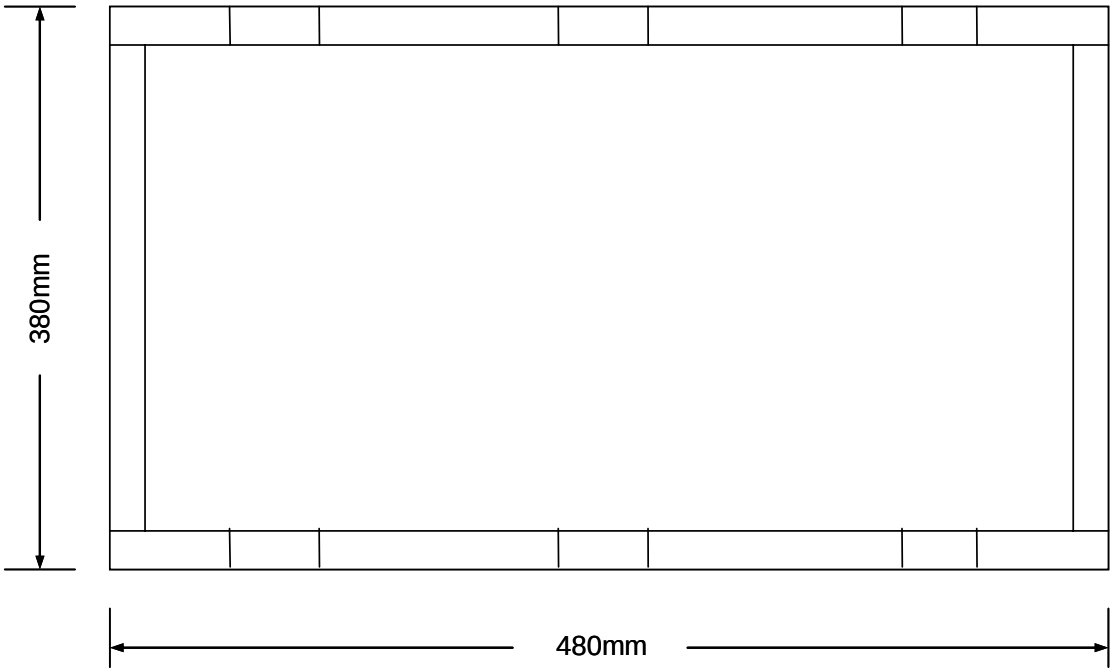

Depth= 100 mm

Figure 3.21 Dimension of the modified box

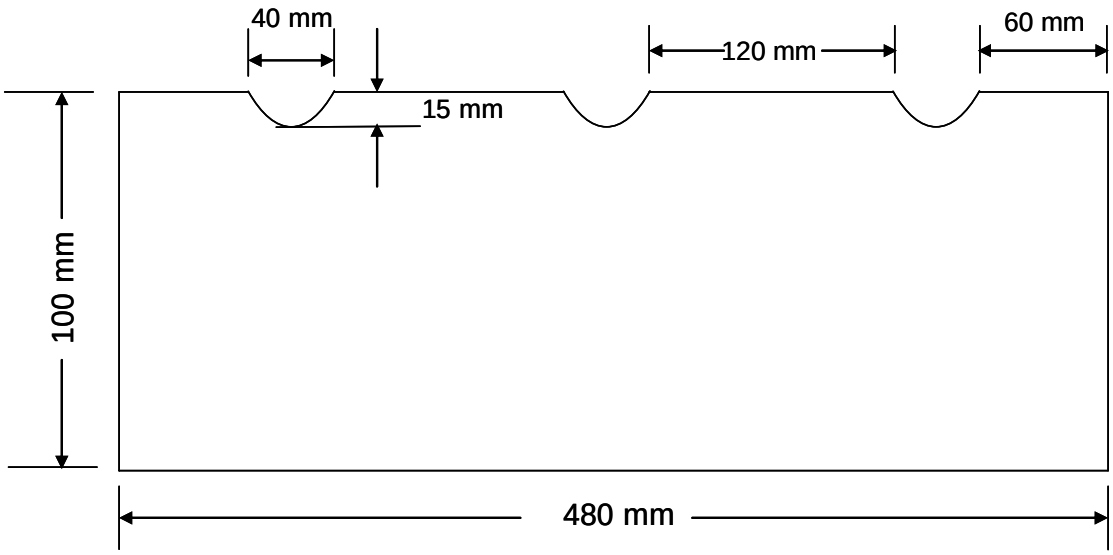

Figure 3.21 Dimension of the modified box (continued)

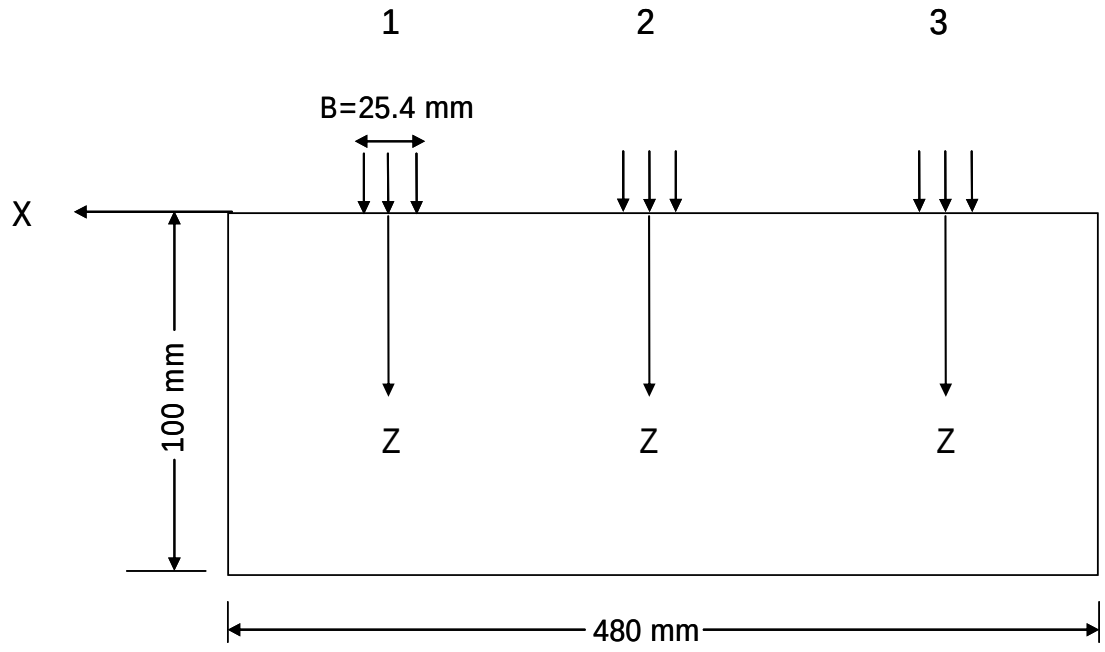

Figure 3.22 Cross section of the box under three wheel loads

Stresses on 480 mm side

In order to know the largest stress the side member may carry, the Boussinesq (1885) solution for the strip load near a retaining wall as shown in Figure 3.23 was used for the calculations. The basic solution for a uniform vertical load is shown in Equation (3.1).

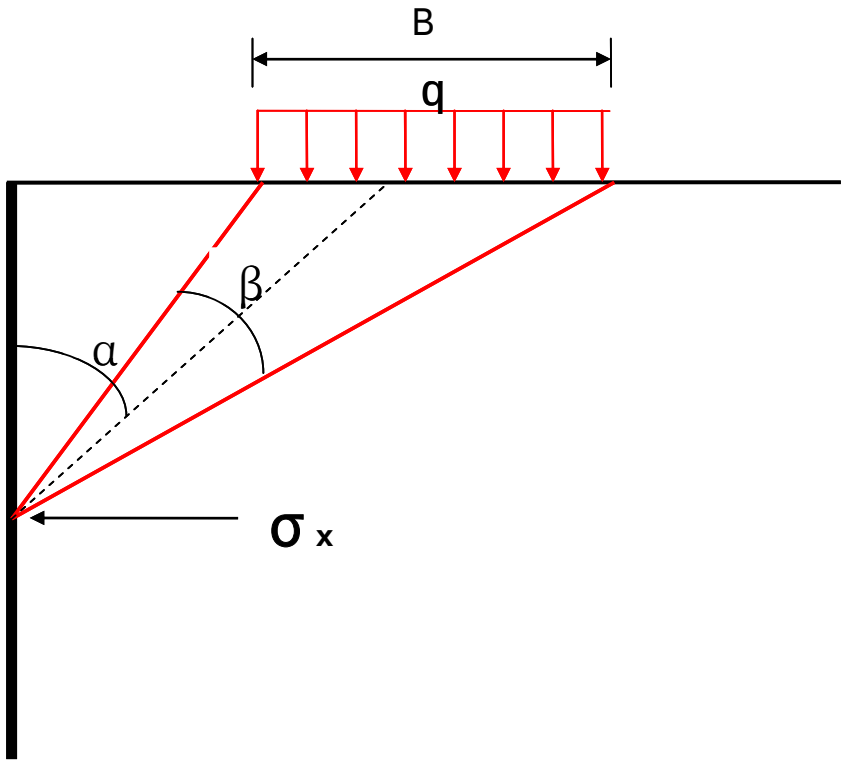

Figure 3.23 Uniform vertical loads near a retaining wall

$$\sigma_x = \frac{2q}{\pi}(\beta - \sin\beta\cos 2\alpha) \qquad (3.1)$$

I. At point 1

where x is 80 mm and b is 25.4 mm

a. z/b= 1

From the geometry, $\alpha = 75.8°$ and $\beta = 3.4°$. From Equation (3.1), the following ratio can be calculated:

$\sigma_x/q = 2.2$

b. z/b= 1.25

$\alpha = 72.5°$, $\beta = 5°$

$\sigma_x/q = 3.23$

c. z/b= 1.5

$\alpha = 69.2°$, $\beta = 4.8°$

$\sigma_x/q = 3.1$

The vertical stress contour under a strip load as shown in Figure 3.24 was used to determine the maximum vertical stress. Then the maximum horizontal stress was calculated using this relationship $\sigma_x =$

$K_o \sigma_z$, where K_o is the lateral earth pressure coefficient at rest. From the calculation of three depths under point 1, the maximum lateral stress was at the depth of approximately 31.8 mm below the surface.

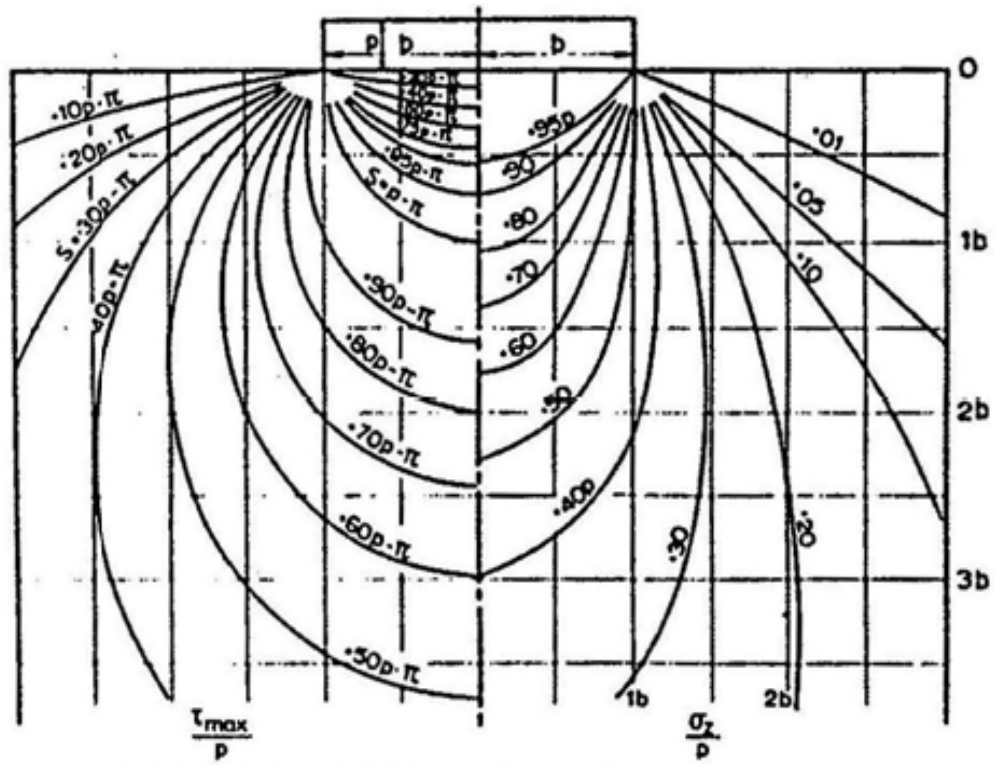

Figure 3.24 Stress below a strip load (Jurgenson, 1934)

The same method was applied to the calculations of the maximum lateral stresses at points 2 and 3.

II. At point 2

where x is 240 mm and b is 25.4 mm

a. z/b= 1

$\alpha = 84.8^\circ$, $\beta = 0.47^\circ$

$\sigma_x/q = 0.3$

b. z/b= 1.25

$\alpha = 83.5^\circ$, $\beta = 1^\circ$

$\sigma_x/q = 0.65$

c. z/b= 1.5

$\alpha = 82.22°$, $\beta = 0.7°$

$\sigma_x/q = 0.45$

III. At point 3

where x is 400 mm and b is 25.4 mm

a. z/b= 0.75

$\alpha = 87.62°$, $\beta = 0.13°$

$\sigma_x/q = 0.084$

b. z/b= 1

$\alpha = 86.82°$, $\beta = 0.176°$

$\sigma_x/q = 0.114$

c. z/b= 1.25

$\alpha = 86.1°$, $\beta = 0.13°$

$\sigma_x/q = 0.084$

From the calculations of the three points shown above, the depths of the maximum stresses were determined at 31.8 mm, 31.8 mm, and 25.4 mm at locations 1, 2, and 3, respectively.

In order to get a conservative design, the total maximum lateral stress was calculated by summing the above three maximum stresses. Assume the maximum hose pressure used for the APA is 552 kPa (80psi), then,

$$\sum \sigma_x = q(3.23 + 0.65 + 0.114) \approx 552 * 4 = 2208 kPa$$

Stresses on 380 mm side

The method included in the book *Elastic Solutions for Soil and Rock Mechanics* by Poulos and Davis (1974) was used. The basic solution is shown in Figure 3.25 and Equation (3.2).

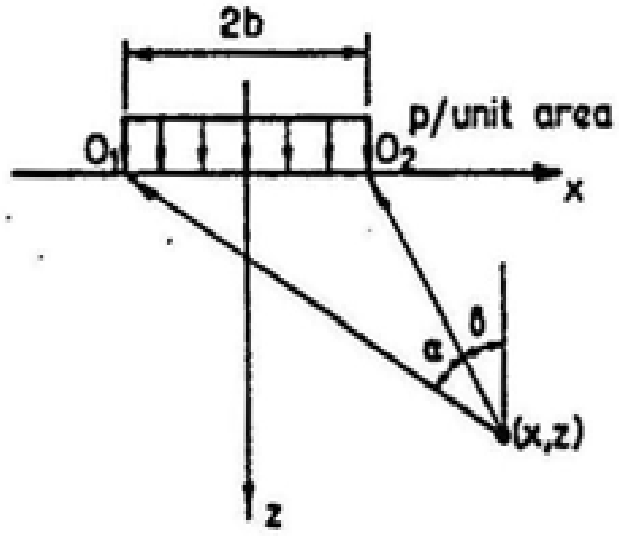

Figure 3.25 Uniform vertical loading

$$\sigma_y = \frac{2p}{\pi} \nu \alpha \quad \text{.....} \quad (3.2)$$

where ν is the Poisson ratio of soil.

The vertical maximum stress occurs when $\alpha = 2\pi$, i.e.:

$$\sigma_y = \frac{2p}{\pi}\nu\alpha = 4p\nu = 4*552*0.3 = 662.4kPa$$

As shown in Figure 3.26, the stress on the 480 mm side can not be added up as that on the 380 mm side because they affect the box side at different locations. Stresses at points 1, 2, and 3 have to be considered independently.

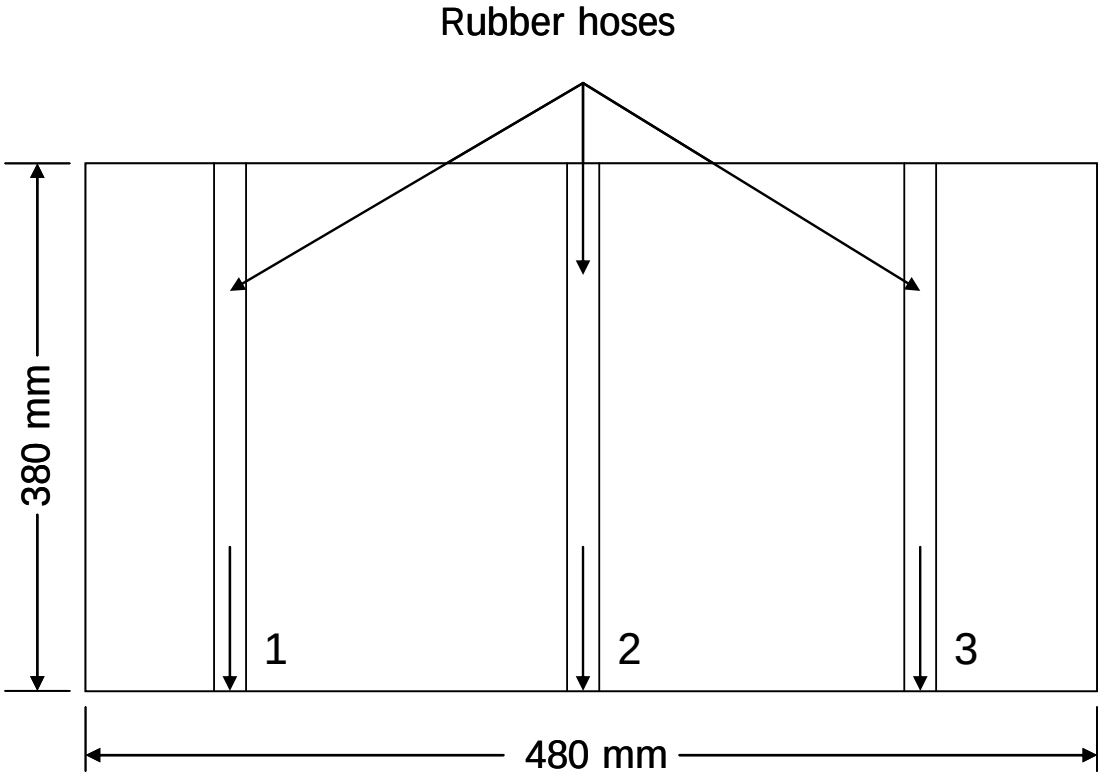

Figure 3.26 Stresses on 480 mm side

Deformation of the two sides

For a conservative design, the classical beam theory was used to calculate the deflection of the walls of the box. The aluminum with the elastic modulus of 7×10^7 kPa (10^7 psi) was selected as the material to build the box.

Use the aluminum thickness of 13 mm, the maximum deflection along the 380 mm side of the box can be calculated as:

$$I = \frac{bh^3}{12} = \frac{100*13^3}{12} = 18308\,mm^4$$

$$\Delta = \frac{PL^3}{48EI} = \frac{2208*380^3}{48*7*10^7*18308} = 0.002\,mm$$

Use the aluminum thickness of 13 mm, the maximum deflection along the 480 mm side of the box can be calculated as:

$$I = \frac{bh^3}{12} = \frac{100*13^3}{12} = 18308\,mm^4$$

$$f_{22} = \frac{pL^3}{48\,EI} = \frac{662.4*480^3}{48*7*10^7*18308} = 0.002\ mm$$

$$f_{12} = \frac{pa}{48EI}\left(3L^2 - 4a^2\right) = \frac{662.4*80}{48*7*10^7*18308}\left(3*480^2 - 4*80^2\right) = 0.00057mm$$

$$\Sigma\Delta = f_{22} + 2f_{12} = 0.002 + 2*0.00057 = 0.003mm$$

The deformation of the 480 mm side seems to be more critical than the 380 mm side.

However, in the real test, after the sample assembly, the 480 mm side is supported by three teeth on both sides as shown in Figure 3.27, exactly at the loading position, which reinforce this side. Therefore, this side is not a problem. The final dimensions of the modified box are shown in Figure 3.28.

Figure 3.27 Three teeth supporting the 480 mm side

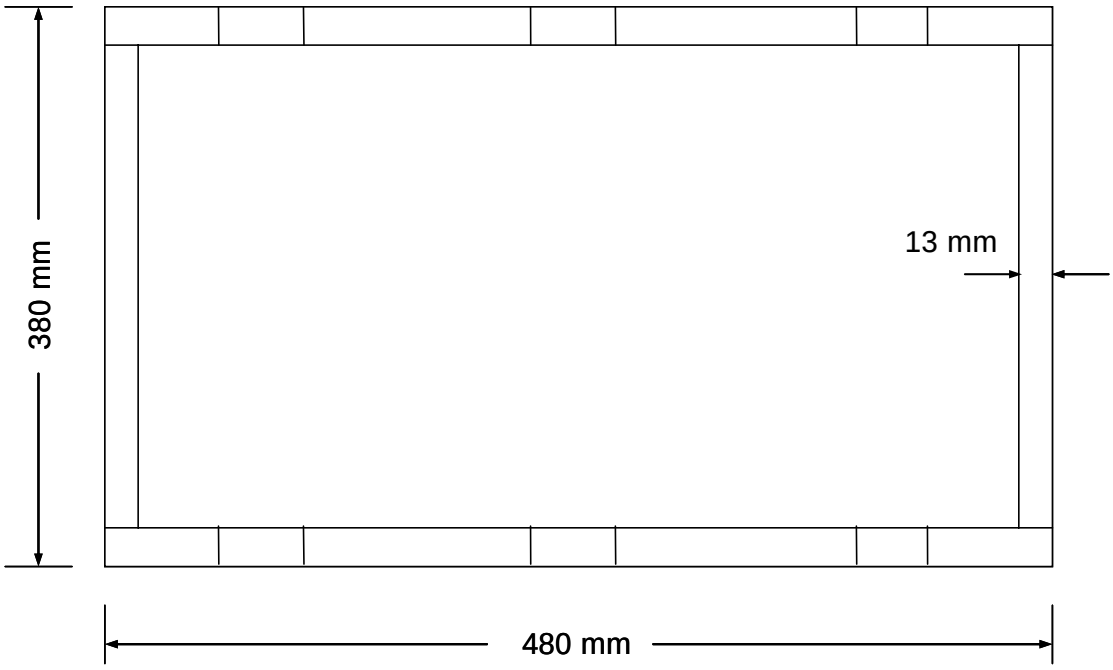

Depth= 100 mm

Figure 3.28 Dimensions of the modified test box

3.6 Test procedures

3.6.1 Sample preparation

Before the confinement test, the soil was compacted to a target density. Considering the relatively large quantity of the soil mass, the soil was placed and compacted in four layers. To control the density of the sample, the soil mass for each layer was measured as calculated. After each layer of soil was filled into the box, compaction was applied by tamping until the soil thickness reached to the desired thickness (the box was marked at different depths). After all the soil layers were filled and compacted, the sample was ready for testing using the APA machine.

Kansas River sand

The relative density of 70% was targeted for the test for Kansas River sand. Based on

the box dimensions as shown in Figure 3.28, the total volume of the sand sample in the box is:

$V=454*354*100= 1.6\times10^7$ mm^3

Based on the property of Kansas River sand,

$$D_r = \frac{e_{max} - e}{e_{max} - e_{min}} = \frac{0.56 - e}{0.56 - 0.384} = 0.7$$, e= 0.4368

$$e = \frac{v_v}{v_s}$$, $V_V=e*V_S=V-V_S$

$1.6\times10^7-V_S= 0.4368V_S$, $V_S= 1.3\times10^7$ mm^3 = 0.013 m^3

$G_S= \gamma_S/ \gamma_W$, $\gamma_S=G_S \gamma_W= 1000*2.651= 2651$ kg/m^3

$W_S=V_S \gamma_S= 0.013*2651= 34$ kg

The total weight of the sand needed for 70% density was 34 kg, which means 8.5 kg for each layer.

AB-3 aggregate

The relative density of 70% was also targeted for AB-3 aggregate. The total volume of the box is $V=1.6\times10^7$ mm^3= 0.016 m^3.

Based on the properties of AB-3,

$$D_r = \left(\frac{\gamma_d - \gamma_{d\,\min}}{\gamma_{d\,\max} - \gamma_{d\,\min}} \right) \frac{\gamma_{d\,\max}}{\gamma_d} = \left(\frac{\gamma_d - 17.011}{21.64 - 17.011} \right) \frac{21.64}{\gamma_d}$$

$\gamma_d = 20.007\ kN/m^3$ (about 97% of the maximum dry unit weight from compaction test, see Figure 3.6)

$$W_s = V * \gamma_d = 0.016 * 20.007 * 1000 / 9.8 = 34 kg$$

The total weight of the AB-3 aggregate needed for 70% relative density was 34 kg, which means 8.5 kg for each layer.

3.6.2 Surcharge

Kansas River sand was tested with and without surcharge. The surcharge was applied by placing the steel bars on the surface of the soil sample as shown in Figure 3.29 to simulate the overburden stresses in the base course under pavement structures. The magnitude of the surcharge was 2.9 kPa.

Figure 3.29 Surcharge

3.6.3 Wheel load and hose pressure

The wheel loads used for tests with Kansas River sand were 44 N (10 lb) and 88 N (20 lb) and the corresponding hose pressures were 69 kPa (10 psi) and 138 kPa (20 psi). The wheel load used for tests with AB-3 course was 353 N (80 lb) and the corresponding hose pressure was 552 kPa (80 psi).

3.6.4 Data acquisition

Both manual and automatic measurements were used for tests with Kansas River sand but only manual measurement was used for tests with AB-3. For tests with Kansas River sand, only the middle wheel was used for loading and only the rut depth under the middle wheel was measured. The final rut depth was the average value of three rut depths measured in the middle portion. For tests with AB-3 course, all the three wheels were used for loading and the rut depths were measured under all three wheels in order to get more accurate results. For AB-3 tests, the final rut depth was the

average value of nine rut depths measured close to the middle portions under three pressure hoses.

Chapter 4 TEST RESULTS AND ANALYSES

4.1 Introduction

The test results obtained from the experimental study are analyzed and discussed in terms of the following aspects: the effect of base material, the effect of surcharge, the effect of geosynthetic types, the traffic benefit ratio, and the rut reduction ratio.

4.2 Repeatability of Test Results

Repeatability tests were conducted in this study to evaluate how repeatable the test results are. Figure 4.1 show the results from one manual test and one automatic test of Kansas River sand without reinforcement. Figure 4.2 shows the results of two manual tests of AB-3 course without reinforcement. Both tests show that the results are reasonably repeatable.

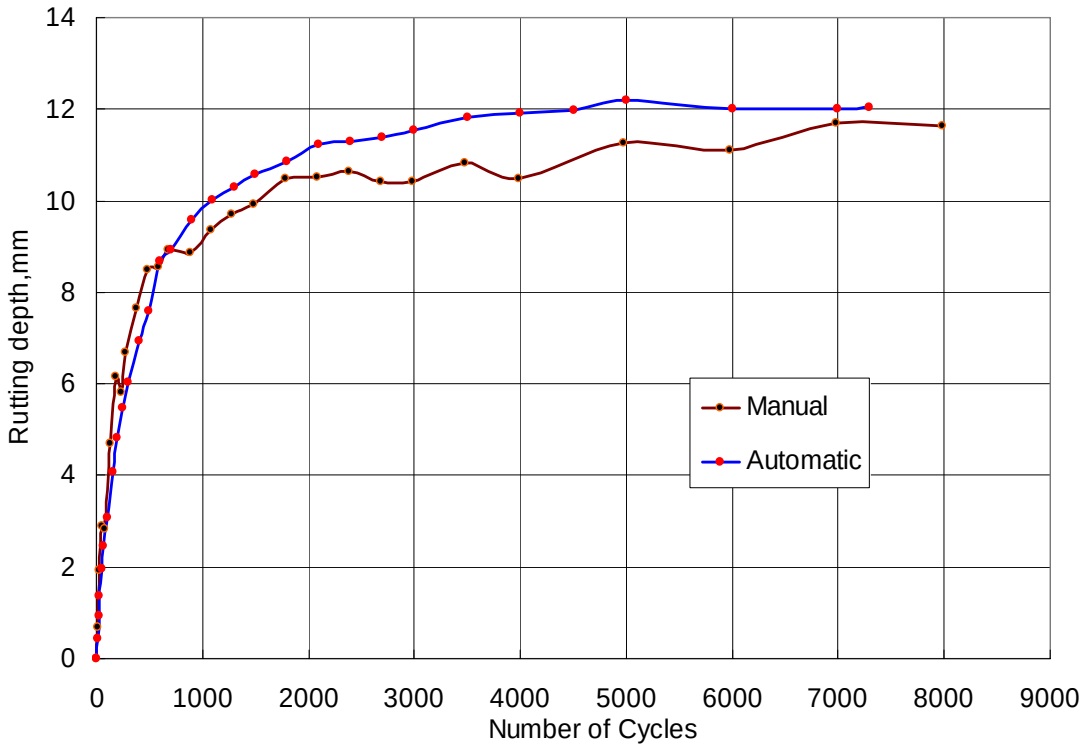

Figure 4.1 Repeatability test of Kansas River sand

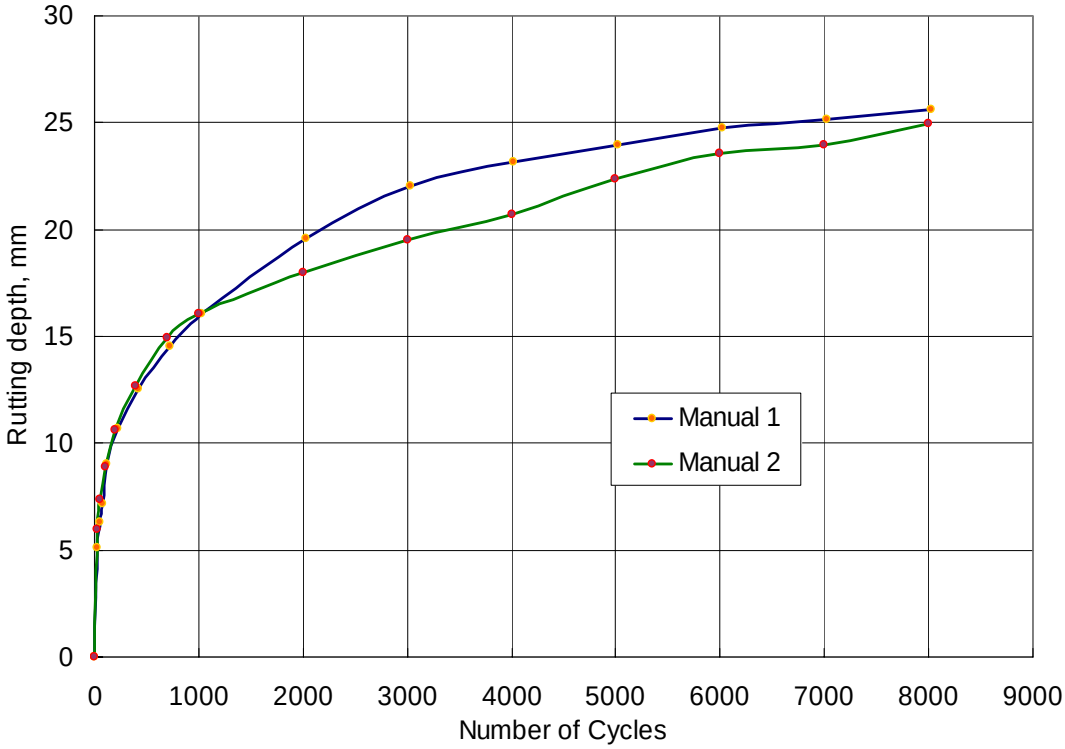

Figure 4.2 Repeatability test of AB-3 aggregate

4.3 Effect of base material

Since Kansas River sand and AB-3 aggregate have different mechanical properties, different load levels and hose pressures were used for testing these two base materials (i.e., 44 N and 88 N loads for Kansas River sand and 353 N loads for AB-3). For comparison purposes, the test results are expressed as the ratio of rut to load with the number of cycles. Figures 4.3 to 4.7 present the rut-load ratio with the number of cycles for these two base materials without reinforcement and with BX1100, BX1200, or BX1500 geogrid, or HP370 geotextile placed at 25 mm below the surface. Figures 4.8 to 4.11 provide the comparisons with the four geosynthetics placed at 13 mm below the surface.

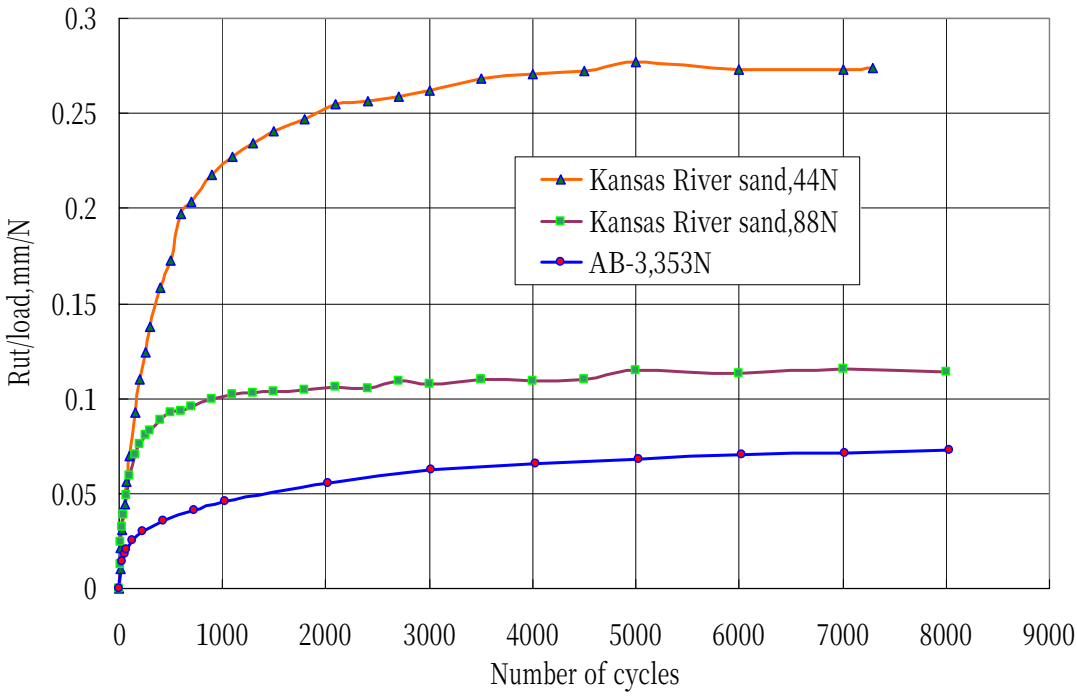

Figure 4.3 Without reinforcement

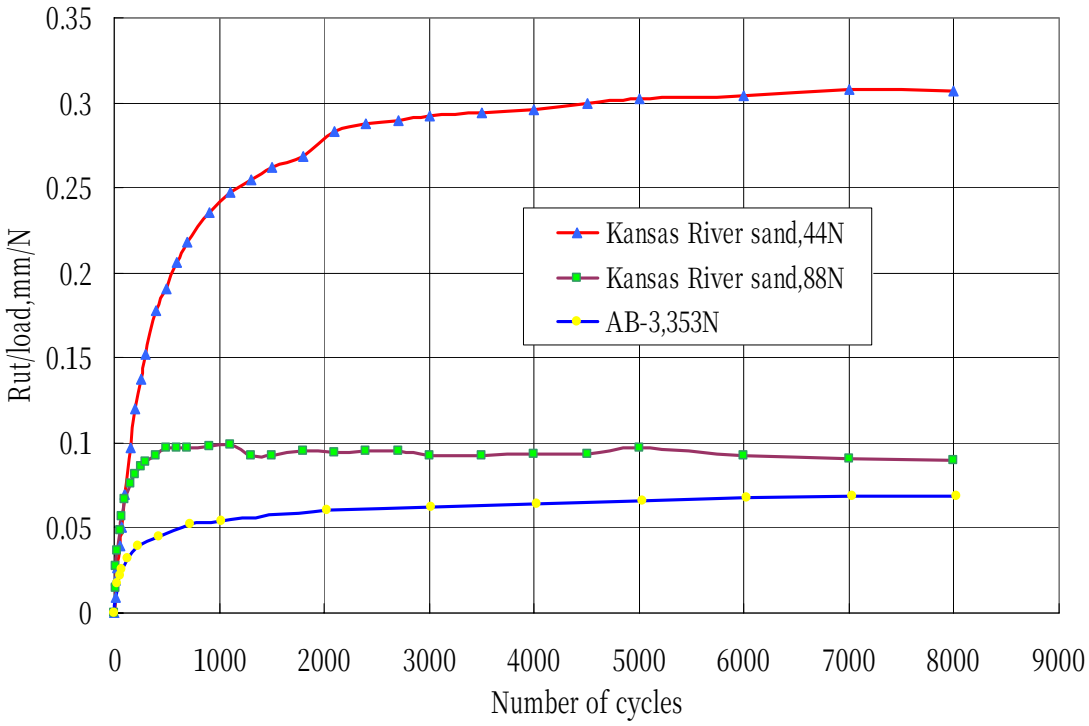

Figure 4.4 BX1100 at 25 mm below the surface

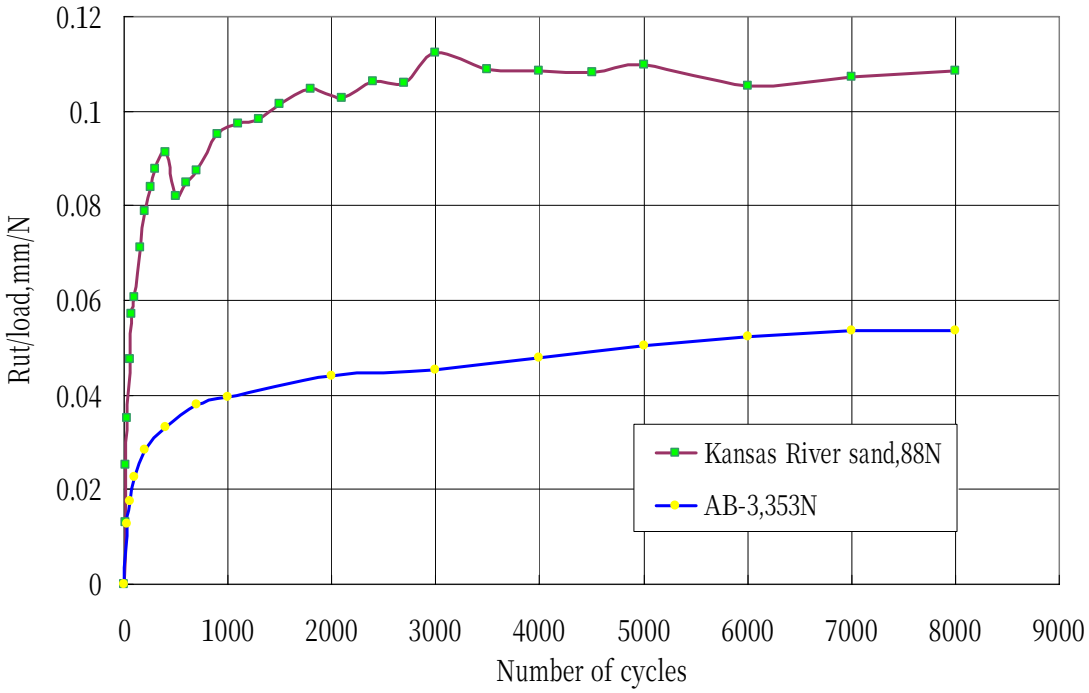

Figure 4.5 BX1200 at 25 mm below the surface

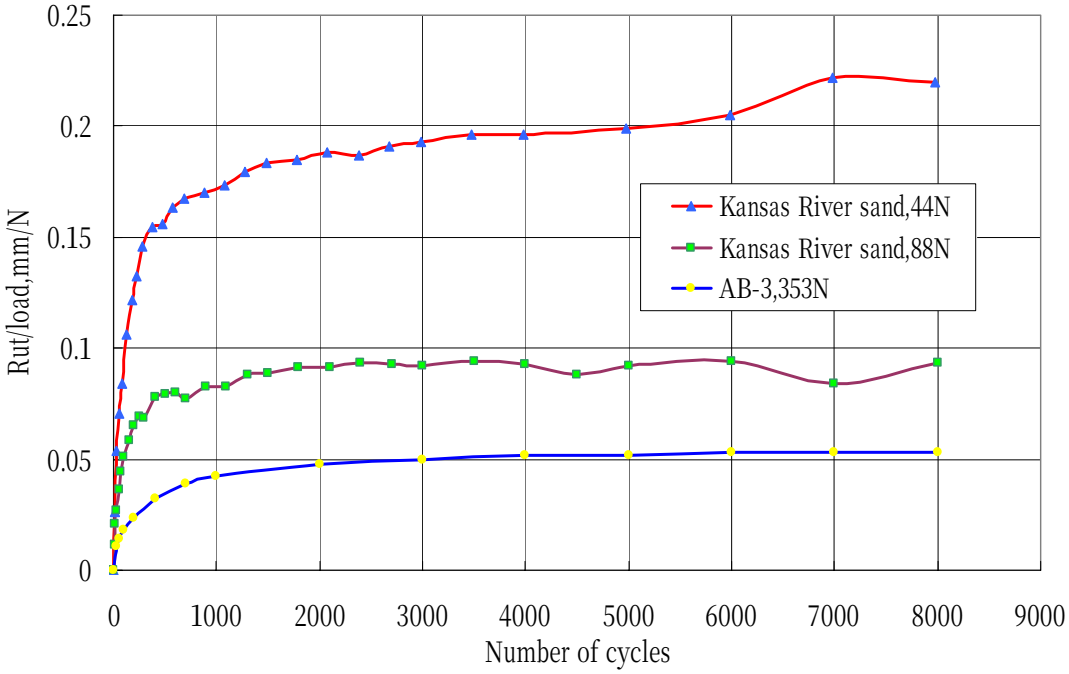

Figure 4.6 BX1500 at 25 mm below the surface

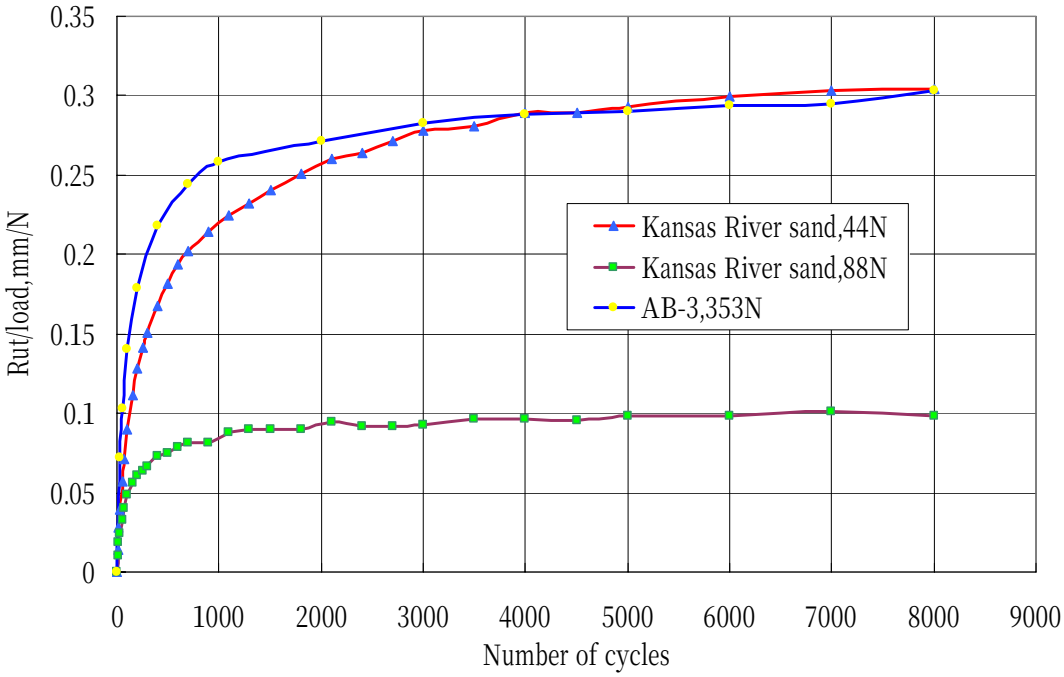

Figure 4.7 Geotextile at 25 mm below the surface

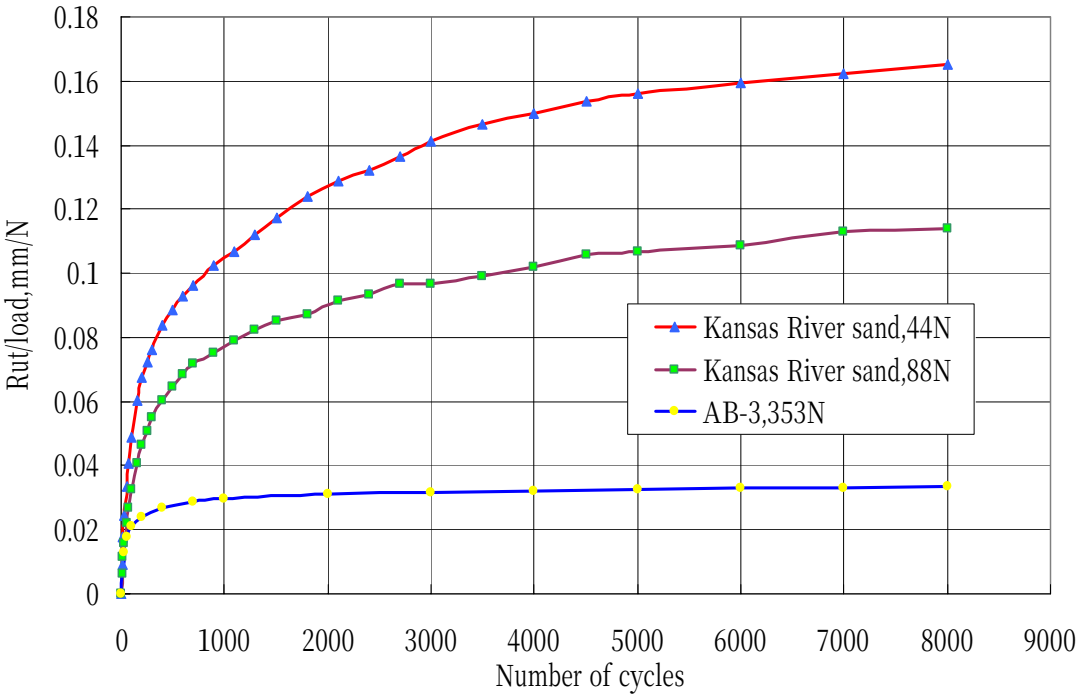

Figure 4.8 BX1100 at 13 mm below the surface

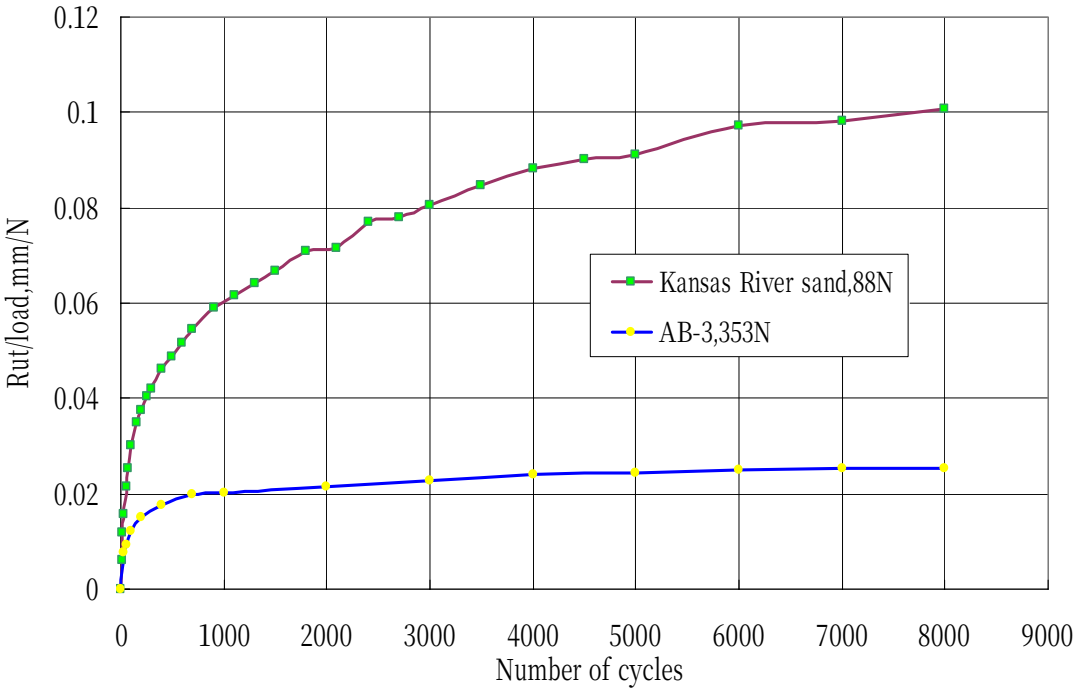

Figure 4.9 BX1200 at 13 mm below the surface

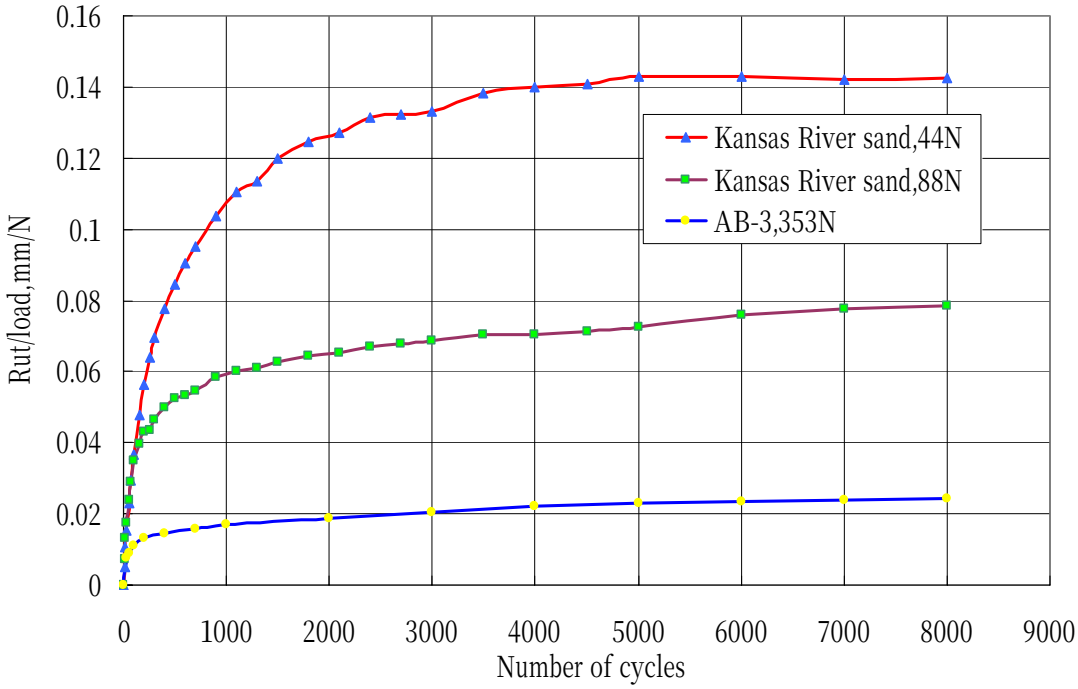

Figure 4.10 BX1500 at 13 mm below the surface

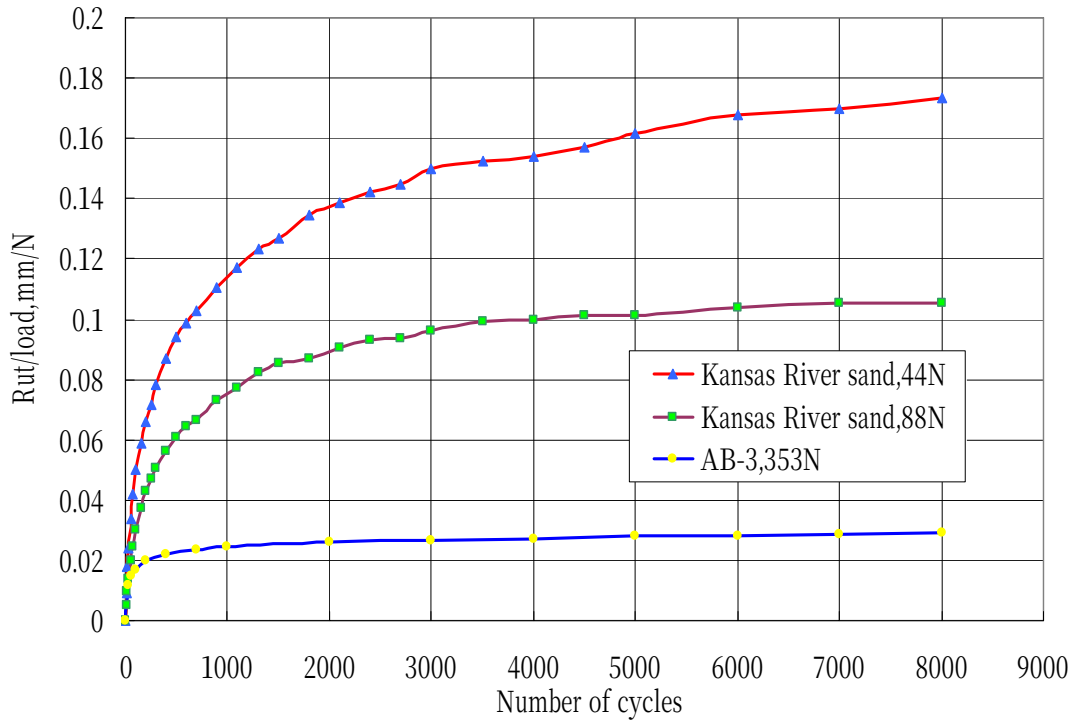

Figure 4.11 Geotextile at 13 mm below the surface

The above figures clearly show that the AB-3 aggregate had much less rut depth than the Kansas River sand. This finding is intuitively correct since the AB-3 aggregate (well-graded with angular particles) was stronger than the Kansas River sand (poorly graded with subrounded particles).

4.4 Effect of surcharge

Surcharge is one kind of confinement on the geosynthetic-soil interaction. In this study, the surcharge was only used in the tests for Kansas River sand. The magnitude of the surcharge was 2.9 kPa.

Figures 4.12 and Figure 4.13 show the comparisons of test results for unreinforced cases without surcharge and with surcharge.

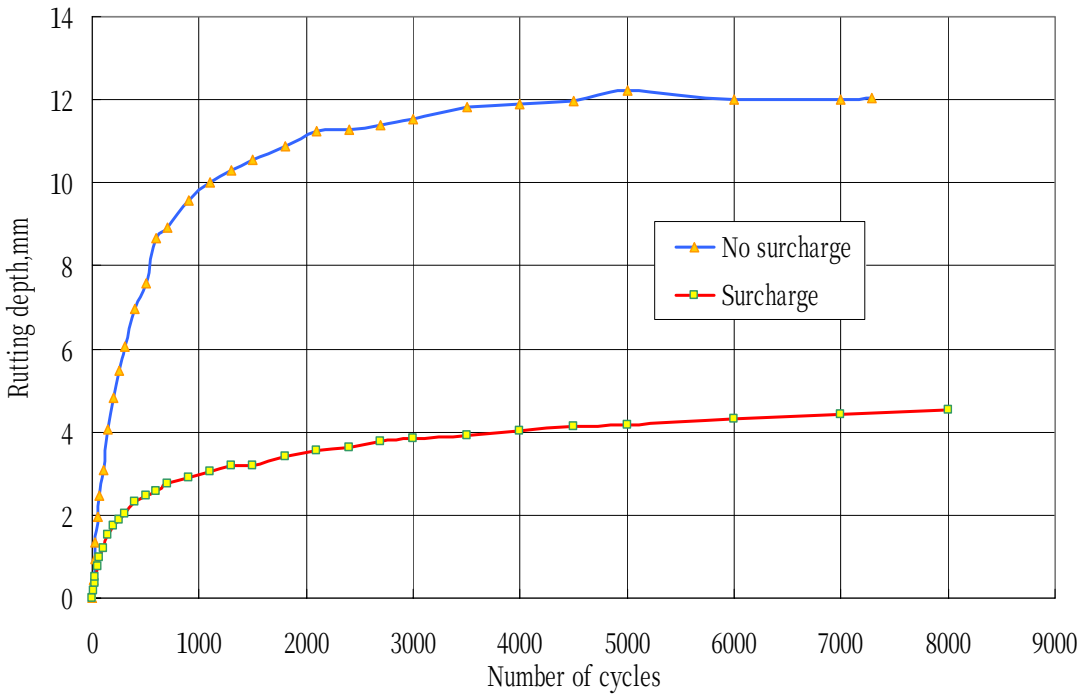

Figure 4.12 Test results of unreinforced cases under 44 N wheel loads without and with surcharge

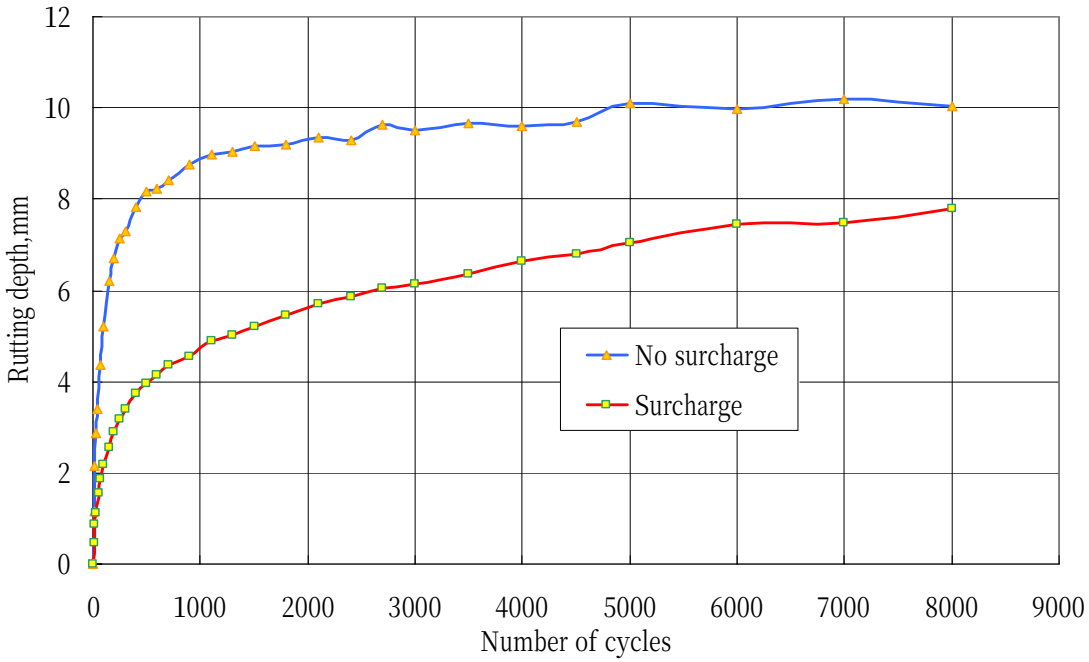

Figure 4.13 Test results of unreinforced cases under 88 N wheel loads without and with surcharge

Figures 4.14 to 4.27 show the comparisons of the reinforced cases with a geosynthetic layer placed at 25mm or 13mm below the surface without or with surcharge.

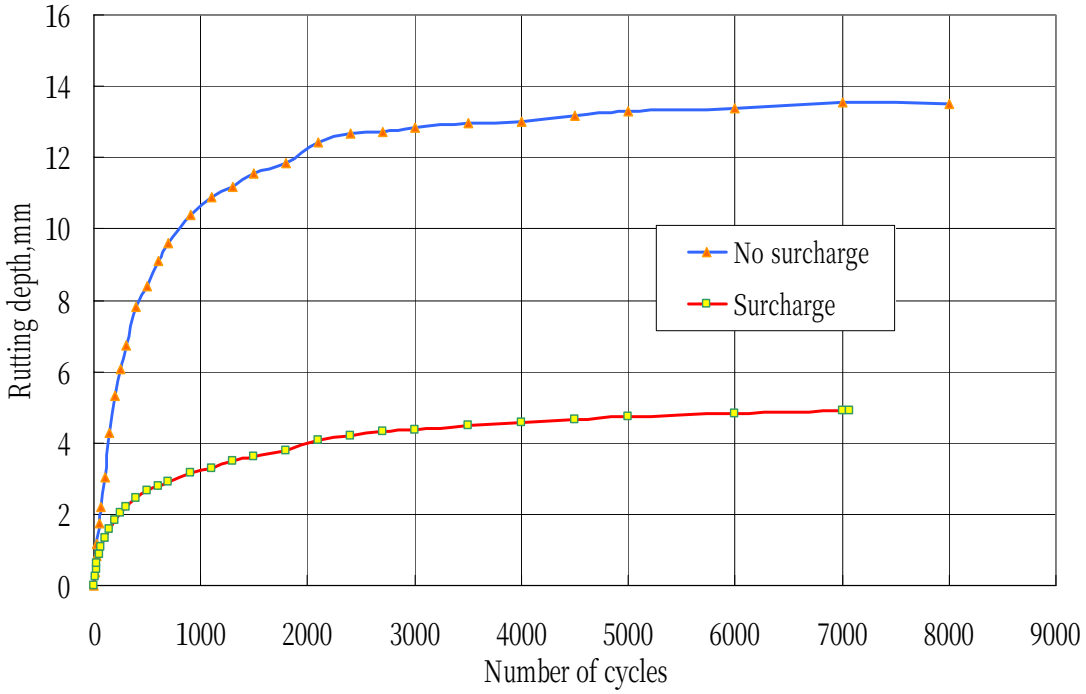

Figure 4.14 Test results of reinforced cases with BX1100 at 25mm deep under 44 N wheel loads without and with surcharge

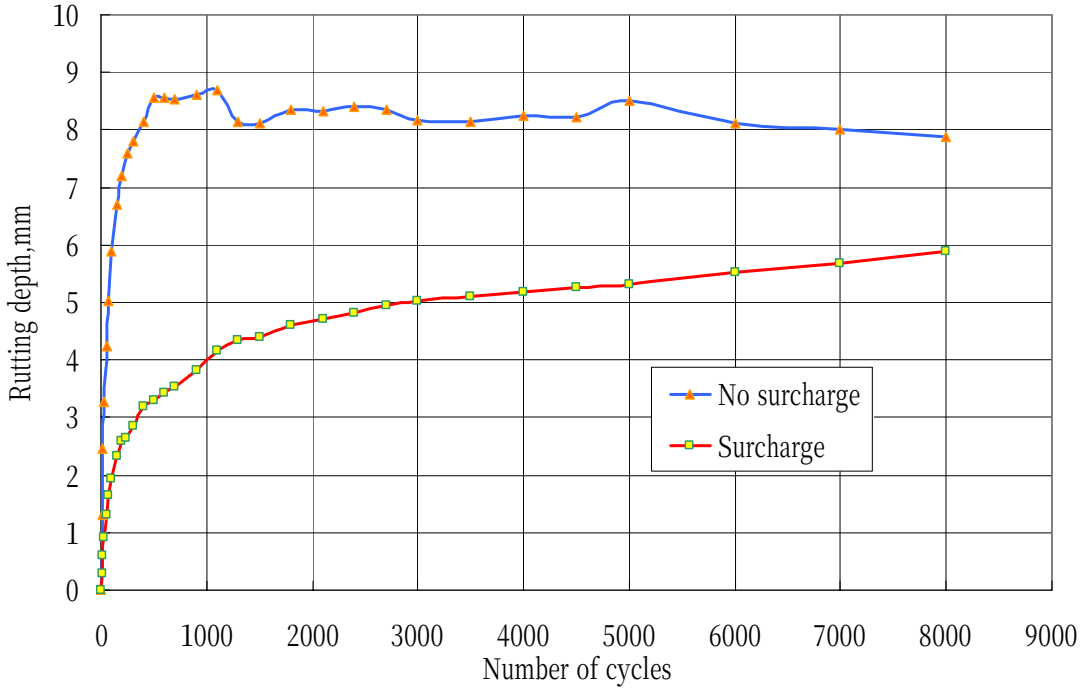

Figure 4.15 Test results of reinforced cases with BX1100 at 25mm deep under 88 N wheel loads without and with surcharge

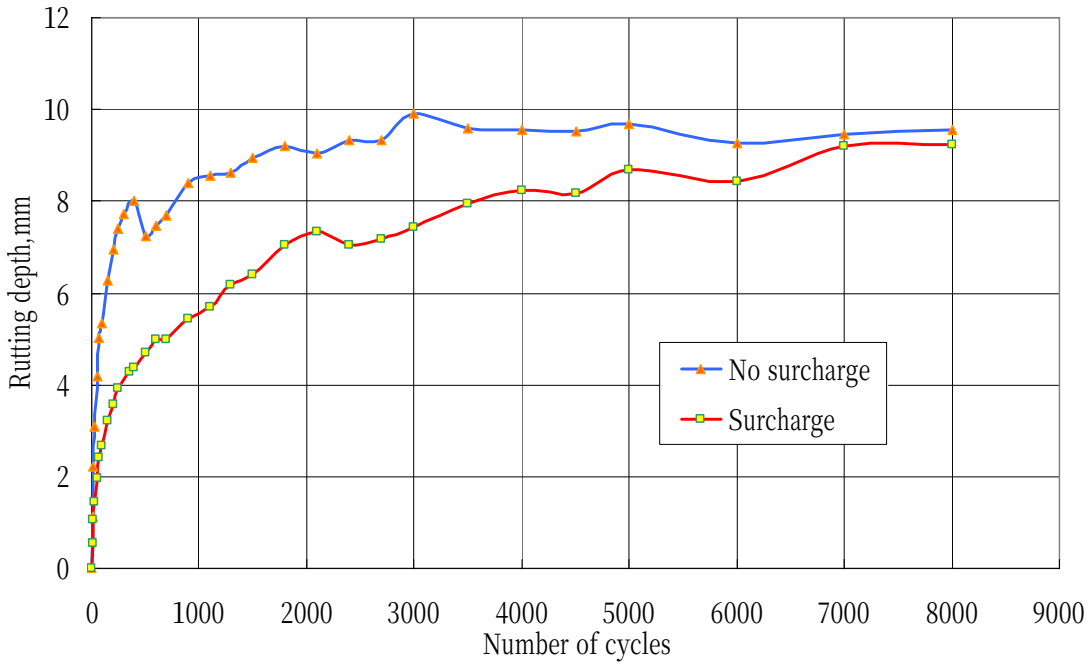

Figure 4.16 Test results of reinforced cases with BX1200 at 25mm deep under 88 N wheel loads without and with surcharge

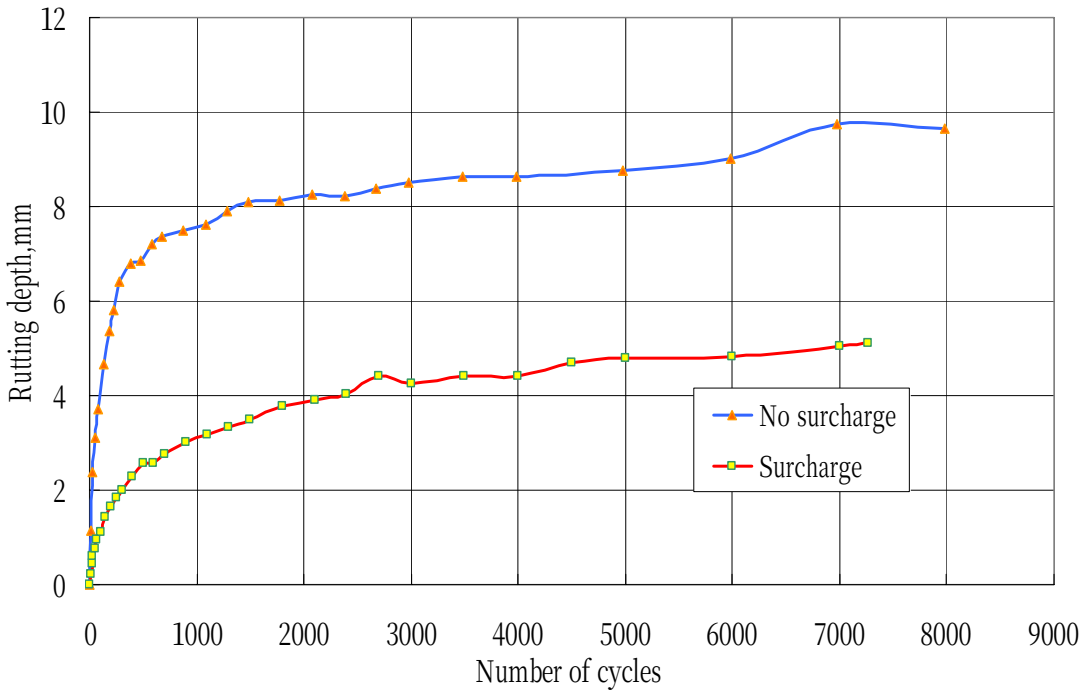

Figure 4.17 Test results of reinforced cases with BX1500 at 25mm deep under 44 N wheel loads without and with surcharge

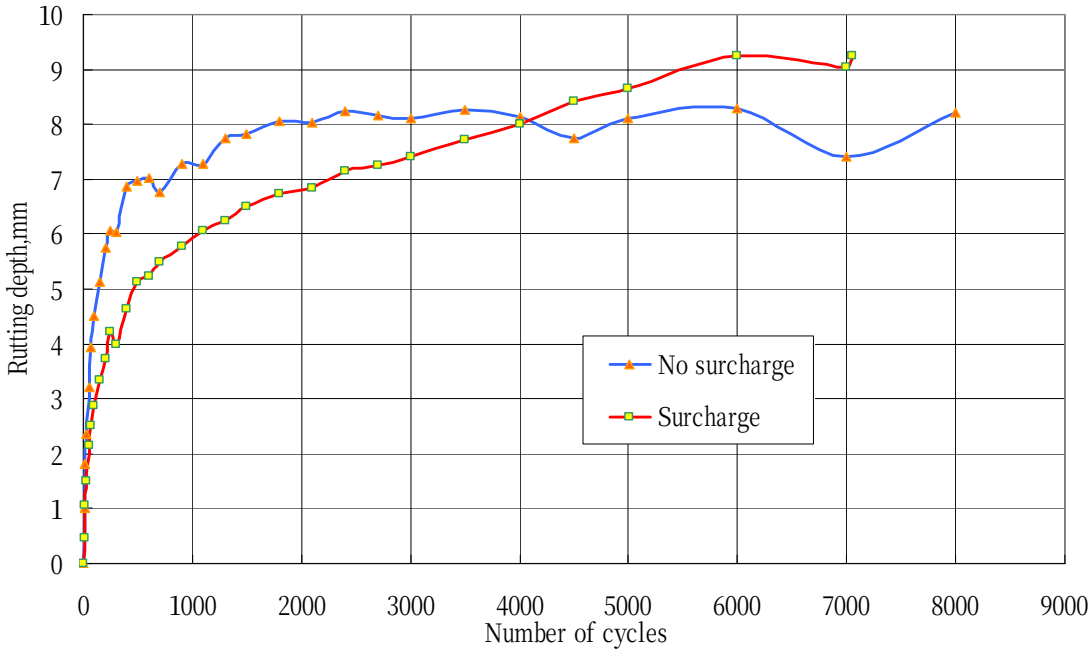

Figure 4.18 Test results of reinforced cases with BX1500 at 25mm deep under 88 N wheel loads without and with surcharge

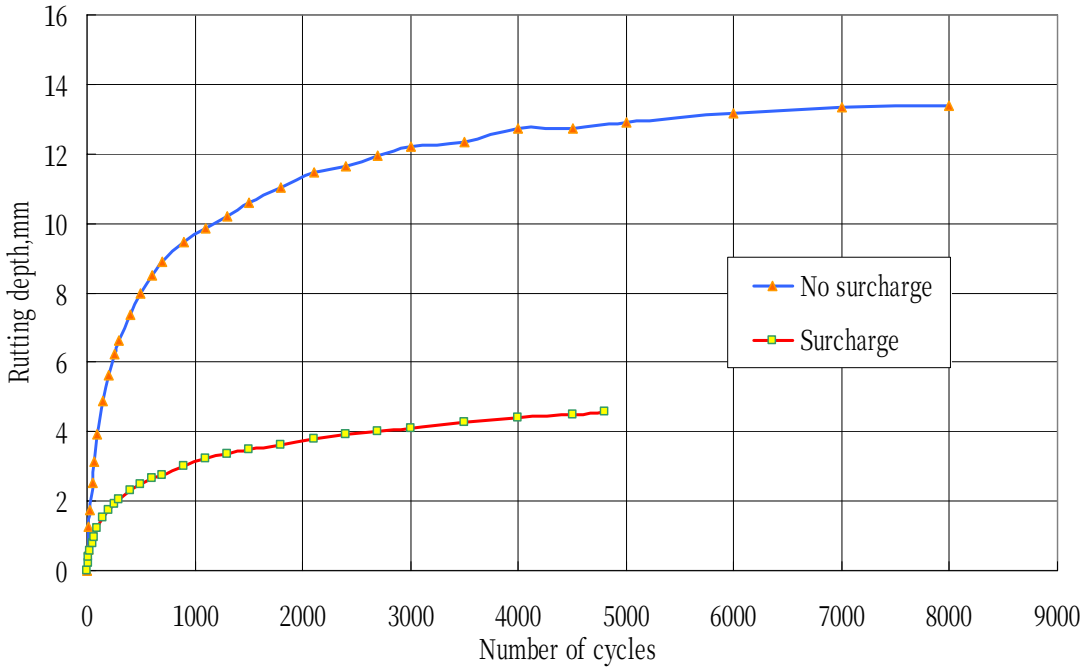

Figure 4.19 Test results of reinforced cases with geotextile at 25mm deep under 44 N wheel loads without and with surcharge

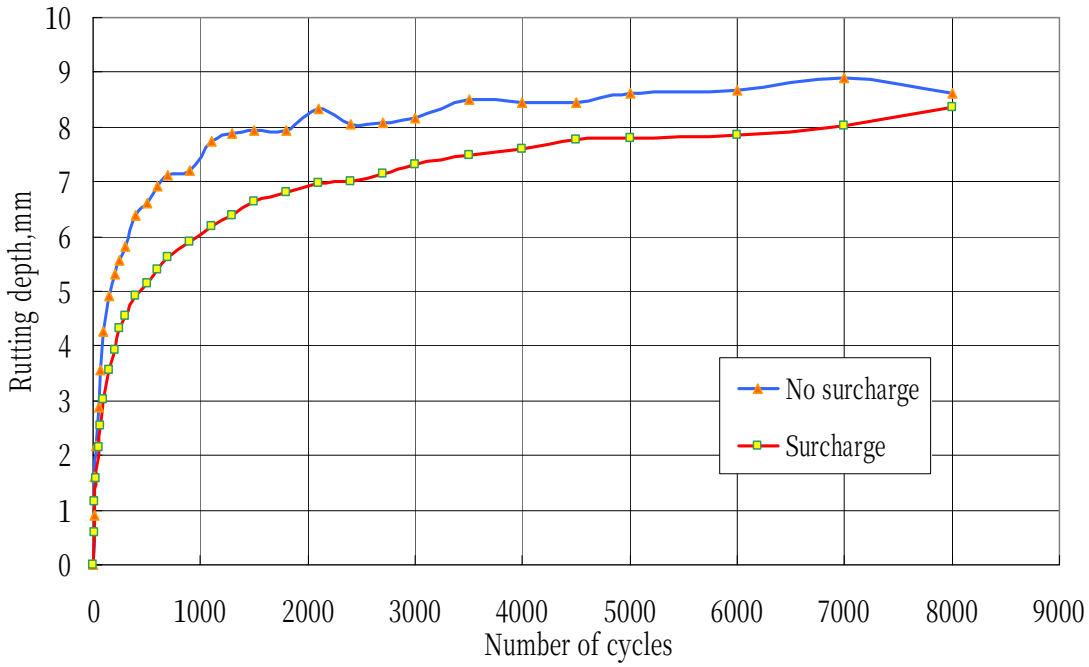

Figure 4.20 Test results of reinforced cases with geotextile at 25mm deep under 88 N wheel loads without and with surcharge

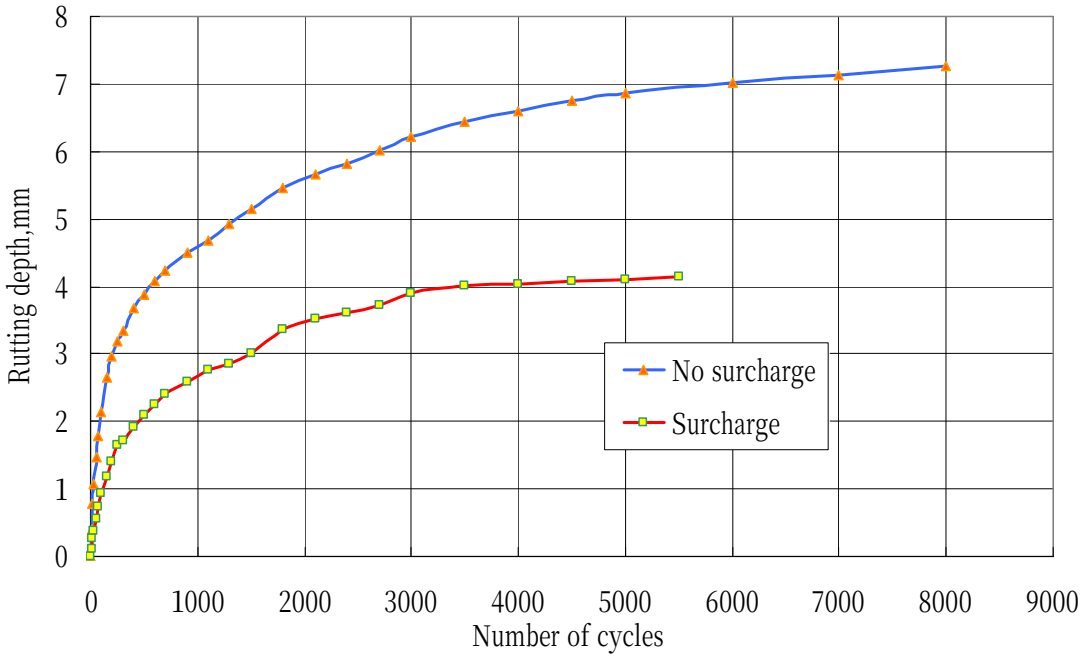

Figure 4.21 Test results of reinforced cases with BX1100 at 13mm deep under 44 N wheel loads without and with surcharge

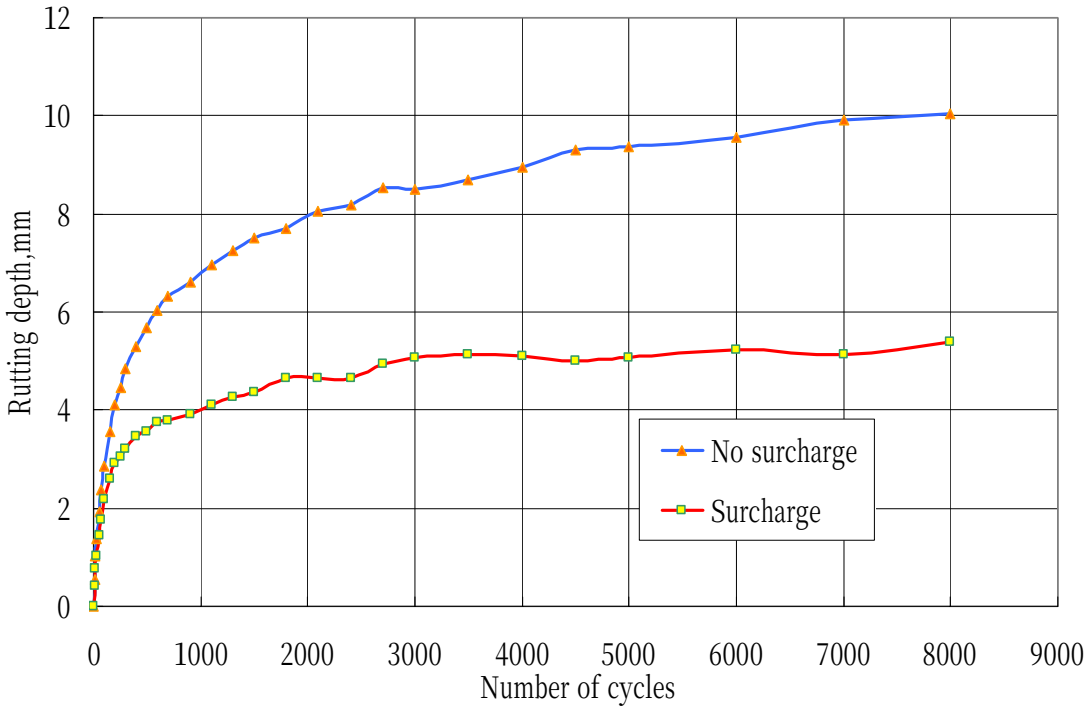

Figure 4.22 Test results of reinforced cases with BX1100 at 13mm deep under 88 N wheel loads without and with surcharge

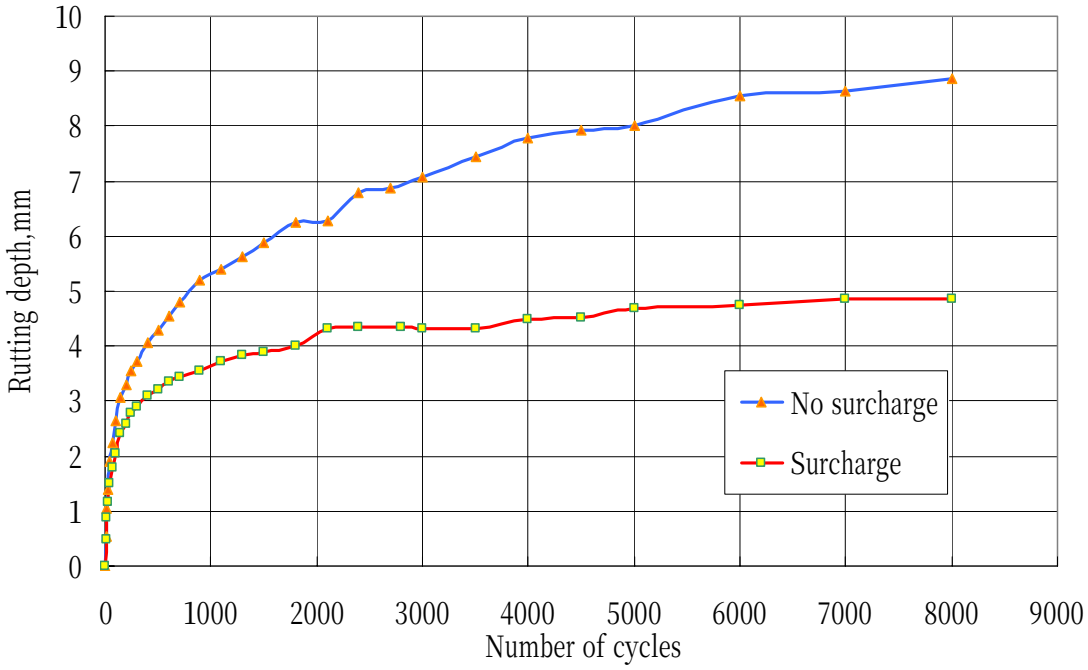

Figure 4.23 Test results of reinforced cases with BX1200 at 13mm deep under 88 N wheel loads without and with surcharge

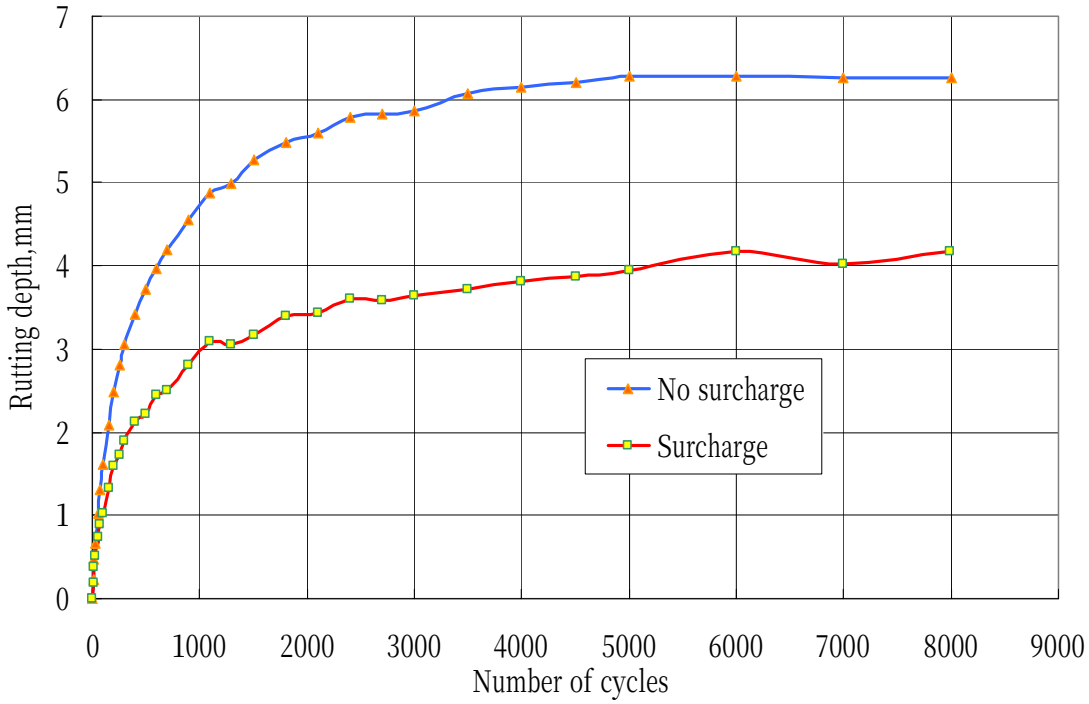

Figure 4.24 Test results of reinforced cases with BX1500 at 13mm deep under 44 N wheel loads without and with surcharge

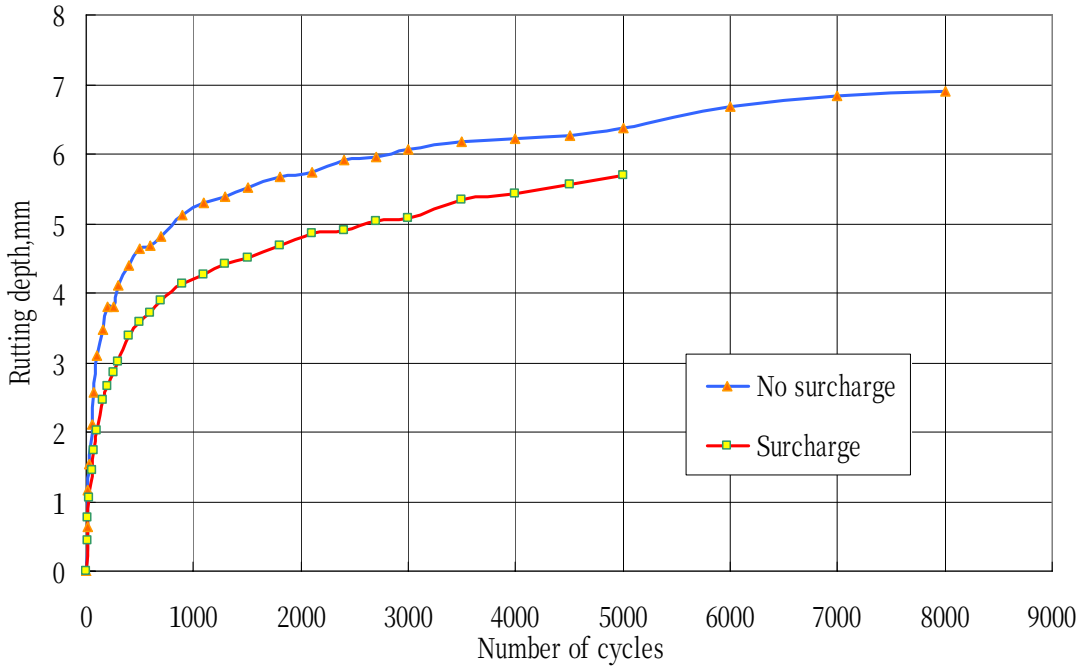

Figure 4.25 Test results of reinforced cases with BX1500 at 13mm deep under 88 N wheel loads without and with surcharge

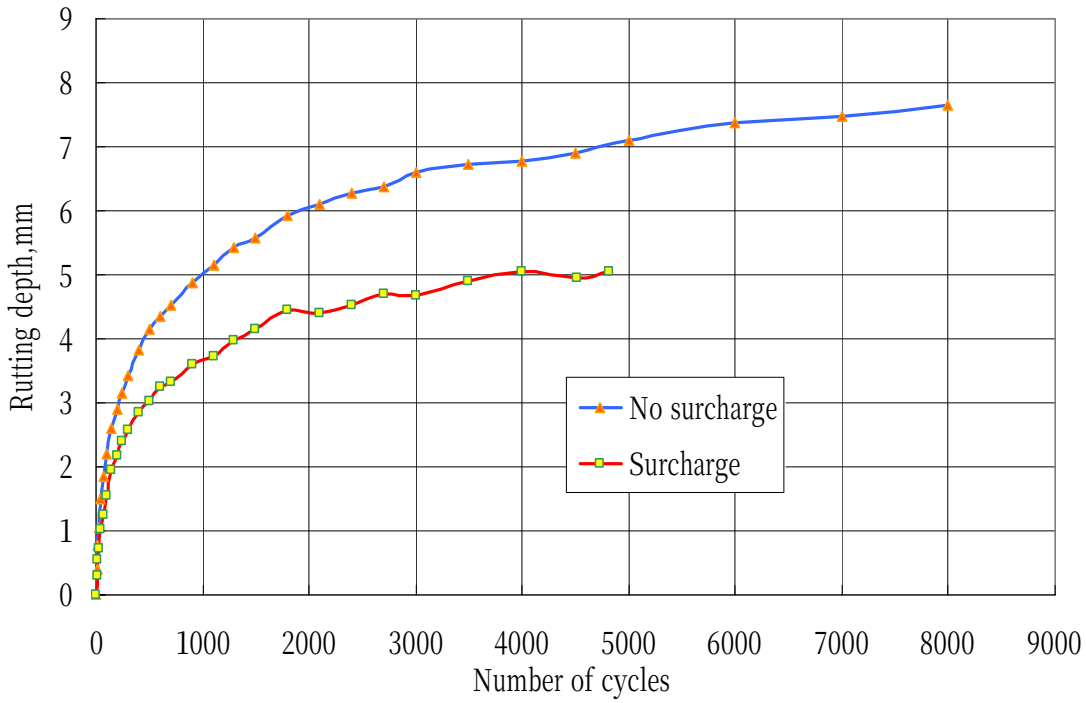

Figure 4.26 Test results of reinforced cases with geotextile at 13mm deep under 44 N wheel loads without and with surcharge

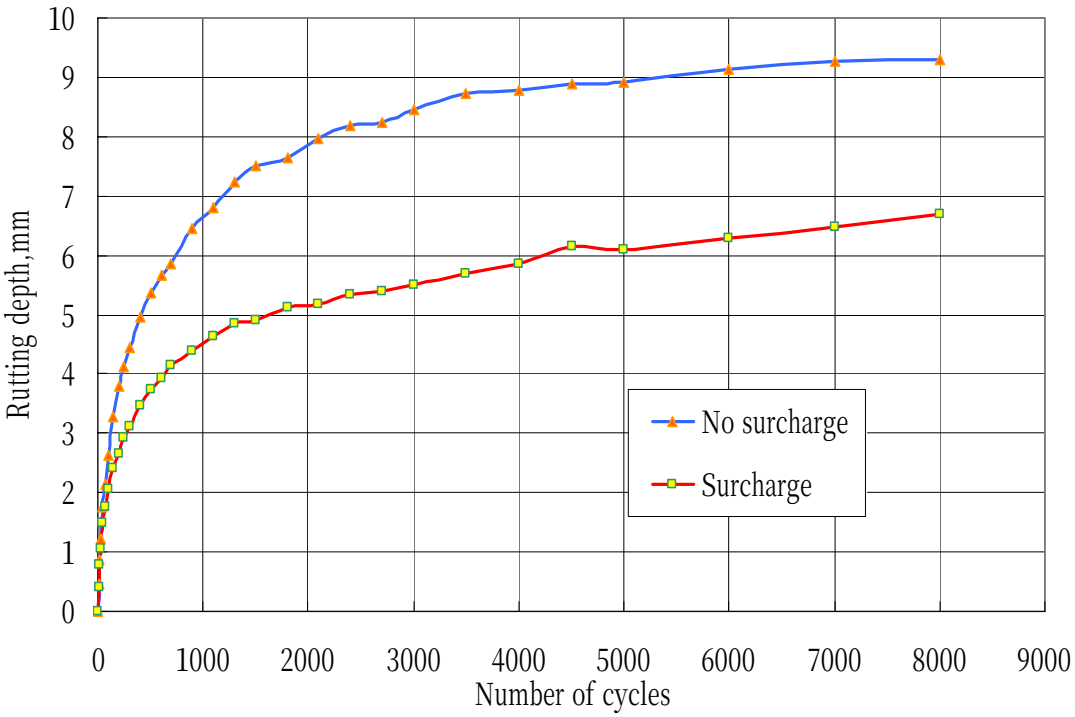

Figure 4.27 Test results of reinforced cases with geotextile at 13mm deep under 88 N wheel loads without and with surcharge

The above comparisons show that the rut depths for almost all the cases with surcharge cases were less than those without surcharge. This effect proves that surcharge can provide confinement to the base course and effectively reduce the rut depth.

4.5 Effect of geosynthetic

The effects of different geosynthetics on the performance of reinforced base courses are presented in this section.

Figures 4.28 to 4.31 present the test results of unreinforced and reinforced Kansas River sands without surcharge.

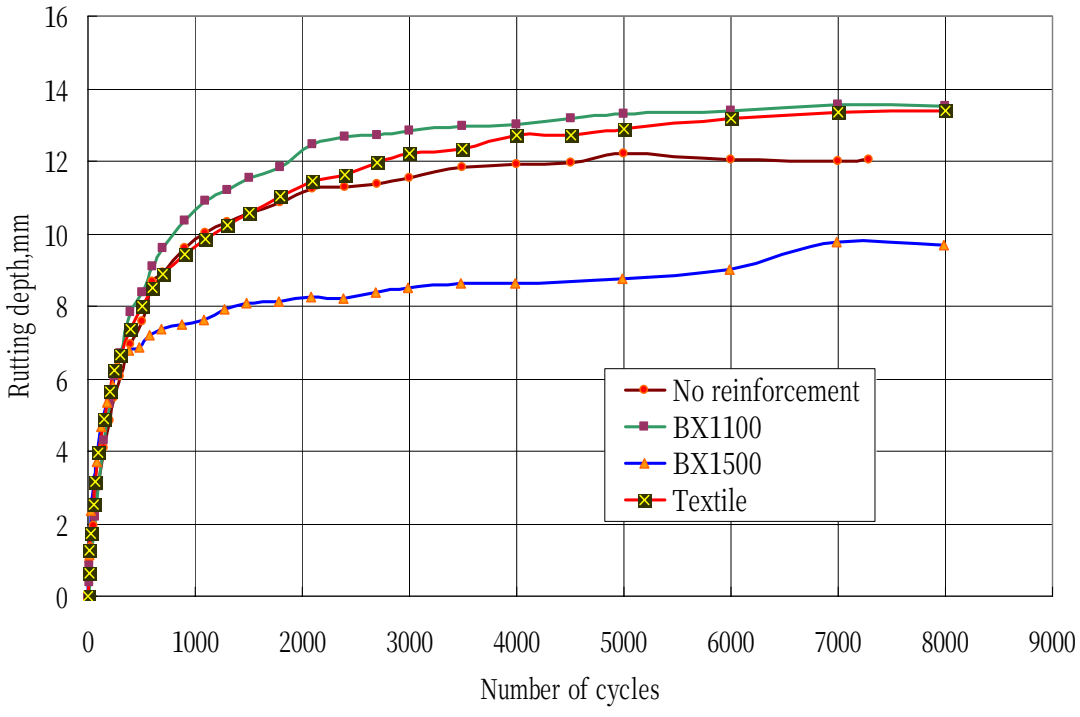

Figure 4.28 Test results of unreinforced and reinforced Kansas River sands with geosynthetics at 25mm deep under 44 N loads

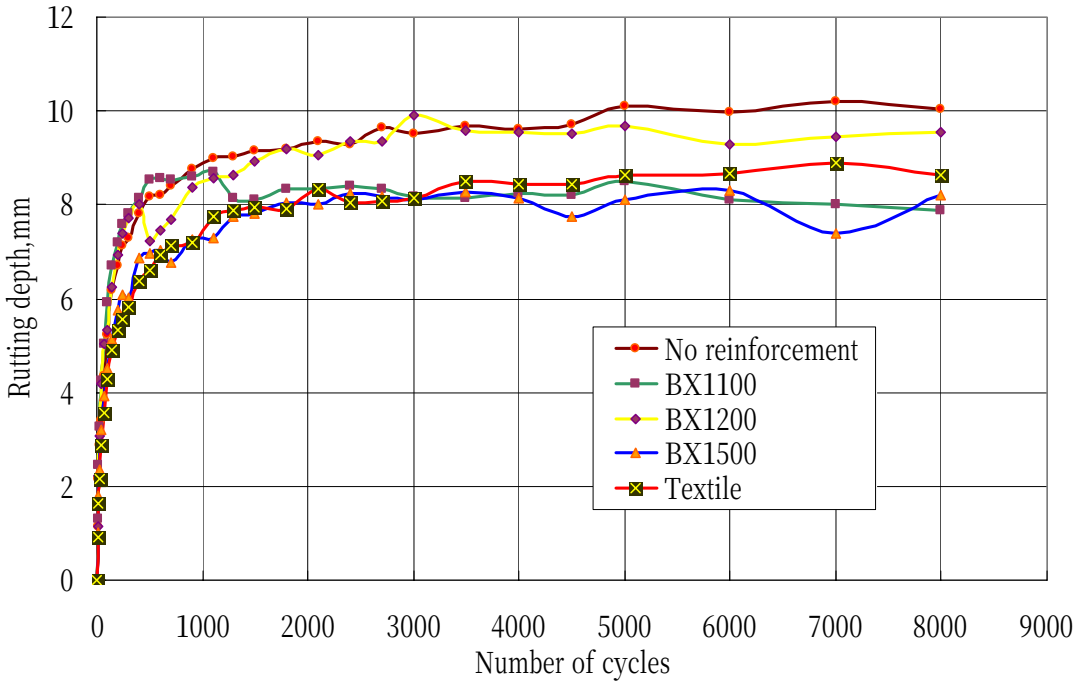

Figure 4.29 Test results of unreinforced and reinforced Kansas River sands with geosynthetics at 25mm deep under 88 N loads

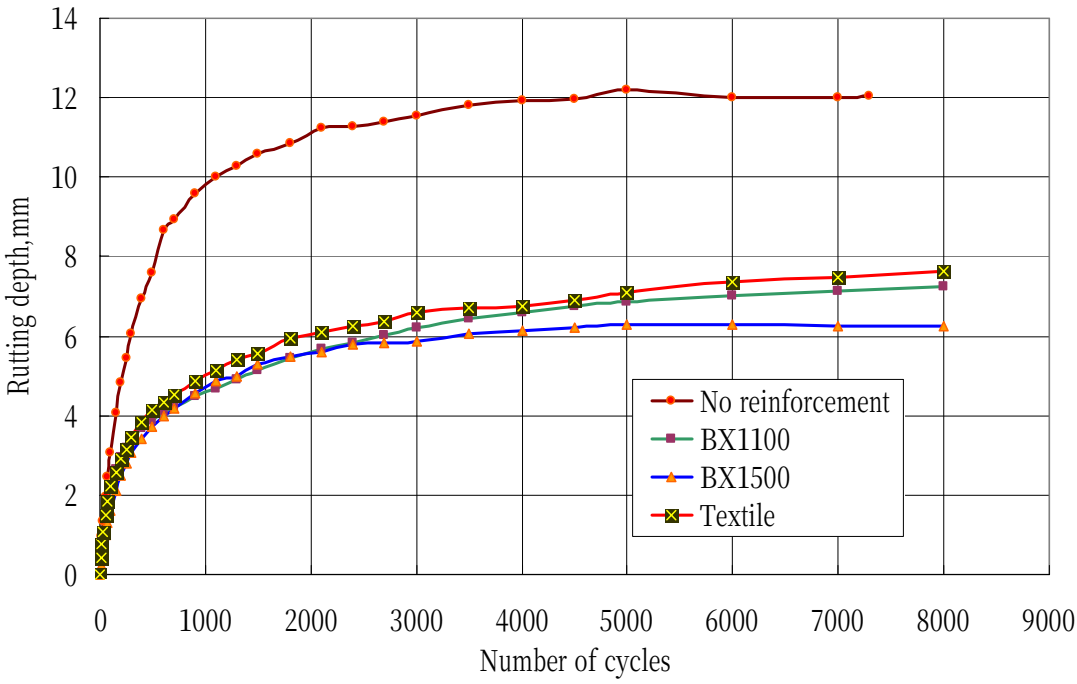

Figure 4.30 Test results of unreinforced and reinforced Kansas River sands with geosynthetics at 13mm deep under 44 N loads

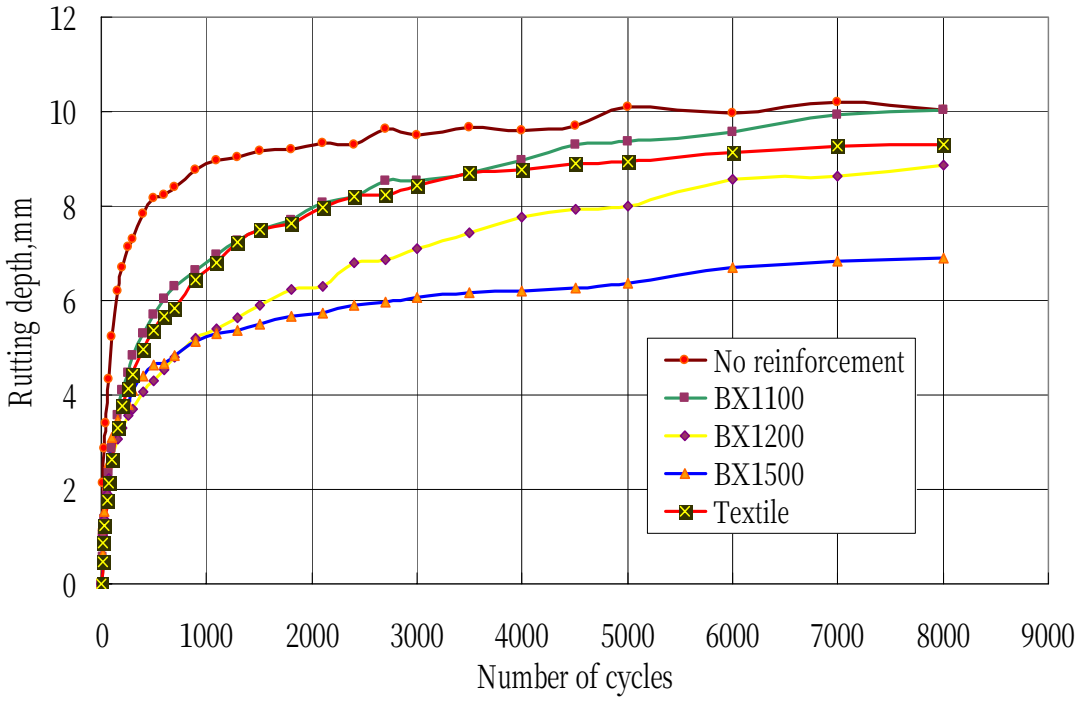

Figure 4.31 Test results of unreinforced and reinforced Kansas River sands with geosynthetics at 13mm deep under 88 N loads

The above four figures show that most geosynthetics had the benefit in reducing the rut depth except for BX1100 geogrid and geotextile at 25mm deep under 44N load. The benefit is more obvious when the geosynthetic layer was placed at 13mm deep. BX1500 geogrid is always the best to reduce the rut depth.

Figures 4.32 to 4.35 present the test results of unreinforced and reinforced Kansas River sands with surcharge.

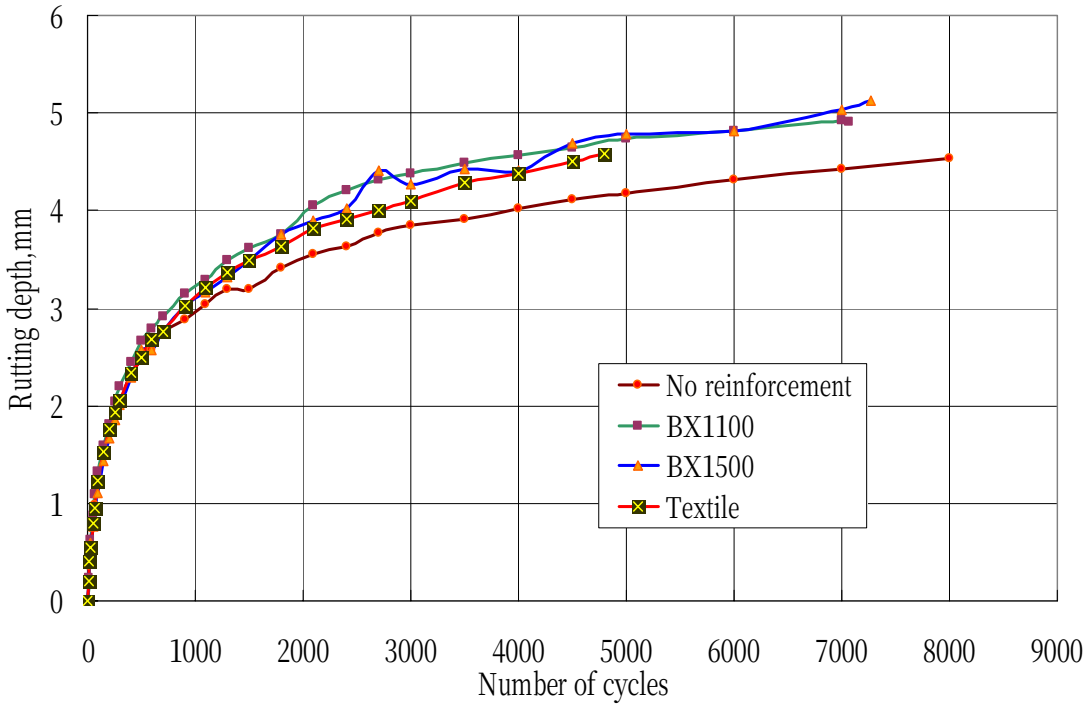

Figure 4.32 Test results of unreinforced and reinforced Kansas River sands with geosynthetics at 25mm deep under 44 N load and with surcharge

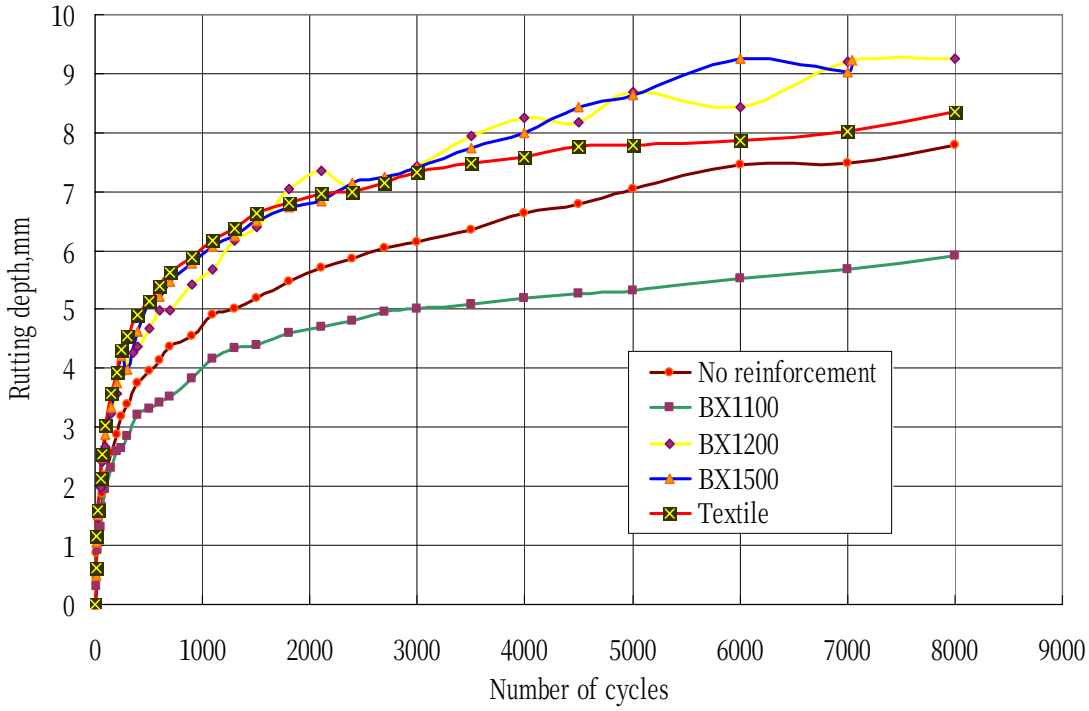

Figure 4.33 Test results of unreinforced and reinforced Kansas River sands with geosynthetics at 25mm deep under 88 N load and with surcharge

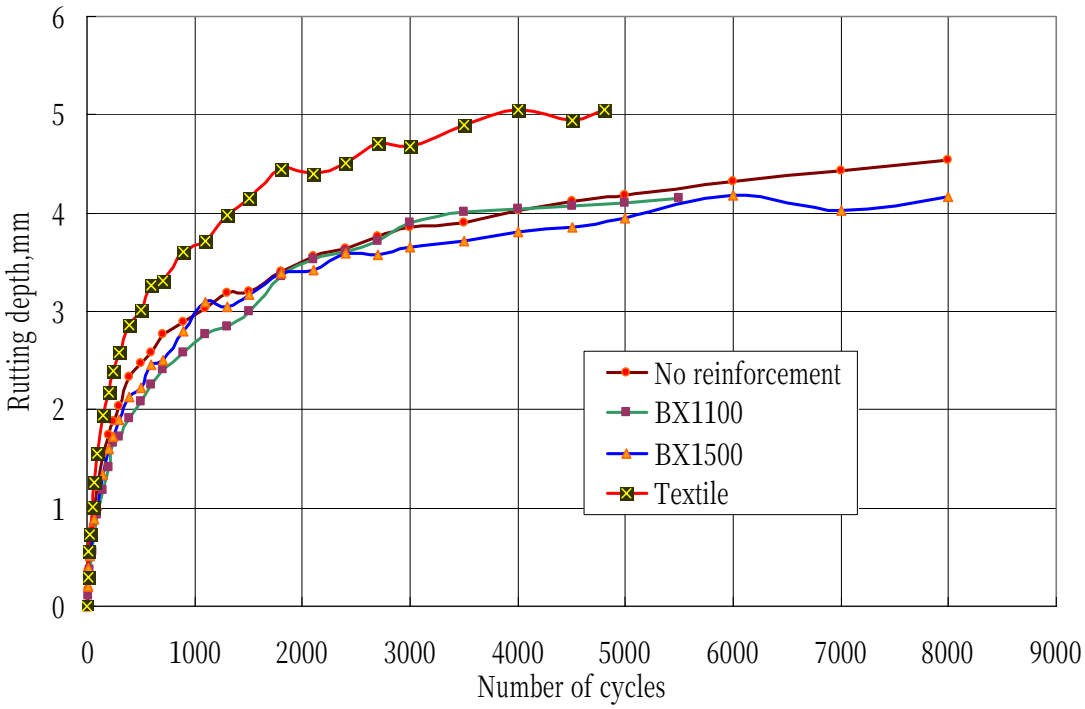

Figure 4.34 Test results of unreinforced and reinforced Kansas River sands with geosynthetics at 13mm deep under 44 N load and with surcharge

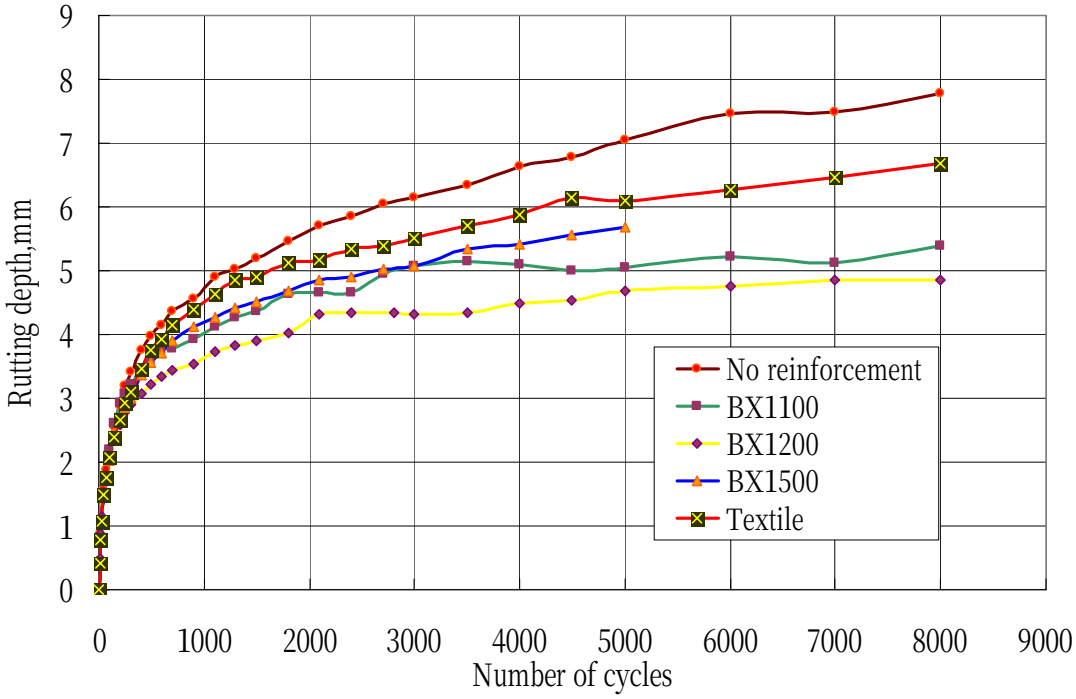

Figure 4.35 Test results of unreinforced and reinforced Kansas River sands with geosynthetics at 13mm deep under 88 N load and with surcharge

As compared with the test results without surcharge, the above figures show that the surcharge minimized the benefit of geosynthetics. This effect can be explained that surcharge is also a kind of confinement and can effectively reduce the rut depth. For smaller rut depths, the contribution of geosynthetics is reduced.

The confinement effect of geosynthetics with AB-3 aggregate was also investigated in this study. Since the AB-3 aggregate is much stronger than Kansas River sand, a high wheel load of 353 N and a high hose pressure of 552 kPa were used. The test results of unreinforced and reinforced AB-3 aggregates with geosynthetics at 25mm or 13mm deep are presented in Figures 4.36 and 4.37.

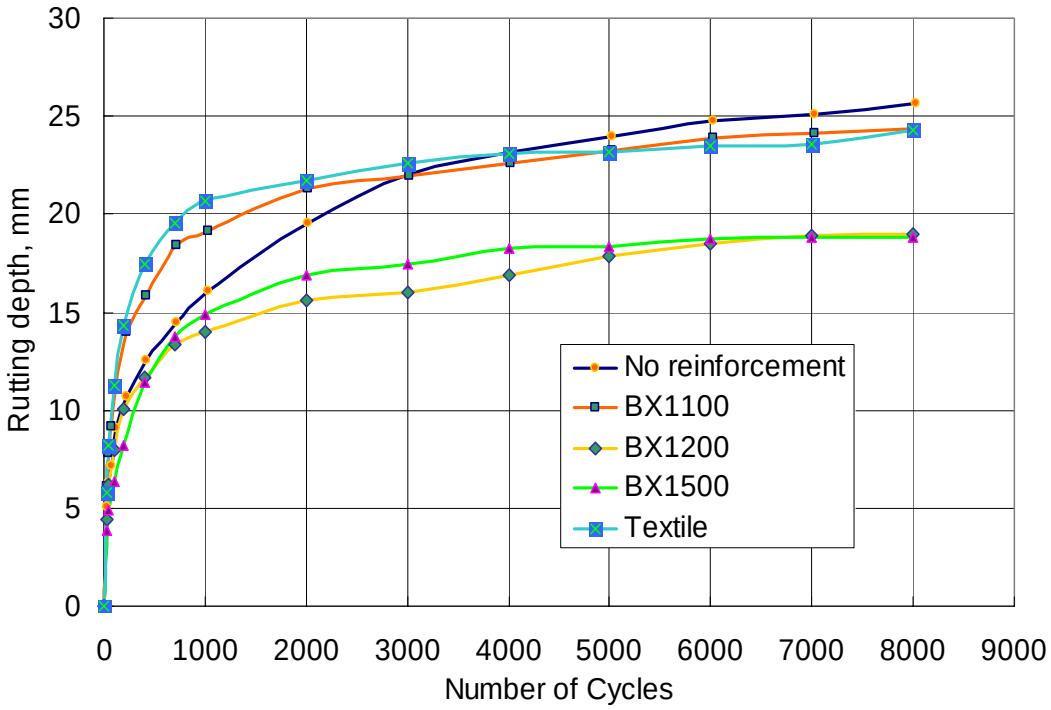

Figure 4.36 Test results of unreinforced and reinforced AB-3 aggregates with geosynthetics at 25mm deep under 353 N loads

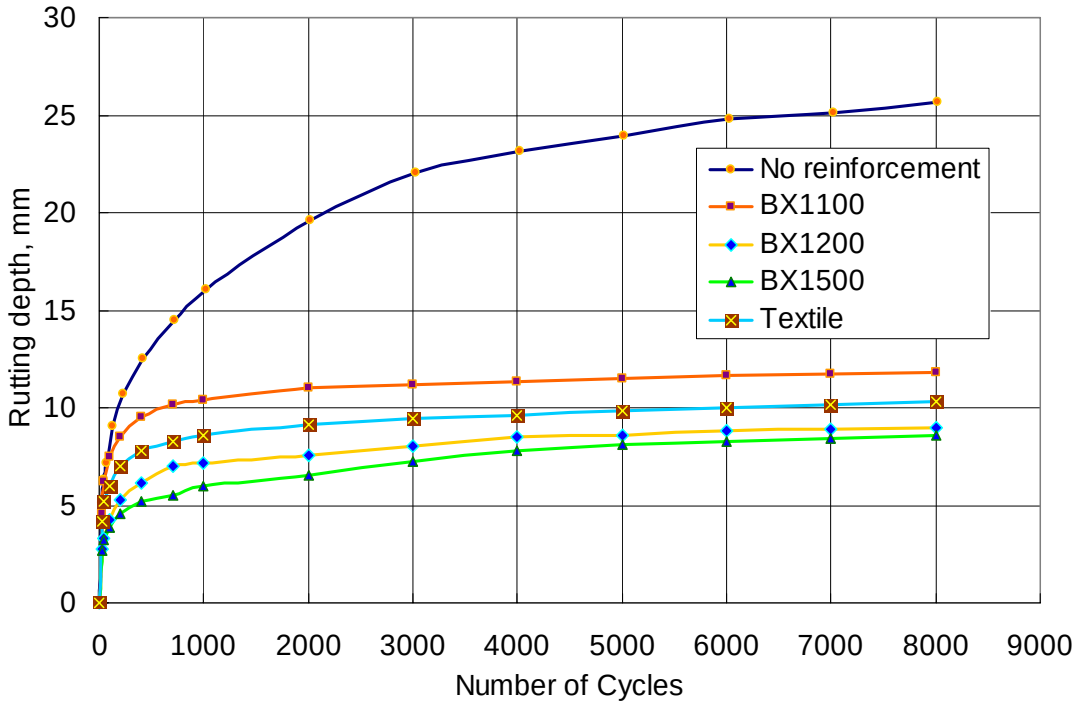

Figure 4.37 Test results of unreinforced and reinforced AB-3 aggregates with geosynthetics at 13mm deep under 353 N loads

The two figures above show that BX1200 and BX1500 geogrids worked well at both 25 mm and 13mm depths. BX1100 and geotextile did not have significant effect on the reduction of rut depth when they were placed at 25 mm depth. When geosynthetics were placed at 13 mm depth, however, all the geosynthetics had obvious enhancement of the performance of the AB-3 aggregate. Figure 4.37 also shows that the proposed test method can clearly distinguish among the benefits of different geosynthetics in the order of BX1100, geotextile, BX1200, and BX1500 for better performance.

4.6 Traffic benefit ratio

Traffic benefit ratio (TBR) is defined as the ratio of the number of cycles to reach a certain rut depth when reinforced to the number of cycles to reach the same rutting depth when unreinforced, which can simply expressed as follows:

$$TBR = \frac{N_{\text{reinforced}}}{N_{\text{unreinforced}}}$$

This parameter has been commonly used to evaluate the effectiveness of geosynthetics in enhancing the road system in term of service life.

TBR depends on the level of rut depth, which varied greatly in the experimental tests with the following factors: base material, surcharge, load and hose pressures, type of geosynthetics and depth of geosynthetics. Therefore, two rutting depths are used as the standard depths to evaluate all the TBRs in this study. One is equal to half of the hose diameter, 13 mm (0.5 in); the other is equal to one quarter of the hose diameter, 6.4 mm (0.25 in). Since the range of rutting depth varies largely in different tests, the abscissa is shown in logarithmic scale. Take AB-3 aggregate as an example. The TBR with 6.4 mm standard depth for BX1500 geogrid at 13 mm depth can be calculated as shown in Figure 4.38.

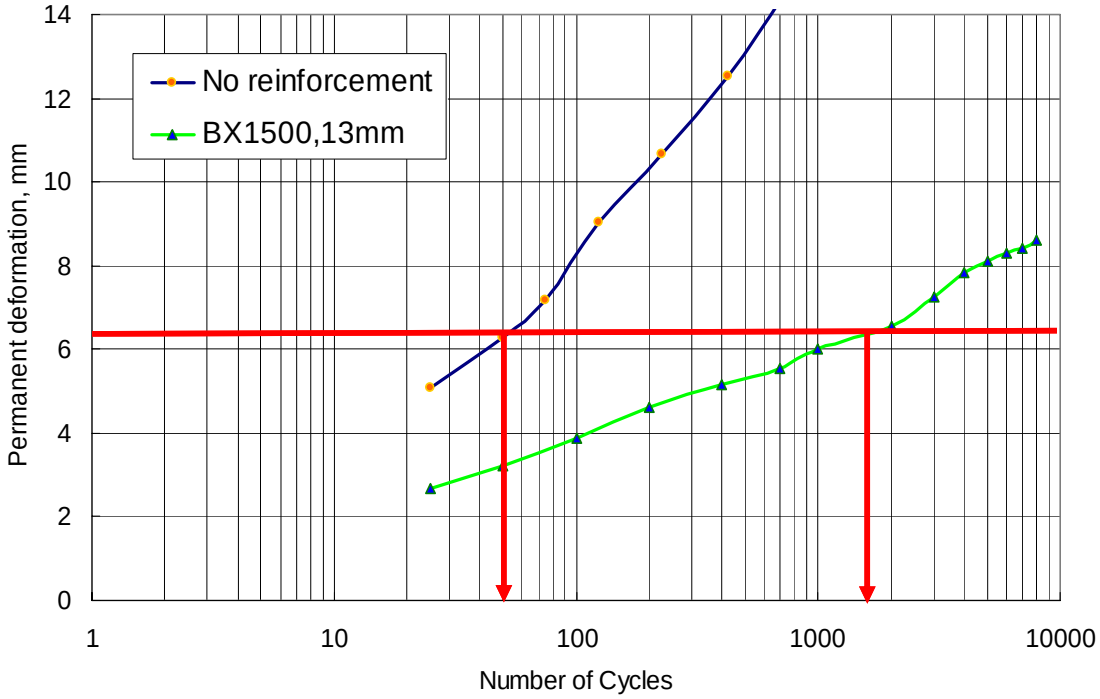

$$TBR = \frac{N_{\text{reinforced}}}{N_{\text{unreinforced}}} = \frac{1600}{50} = 32$$

Figure 4.38 Sample calculation of TBR

The TBRs corresponding to Figures 4.28 to 4.37 were calculated and are tabulated in Table 4.1.

Base	Surcharge	Loads, N	Geosyn. Depth, mm	Based on rut depth of 13 mm				Based on rut depth of 6.4 mm			
				BX1100	BX1200	BX1500	HP370	BX1100	BX1200	BX1500	HP370
Kansas River sand	No	44	25	0.33	N/A	50	0.5	0.76	N/A	0.76	0.76
			13	28.6	N/A	143	28.6	10.3	N/A	31.3	8.4
		88	25	1.4	1.4	5.7	1.6	0.7	1	2.1	2.7
			13	0.2	0.4	30	0.35	5.7	7.9	36.4	6.4
	Yes	44	25	0.038	N/A	0.075	0.21	0.24	N/A	0.35	0.47
			13	0.2	N/A	0.8	0.28	1	N/A	1.4	0.26
		88	25	60	0.33	0.33	1	4.6	0.4	0.37	0.37
			13	300	3000	50	10	5.7	28.6	2.9	1.9
AB-3	No	353	25	0.4	1.3	1.2	0.33	0.5	1.1	2	0.6
			13	70.6	941	706	235	1	9.6	32	2.3

Table 4.1 TBR of four geosynthetics at all conditions

The TBR results in this table show that the geosynthetic placed at 13mm had more benefit than that at 25mm. Surcharge reduced the effect of geosyntheics. In general, BX1500 geogrid performed the best among all the geosynthetics tested in this study and it is followed by BX1200 geogrid, HP370 woven geotextile, and BX1100 geogrid. All the geosynthetics had better interaction with AB-3 than Kansas River sand.

4.7 Rut reduction ratio

Rut reduction ratio (RRR) is defined as the ratio of the rut depth of the reinforced case at a certain number of cycles to the rut depth of the unreinforced case at the same number of cycles, simply expressed below:

$$RRR = \frac{r_{\text{reinforced}}}{r_{\text{unreinforced}}}$$

Since most tests in this research reached the cycle number of 8000, the number of cycles of 8000 is used as the standard cycle number. Take AB-3 aggregate as an example. The RRR of BX1500 at 25 mm depth is calculated as shown is Figure 4.39. The RRR is equal to 0.74 in the example which means the rut depth of the reinforced case at 8000 cycles is only 0.74 that of the unreinforced one.

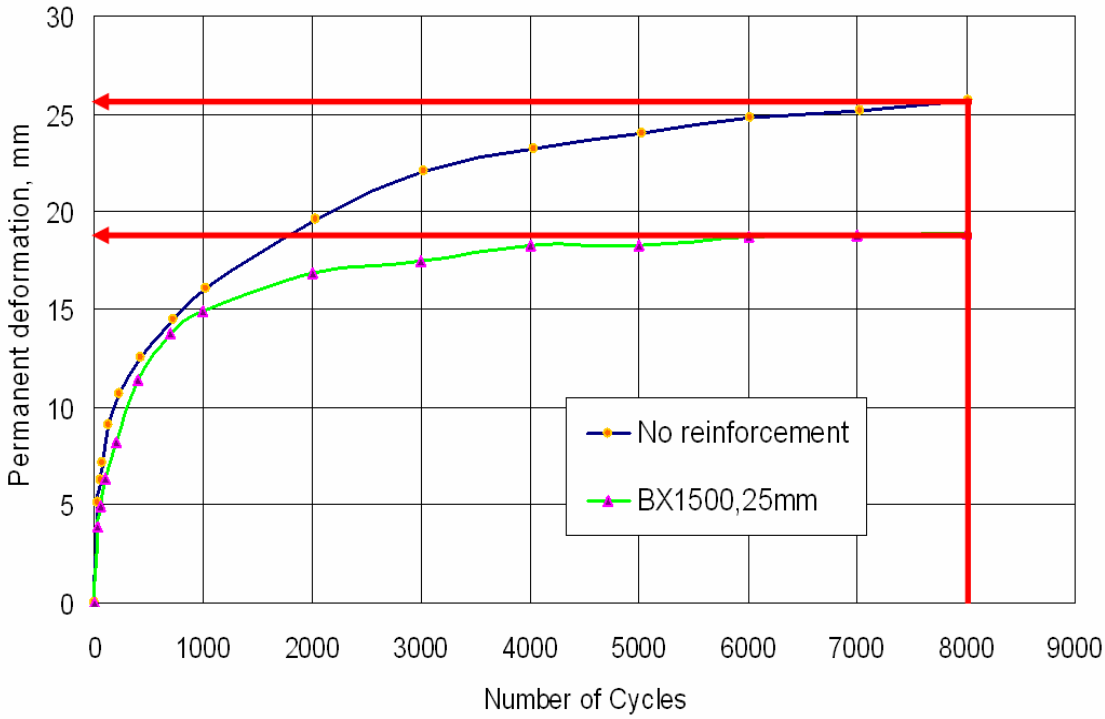

$$RRR = \frac{r_{\text{reinforced}}}{r_{\text{unreinforced}}} = \frac{18.85}{25.64} = 0.74$$

Figure 4.39 Sample calculation of RRR

The RRR for all the other cases were calculated and are tabulated in Table 4.2. These results show again that geosynthetics placed at 13 mm show more benefit than when placed at 25 mm. The effect of geosynthetics is reduced by the surcharge. All geosynthetics had better interaction with AB-3 than Kansas River sand.

Base	Surcharge	Loads, N	Geosyn. Depth, mm	BX1100	BX1200	BX1500	HP370
Kansas River sand	No	44	25	1.1	N/A	0.8	1.1
			13	0.6	N/A	0.52	0.63
		88	25	0.79	0.95	0.82	0.86
			13	1	0.88	0.69	0.93
	Yes	44	25	1.1	N/A	1.1	1.1
			13	0.95	N/A	0.92	1.17
		88	25	0.76	1.19	1.19	1.1
			13	0.69	0.62	0.81	0.86
AB-3	No	353	25	0.95	0.74	0.74	0.95
			13	0.46	0.35	0.34	0.4

Table 4.2 RRR of four geosynthetics at all conditions

Chapter 5 CONCLUSIONS AND RECOMMENDATIONS

5.1 Summary

A review of the literature showed that geosynthetics could reduce the rut depth and enhance the performance of roadways. Current test methods used to evaluate geosynthetic-soil confinement include the aperture stability modulus test, the TRI bending stiffness test, the cyclic plate loading test, the cyclic triaxial test, the accelerated pavement facility, and the field track test. However, all these test methods have some of the following deficiencies:

1. Cannot evaluate the interaction of geosynthetic with soil.
2. Cannot be used for different types of geosynthetics.
2. Cannot simulate the rolling wheel load.
3. Influence of shear resistance between soil and chamber (for example, the TRI stiffness test).
4. Tedious, difficult, slow, and costly.

This research was conducted to develop a new test method to evaluate geosynthetics-soil confinement using an Asphalt Pavement Analyzer (APA) in order to avoid the deficiencies listed above. Four types of geosynthetics - BX1100, BX1200, BX1500 geogrids, and HP370 geotextile - were placed at 25 mm or 13mm depths below the surface in a modified test box, interacting with Kansas River sand under 44 N or 88 N load without or with surcharge or with AB-3 aggregate under 353 N load without surcharge.

5.2 Conclusions

Based on the test results from this study, the following conclusions can be made:

1. AB-3 aggregate had better interaction with geosynthetics than Kansas River sand.

2. Surcharge could provide the confinement and reduce the rut depth so that it minimized the benefit of geosynthetics.

3. Without surcharge, all the geosynthetics were beneficial especially at large deformations.

4. Geosynthetics placed at a depth of 13mm performed much better than those placed at 25mm.

5. The proposed new test method can be used for different geosynthetic products (geogrid and geotextile) and distinguish among the confinement effects of these products. Based on this study, BX1500 geogrid performed the best, followed by BX1200, geotextile HP370, and BX1100.

5.3 Recommendations

Additional tests are necessary to further verify the proposed method for evaluating the geosynthetic-soil confinement including more load combinations, different locations of geosynthetics, different types of geosynthetics (such as woven geogrids) and surcharge conditions. Studies are also needed for base course materials under an as-compacted moisture condition.

REFERENCES

Adams, M. T. and Collin, J. G., *Large model spread footing load tests on geosynthetic reinforced soil foundations*, Journal of Geotechnical and Geoenvironmental Engineering, ASCE, January, 1997, Vol.123, p 66-72.

Bardet, J. P., *Experimental soil mechanics*, Prentice Hall, 1997.

Barksdale, R. D., Brown, S. F., and Chan, F., *Aggregate base reinforcement of surfaced pavement*, Geotextile and Geomembranes, 1989, 8, 165-189.

Berg, R. R., Christopher, B. R., and Perkins, S. W., *Geosynthetic reinforcement of the aggregate base course of flexible pavement structures*, GMA White Paper II, Geosynthetic Materials Association, 2000.

Blackman, D. I., Green, M. J., and Watts, G. R. A., *Tensar International Limited: Trafficking trials for sub-base reinforcement*, TRL Report PR/IS/13/2001, 2001.

Budhu, M., *Soil mechanics and foundations*, 2nd Ed., John Wiley &. Sons, 2007.

Cancelli, A. and Montanelli, F., *In-ground test for geosynthetic reinforced flexible paved roads*, Proc. Geosynthetics, 1999, Boston, 863–878.

Chaddock, B. C. J., *Deformation of road foundations with geogrid reinforcement*, TRL Research Report, 140, 1988.

Chang, T. T. D., Ho, H. N., Chang, Y. H., and Yeh, H. S., *Laboratory and case study for geogrid-reinforced flexible pavement overlay*, Transportation Research Record 1687, Transportation Research Board, National Research Council, 1988, Washington, D. C., 125-130.

Collin, J. G., Kinney, T. C., and Fu, X., *Full scale highway load test of flexible pavement system with geogrid reinforcement base courses*, Geosynthetics International, 1996, 3(4).

Dondi, G., *Three-dimensional finite element analysis of a reinforced paved road*, 5th International Conference on Geotextile, Geomembranes and Related Products, 1994, Vol. 1, Singapore, 95-100.

Hass, R., Walls, J., and Carroll, R. G., *Geogrid reinforcement of granular bases in flexible pavement*, Transportation Research Record 1188, Transportation Research Board, National Research Council, 1988, Washington, D. C., 19-27.

Hufenus, R., Rueegger, R., Banjac, R., Mayor, P., Springman, S. M., and Brönnimann, R., *Full-scale field test on geosynthetic reinforced unpaved roads on soft subgrade*, Geotextile and Geomembranes, 2006, 24, 21-37.

Huntington, G. and Ksaibati, K., *Evaluation of geogrid reinforced granular bases*, Geotechnical Fabrics Report, January/February, 2000, Vo.18, No.1, 22-88

Kinney, T. C. and Xiaolin, Y., *Geogrid aperture rigidity by in-plane rotation*, Proceedings of Geosynthetics, 1995, Nashville, Vol.2, 525-537.

Kwon, J., Tutumluer, E., and Kim, M., *Development of a mechanistic model for geosynthetic-reinforced flexible pavements*, Geosynthetics International, 2005, 12(6), 310-320.

Laurinavičius, A. and Oginskas, R., *Experimental research on the development of rutting in asphalt concrete pavements reinforced with geosynthetic materials*, Journal of Civil Engineering and Management, 2006, Vol.XII, 4, 311-317.

Ling, H. I., and Liu, H., *Finite element studies of asphalt concrete pavement reinforced with geogrid*, Engineering Mechanics, 2003, 129(7), 801-811

Ling, H. I. and Liu, Z., *Performance of geosynthetic-reinforced asphalt pavements*, Journal of Geotechnical and Geoenvironmental Engineering, February, 2001, 127(2), 177-184.

Liu, C. and Evett, J. B., *Soil properties – testing, measurement, and evaluation*, 5th Ed., Prentice Hall, 2003.

Miura, N., Sakai, A., Taesiri, Y., Mouri, K., and Ohtsubo, M., *Model and field tests of reinforced pavement on soft clay ground*, International Geotechnical Symposium on Theory and Practice of Earth Reinforcement, 1988, 2, Fukuoka, Japan, 227-232.

Mofiz, S. A., Taha, M. R. and Sharker, D. C., *Mechanical stress-strain characteristics and model behavior of geosynthetic reinforced soil composites*, 17th ASCE Engineering Mechanics Conference, June 13-16, 2004.

Montanelli, F., Zhao, A., and Rimoldi, P., *Geosynthetic-reinforced pavement system: testing &. Design*, Proceedings of Geosynthetics, 1997, IFAI, 2, Long Beach, California, 619-632.

Perkins, S. W., *Numerical modeling of geosynthetic reinforced flexible pavements: Final report*, Report No.FHWA/MT-01/003/99160-2, Montana Department of Transportation, 2001, Helena, Montana.

Perkins, S. W. and Cortez, E. R., *Evaluation of base-reinforced pavements using a heavy vehicle simulator*, Geosynthetics International, 2005, 12(2), 86-98.

Perkins, S. W. and Edens, M. Q., *Finite element modeling of a geosynthetic pullout test*, Geotechnical and Geological Engineering, 21, 357-375, 2003.

Poulos, H. G. and Davis, E. H., *Elastic Solutions for Soil and Rock Mechanics*, John Wiley &. Sons, 1974.

Saad, B., Mitri, H., and Poorooshasb, H., *3D FE analysis of flexible pavement with geosynthetic reinforcemen*t, Journal of Transportation Engineering, ASCE, May 2006, 132(5), 402-415.

Skok, E., Johnson, E., and Turk, A., *Asphalt pavement analyzer (APA) evaluation*, MN/RC 2003-02, Minnesota Department of Transportation, 2002.

Tensar Earth Technologies, Inc., *The properties and performance of Tensar Biaxial Geogrids*, January 2003.

Wasage, T. L. J., Ong, G. P., Fwa, T. F., and Tan, S. A., *Laboratory evaluation of rutting resistance of geosynthetics reinforced asphalt pavement*, Journal of the Institution of Engineers, Singapore, 2004, 44(2), 29-44.

Wathugala, G. W., Huang, B., and Pal, S., *Numerical simulation of geogrid reinforced flexible pavements*, Transportation Research Record 1534, Transportation Research Board, National Research Council, 1996, Washington, D. C., 58-65.

陈心爽 袁耀良，*材料力学*，第一版，同济大学出版社，1996. (Chen, X. S., Yuan, Y. L., *Mechanics of materials*, 1st Ed., Tongji University Press.)